# The Role of Cardiac Energy Metabolism during Stress in Hypertrophic and Dilated Cardiomyopathy.

***Sairia Dass MBBS MRCP (UK)***

*St Catherine's College*

*Department of Cardiovascular Medicine*

*University of Oxford*

*Oxford, OX3 9DU*




***Thesis Submitted for the Degree of***

***Doctor of Philosophy***

***Trinity Term 2011***

I dedicate this work to my children Chloe and Zachary

# *Acknowledgements*

It was an honour to be supervised by Prof Hugh Watkins, Prof Stefan Neubauer and Dr Theodoros Karamitsos. I am very grateful for their support, steer and advice through the many learning stages of this thesis. Special thanks to Dr. Joseph Suttie who gave willingly of his time and expertise, for this I am forever grateful.

I am indebted to my colleagues for their willingness to help with the day to day running of this project. I would like to thank Dr. Vanessa Ferreira for the daily inspection of my 'to do list'; Dr. Ntobeko Ntusi and Dr. Erica Dall'Armelina for well-timed words of encouragement. Dr. Cameron Holloway has been a rock, I depended on him for advice and he never disappointed. Every D Phil student needs an angel, for me I was blessed with Dr Lowri Cochlin. Lowri supported me with her intellect and her friendship and for this I am truly thankful.

I especially want to thank my family. My parents, brother and grandmother have always encouraged me to work hard and aim high. My husband, Roger, has inspired me through his own achievements and has quietly guided me throughout this experience. He has provided unconditional, limitless support over the years without which none of this would be possible. Finally, a special thanks to my dearest children for their endless supply of hugs and kisses which have kept me smiling throughout this experience.

# *Declaration*

The work in this thesis is my own. Dr. Lowri Cochlin provided physics support leading to the results in chapter 3 and 4. Dr. Cameron Holloway assisted in conducting the study leading to the results in chapter 7.

# *Abbreviations*

| | |
|---|---|
| 2, 3 DPG | 2.3 diphosphoglycerate |
| $^{31}$P MRS | 31Phosphorus magnetic resonance spectroscopy |
| AMARES | Advanced Method of Accurate, Robust and Efficient Spectroscopic fitting |
| ATP | Adenosine triphosphate |
| AW | Acquisition Weighting |
| BOLD | Blood oxygen level dependent imaging |
| CAD | Coronary artery disease |
| CMR | cardiac magnetic resonance |
| CO | cardiac output |
| COV | Coefficient of variance |
| CSI | Chemical shift imaging |
| DCM | Dilated cardiomyopathy |
| ECG | Electrocardiogram |
| EDV | End diastolic volume |

| | |
|---|---|
| EF | Ejection fraction |
| ESV | End systolic volume |
| HCM | Hypertrophic cardiomyopathy |
| jMRUI | Java Magnetic Resonance User Interface |
| LGE | Late gadolinium enhancement |
| LV | left ventricle |
| MPRI | Myocardial perfusion reserve index |
| MRI | Magnetic resonance imaging |
| MYBPC3 | Myosin binding protein C |
| MYH7 | β myosin heavy chain |
| NOE | Nuclear Overhauser Effect |
| NS | Not significant |
| NYHA | New York Heart Association |
| PCr | Phosphocreatine |
| PET | Positron emission tomography |
| PPA | Phenyl phosphoric acid |

| | |
|---|---|
| PSF | Point spread function |
| RF | Radio frequency |
| RPP | Rate pressure product |
| SERCA | Sarco/endoplasmic reticulum $Ca^{2+}$-ATPase |
| ShMOLLI | Shortened Modified Look- Locker inversion recovery |
| SI | Signal intensity |
| SNR | Signal to noise |
| SSFP | Steady state free precession |
| SV | Stroke volume |
| TE | Echo time |
| TR | Repetition time |

# Table of Contents

**DECLARATION** ..... **3**

**ABBREVIATIONS** ..... **3**

**TABLE OF CONTENTS** ..... **7**

**THESIS ABSTRACT** ..... **10**

**CHAPTER 1** ..... **12**

**INTRODUCTION** ..... **12**

1.1 OVERVIEW ..... 13

1.2 HYPERTROPHIC CARDIOMYOPATHY ..... 16

1.3 DILATED CARDIOMYOPATHY (DCM) ..... 21

1.4 MEASURING CARDIAC ENERGY METABOLISM ..... 22

1.5 AIMS OF THIS RESEARCH ..... 23

**CHAPTER 2** ..... **25**

**GENERAL METHODS** ..... **25**

2.1 GENERAL METHODS ..... 26

2.2 ELIGIBILITY CRITERIA ..... 26

2.3 CLINICAL ASSESSMENT ..... 28

2.4 SCAN PROTOCOLS ..... 28

**CHAPTER 3** ..... **39**

**8 MINUTE CARDIAC $^{31}$P MRS ACQUISITION PROTOCOL: APPLICATION TO CARDIAC PHYSIOLOGICAL STRESS TESTING.** ..... **39**

3.1 INTRODUCTION ..... 40

3.2 METHODS ..... 43

3.3 RESULTS ..... 48

3.4 DISCUSSION ..... 51

3.5 CONCLUSION ..... 58

**CHAPTER 4 ..... 60**

**$^{31}$P MRS ANALYSIS DEVELOPMENT: IMPROVED FITTING OF 2, 3 DPG ..... 60**

4.1 INTRODUCTION ..... 61

4.2 METHOD ..... 66

4.3 RESULTS ..... 68

4.4 DISCUSSION ..... 76

4.5 CONCLUSION ..... 80

**CHAPTER 5 ..... 81**

**EFFECT OF EXERCISE ON CARDIAC ENERGY METABOLISM IN HYPERTROPHIC CARDIOMYOPATHY ..... 81**

5.1 INTRODUCTION ..... 82

5.2 METHOD ..... 84

5.3 RESULTS ..... 85

5.4 DISCUSSION ..... 91

5.5 LIMITATIONS ..... 97

5.6 CONCLUSION ..... 98

**CHAPTER 6 ..... 99**

**MYOCARDIAL TISSUE OXYGENATION IN HYPERTROPHY ASSESSED WITH BLOOD-OXYGENATION-LEVEL-DEPENDENT (BOLD) MRI ..... 99**

6.1 INTRODUCTION ..... 100

6.2 METHODS ..... 102

6.3 RESULTS ..... 103

6.4 DISCUSSION ..... 111

6.5 CONCLUSION ..... 119

6.6 FUTURE WORK ..... 119

**CHAPTER 7 ..... 121**

**EFFECT OF SHORT TERM EXERCISE TRAINING ON CARDIAC FUNCTION AND CARDIAC ENERGY METABOLISM IN DILATED CARDIOMYOPATHY ..... 121**

7.1 INTRODUCTION ..... 122

7.2 METHODS ..... 123

7.3 RESULTS ..... 126

7.4 DISCUSSION ..... 134

7.5 CONCLUSION ..... 136

**CHAPTER 8 SUMMARY ..... 137**

**BIBLIOGRAPHY ..... 142**

**TABLE OF TABLES AND FIGURES ..... 152**

**APPENDIX 1 MINNESOTA ..... 156**

**QUESTIONNAIRE ..... 156**

**APPENDIX 2 ..... 158**

**BORG SCORE ..... 158**

**APPENDIX 3 ..... 159**

**PAPERS IN PREPARATION ..... 159**

# *Thesis Abstract*

Both hypertrophic (HCM) and dilated cardiomyopathy (DCM), though differing in their aetiologies, share features of impaired resting energetics. The aim of this thesis was to determine if cardiac high energy phosphate metabolism, measured as the phosphocreatine (PCr)/ATP ratio using $^{31}$Phosphorus magnetic resonance spectroscopy ($^{31}$P MRS), is further impaired during exercise in these pathologies. This would provide a possible explanation for the high incidence of exercise related death in HCM and DCM as well as the blunted inotropic response to exercise in DCM. Furthermore, this thesis investigates the role of stress perfusion and stress tissue oxygenation in HCM (as these are hypothesized to exacerbate the primary defect in energetics) and exercise training in DCM (which is hypothesized to improve function though the mechanisms are uncertain).

This work developed a novel protocol for measuring $^{31}$P MRS in a clinically acceptable time frame. The traditional acquisition is at least 20 minutes (as much as 40 minutes in subjects with lower pulse rates). This is a particularly long time to allow for exercise in the magnet particularly in the symptomatic DCM cohort. Hence this work meticulously developed a shorter 8 minute protocol. Its validity, reproducibility and application to exercise were confirmed. The post processing of the MRS data was further improved for calculating blood contamination and tested with both simulated and patient data, including normal, hypertrophied and thinned myocardium.

Applying this new method, this thesis is the first to report a further decrease in exercise energetics in HCM. The relationship between perfusion, tissue de-oxygenation and energetic compromise during exercise was then explored in HCM. Athletes, with physiological hypertrophy, were used as an additional control group in these experiments. These results demonstrated a strikingly blunted oxygenation response of the HCM heart to stress even in the pre-hypertrophy HCM mutation carriers. However, as a group, the data did not show a correlation between the blunted oxygenation response and the percentage change in PCr/ATP during exercise. None-the-less, these results can potentially be useful for distinguishing between hypertrophy in the athletes and pathological hypertrophy in HCM and for distinguishing HCM mutation carriers' pre hypertrophy and the normal heart.

In the DCM cohort, this thesis explored the impact of exercise training on cardiac metabolism and function. The results showed no change in cardiac energetics and left ventricular ejection fraction during 8 minutes of exercise. In addition, an eight week home exercise programme did not alter resting or exercise cardiac PCr/ATP, but improved cardiac function during rest and exercise, and increased exercise tolerance and quality of life scores.

In conclusion, this thesis reports further insights into cardiac exercise energetics in HCM and DCM and its relationship to perfusion and oxygenation in HCM and to exercise training in DCM. Therapies that decrease the energy cost of cardiac work during exercise may prove beneficial targets to explore further in these conditions.

# *Chapter 1*
# *Introduction*

# 1.1 Overview

Cardiomyopathies encompass a diverse spectrum of inherited and acquired disorders characterized by impaired myocardial contractility and pathological ventricular remodelling[1, 2]. Although gross (figure1.1) and histologic findings in primary cardiac hypertrophy and dilatation are well described, the cellular and molecular triggers of these forms of remodelling are largely unknown[3] . Identification of genetic mutations as well as insight into cellular metabolism in these cardiomyopathies has provided insight into disease aetiology. Deranged cardiac energy metabolism has been implicated in both hypertrophic [4, 5, 6, 7] and dilated cardiomyopathy [8,9, 10] .

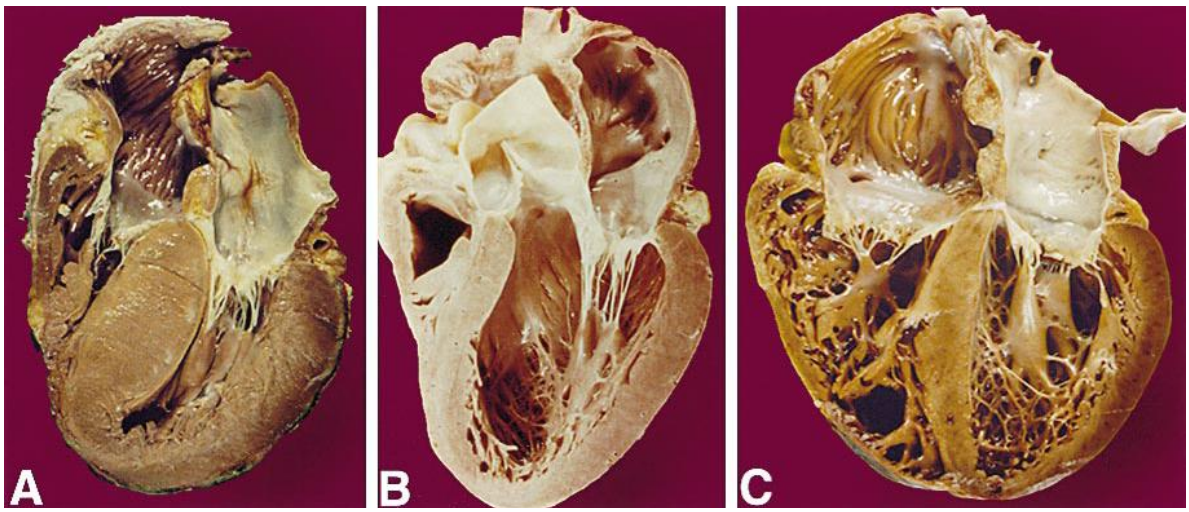



***Figure 1.1:*** *Patterns of Cardiac Remodelling. The normal myocardium can be remodelled by heritable gene mutations and acquired diseases into hypertrophic or dilated morphologies. Note the normal left ventricular wall thickness and chamber volume of the healthy heart (B) in comparison to the robust increase in left ventricular wall thickness of hypertrophic cardiomyopathy (A) and the marked increase in left ventricular chamber volumes of dilated cardiomyopathy(C). (ref Seidman[3])*

The heart is an energy expensive organ. With an average heart rate of 72 beats per minute, the heart will pump about 7 liters total per minute. The cardiac output of the average human heart over a life time of 70 years would be about 300 million liters. Therefore, maintenance of adequate levels of cardiac high-energy phosphate metabolites, adenosine triphosphate (ATP), the energy source for contraction, and phosphocreatine (PCr), the major energy storage compound, is essential for normal heart function. As such, the heart consumes about 6kg of ATP every day, more energy than any other organ[11]. Hence it is not surprising that derangements in cardiac energetics can contribute significantly to disease aetiology and progression.

Abnormal resting cardiac energetics has already been demonstrated in hypertrophic cardiomyopathy (HCM) [4 5 6, 7], non-ischaemic heart failure [8 9 10], ischaemic heart disease [12,13] hypertension [14, 15] and valvular disease [16,12].

There are four major factors necessary for effective cardiac metabolism (Figure 1.2).

1. Adequate perfusion: A healthy myocardial blood supply with an appropriate hyperemic response during exercise is necessary to deliver both substrate and oxygen under resting and exercise condition.
2. Substrate utilisation: This involves uptake of mainly free fatty acids and glucose and its subsequent breakdown via beta oxidation and glycolysis. These processes result in the formation of acetyl coenzyme A (CoA), which is fed into the Krebs cycle and produces NADH and carbon dioxide ($CO_2$).

3. Energy production: High energy phosphate bonds are made in the form of ATP via a series of electron transfers in the mitochondria. Respiratory-chain complexes I through IV transfer electrons from NADH to oxygen, thereby creating a proton electrochemical gradient across the inner mitochondrial membrane as well as NAD and water. This gradient drives ATP synthase, which produces ATP by phosphorylating ADP (adenosine di phosphate). Uncoupling proteins cause mitochondria to produce heat rather than ATP.
4. Energy transfer and utilisation: The heart energy transfer mechanism is the creatine kinase energy shuttle. Mitochondrial creatine kinase catalyzes the transfer of the high energy phosphate bond in ATP to creatine to form PCr. This molecule is smaller and less polar and hence diffuses out of the mitochondria into the cytoplasm. At the site of energy usage, mainly at the sarcomere and for ion pump function, ATP is reformed in the reverse reaction. Creatine, which is not produced in the heart, is taken up by the creatine transporter.

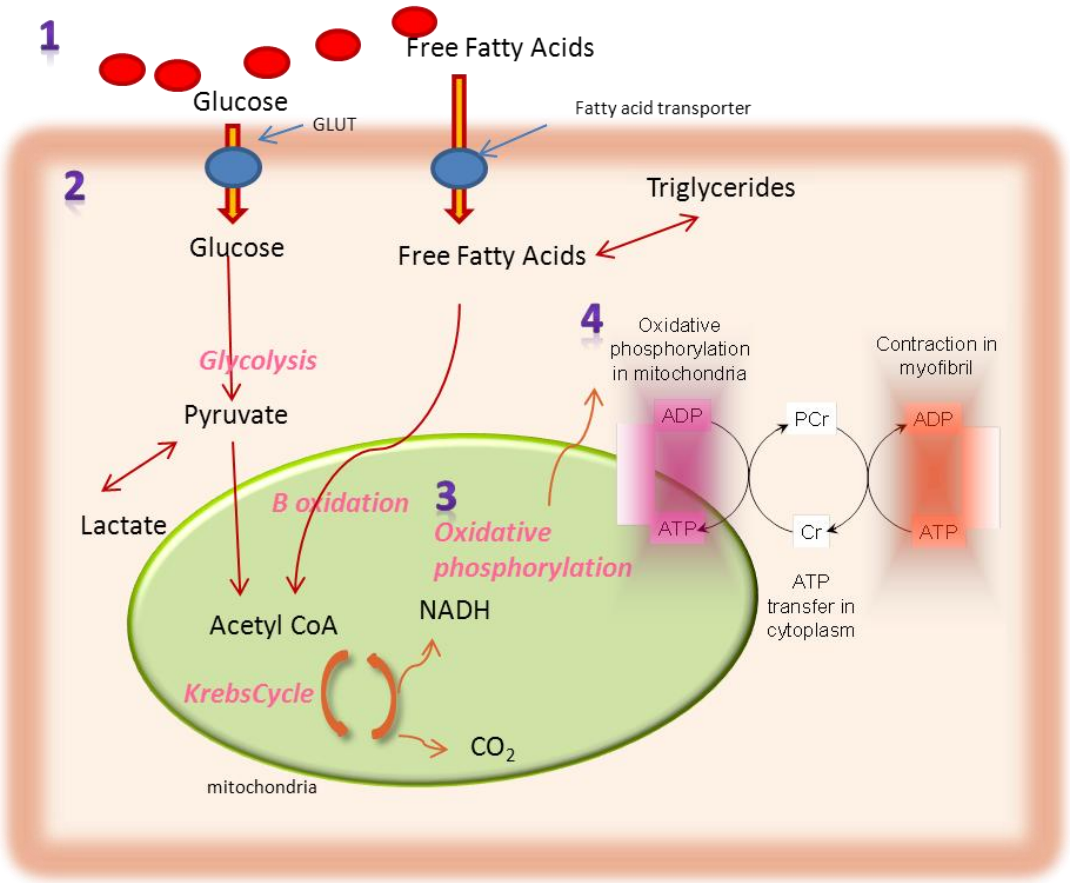



***Figure1.2:*** *Cardiac Energy Metabolism**.** Energy metabolism in the heart has four components. 1. Adequate blood supply; 2.substrate utilisation; 3. Oxidative phosphorylation; 4. Energy transfer and utilisation; GLUT denotes glucose transporter, PCr phosphocreatine, Cr free creatine.*

## 1.2 Hypertrophic cardiomyopathy

Hypertrophic cardiomyopathy (HCM) affects 1 in 500 individuals and is the commonest cause of sudden cardiac death in the young (including competitive athletes) and this is perhaps the most devastating component of its natural history[1, 2, 17-19].

Despite being a common genetic cardiomyopathy, determining disease progression and risk stratification remains a clinical dilemma. This is mainly attributed to the marked heterogeneity in the following:

(i) Molecular expression exhibited both at a gene and allele level. HCM is an autosomal dominant disease caused by mutations in sarcomeric proteins. Over 1000 mutations in nine genes encoding sarcomeric proteins have now been implicated[20]. Mutations in genes encoding the β- myosin heavy chain( MYH7) and the cardiac myosin- binding protein C ( MYBPC3) are the most common, with each accounting for 25 -33% of all cases[1] ( figure 1.3). Interestingly, the genetic basis of ventricular hypertrophy does not directly correlate with prognostic risk stratification. Patients with some mutations, such as specific tropomyosin substitutions, have only a mild degree of ventricular hypertrophy, with little or no left ventricular outflow tract obstruction, but they still carry a disproportionately high risk of sudden death[21].

(ii) Clinical expression. There is significant inter and intra familial variation in degree of hypertrophy, symptoms and disease progression. Clinical risk factors for sudden death (i.e., age, syncope, family history of sudden cardiac death, cardiac arrest survivor, non-sustained ventricular tachycardia and abnormal blood pressure response to exercise) have been identified. However, as evidenced by differing international guidelines, controversy abounds with regards to defining levels of risk of sudden death.

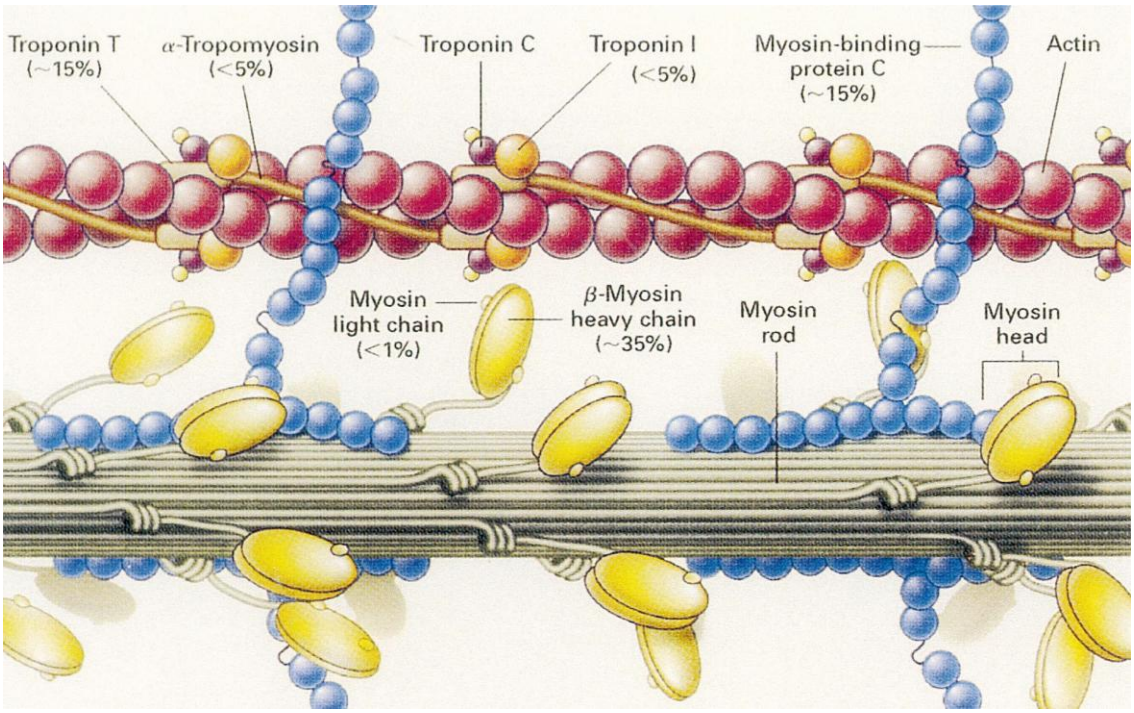



***Figure 1.3****:Diagrammatic representation of the molecular structure of the sarcomere showing the thick (myosin) and thin (actin) filaments and the location of the proteins–β myosin heavy chain, myosin light chains, myosin binding protein-C, α-tropomyosin, troponin T and troponin I – that are mutated in HCM. From Ref. [Redwood 1999]*

With the availability of therapeutic measures that prevent sudden death (i.e. implantable cardioverter defibrillator), the identification of high-risk patients is now of even greater importance. Abnormal myocardial energy utilisation has been implicated in playing a crucial role in the pathophysiology of HCM[1, 22, 23]. Further interrogation of this, particularly during exercise, when sudden death is more likely to occur, might in fact lead to a more comprehensive understanding of disease mechanism and assist in identifying persons at risk of sudden death and in the monitoring of treatment interventions.

## *Energy metabolism in HCM*

The aetiology of hypertrophy in HCM occurs in the absence of increased external load, thus it is likely due to the primary pathogenic mutation. This phenomenon is believed by many experts in the field to be due to an underlying energetic defect[1, 22, 23] . Little is known about the specific changes in substrate utilisation, oxidative phosphorylation and energy transfer in HCM but it is well established that the energy cost of force production is increased[22].

Traditionally it was thought that the mutant HCM proteins depressed cardiac function and that subsequently activated neuroendocrine and mechanical responses leading to compensatory hypertrophy. However, in vitro and mouse models have subsequently shown *increased* contractility of the mutant myofilaments due to altered myosin kinetics, increased thin filament calcium sensitivity or changes in myosin binding regulation[3, 24]. Mutations in myosin can alter cycling rate of myosin heads thus leading to more cross bridge detachment before completion of the power stroke[25]. Most HCM mutations in thin filament regulatory proteins increase calcium sensitivity, this increases force at submaximal calcium concentrations[26-28]. In addition, mutations in these regulatory proteins can also alter velocity of cross bridge formation[29].

The energy depletion hypothesis proposes that the increased energy demand compromises the cardiomyocytes ability to maintain energy levels necessary for contraction, pump function and homeostatic function such as calcium re up-take. This myocyte dysfunction results in hypertrophy. This hypothesis is supported by findings of abnormal resting energetics in patients with HCM[4, 6] even in the pre hypertrophied state[4]. Further support

comes from the observation that diseases which directly affect glucose transport (GLUT 4 knockout); free fatty acid transport (cd36 deficiency) and mitochondrial function cause HCM phenocopies.

Furthermore, abnormal energetics may be compounded by the microvascular dysfunction which occurs in HCM with possible resultant tissue hypoxia. Microvascular dysfunction in HCM has been extensively investigated using many modalities including MRI[30, 31], positron emission tomography (PET) [32] and thallium scanning[33]. Ischaemia has been assumed as a result of perfusion deficits.

Angina and symptoms suggesting myocardial ischemia are frequent features in the natural history of HCM, and there is pathological evidence that ischemia can be related to sudden death even in young asymptomatic patients[34]. Two possible mechanisms may be responsible for de-oxygenation in HCM. Firstly, abnormal intramural coronary arteries, with a reduction in the size of the lumen and thickening of the vessel wall are a consistent feature in HCM[35]. The prominence of abnormal intramural coronary arteries in areas of extensive myocardial fibrosis is consistent with the hypothesis that these abnormalities are responsible for the development of myocardial de-oxygenation. Secondly, capillary density and distribution are of crucial importance for the process of oxygen exchange between blood and tissue. Thus, de-oxygenation might also exist in HCM due to an increased oxygen diffusion distance caused by an inadequate growth of capillaries[36] .

## 1.3 Dilated cardiomyopathy (DCM)

DCM is the second most common cause of heart failure after coronary artery disease. Despite advances in medical and resynchronization device therapy , in the United Kingdom, heart failure affects one in every 100 people and within the year of admission, 32% of patients die[37]. On the whole, heart failure consumes about 2% of the National Health Service budget in the United Kingdom; and in the United States, the annual cost of treatment is in excess of $28 billion. The prevalence of heart failure and its associated morbidity and financial burden is expected rise given an aging population and improved treatments of its causes.

Dilated cardiomyopathy (DCM) is the end phenotype of non ischaemic insults and has a very poor clinical prognosis[1, 2, 17, 38].Left ventricular dilatation, systolic dysfunction, myocyte death and myocardial fibrosis are the main features of DCM. Familial disease accounts for one third to one half of cases[39].

There is  growing evidence that altered energetics play an important role in the mechanism of heart failure[11]. Investigating myocardial energetics during stress might further clarify a mechanism for sudden cardiac death, (i.e. impaired pump function leading to poor calcium handling and lower threshold for ventricular arrhythmias) and loss of inotropic reserve/progression of contractile dysfunction.

### *Energy metabolism in heart failure*

Abnormalities of cardiac energy metabolism in heart failure are multifactorial.

1. Substrate utilisation: There are reported changes in fatty acid as well as glucose substrate utilisation with an initial increase in glucose metabolism. However, in advanced heart failure insulin resistance develops in the myocardium with a subsequent decline in glucose metabolism. Fatty acid metabolism also declines in advanced heart failure.

2. Oxidative phosphorylation: Cardiac mitochondria have structural abnormalities and are probably increased in number[40]. The activity of the electron transport chain complexes and of ATP synthase is reduced. Absolute phosphocreatine concentrations can be reduced by more than half, with ATP concentrations reduced by as much as a third.

3. ATP transfer: There are significant changes in the creatine kinase system in heart failure. Both mitochondrial and myofibrillar creatine kinase activities are reduced resulting in a decline in ATP transfer. ATP turnover rates via CK were shown to be as much as 50% reduced.[41]

## 1.4 Measuring cardiac energy metabolism

ATP is used for most energy consuming reactions in the heart, including contraction of cardiac myofilaments (70%) and for active pump function and calcium uptake via sarco/endoplasmic reticulum $Ca^{2+}$-ATPase (SERCA). Myocardial levels of ATP are kept

relatively constant over a wide range of cardiac loads in the normal heart, buffered by the transfer of energy from PCr. The equilibrium constant of this creatine kinase reaction, figure 1.2, favours the synthesis of ATP over PCr, by a factor of approximately 100. Hence in disease states with inefficient energy production or energy utilisation, the ATP levels would initially remain constant at the expense of PCr; the ratio of PCr/ATP is therefore a sensitive indicator of the underlying energetic state of the heart.

Measurement of PCr and ATP content in myocardial biopsies is problematic as it is invasive and these molecules are unstable when analysed with wet chemical techniques.

Cardiac $^{31}$P MRS is the only technique that allows non-invasive measurement of cardiac high-energy phosphate metabolism in vivo. The first publication in 1980 on *in vivo* spectroscopy on the rat heart[42] paved the way for this non-invasive technique to be applied to the human heart, some ten years later[43]. The technique is now an established research method used for investigating cardiac energetics and its response to treatment.

## 1.5 Aims of this research

This is a multi-parametric cardiac magnetic resonance imaging (CMR) study.

This work aims to investigate the resting and exercise energetic profile of both HCM and DCM. In order to accomplish this, the work of this thesis begins with the development of a robust and accurate method to measure and process exercise $^{31}$P MRS in a clinically acceptable time frame.

The following were then explored:

1. The high incidence of exercise-related death in HCM may be explained by an acute impairment of myocardial energetics. As a proof-of-principle study, this thesis examined whether cardiac energetics are further impaired during exercise in HCM.

2. Microvascular dysfunction is a well known component of HCM. This thesis explores for the first time, tissue oxygenation in HCM in the presence of hypertrophy and also in pre-hypertrophied mutation carriers. The relationship between exercise energetics, stress perfusion reserve and tissue oxygenation during stress was interrogated.

3. In DCM, exercise training may play a beneficial role, however, the time course for improvements and mechanisms is poorly understood. The effects of short term exercise training on rest and exercise energetics, cardiac function and quality of life are investigated.

# *Chapter 2*
# *General Methods*

## 2.1 General Methods

This study was approved by the Mid and South Buckinghamshire Research Ethics Committee (ref: 07/Q1607/66). Each participant gave written informed consent to be involved. Subjects were recruited from the cardiovascular clinics at the John Radcliffe hospital. Athletes were recruited from the city of Oxford rowing club tier 1 team and normal volunteers were recruited via word of mouth.

## 2.2 Eligibility Criteria

Subjects were eligible for inclusion in the study if:

- Aged between 18 and 65
- Willing to participate in a research study on a voluntary basis.
- **HCM**:

  With hypertrophy:

  Gene positive for beta-Myosin heavy chain, Myosin Binding Protein C or Troponin T mutations *OR* evidence of asymmetrical hypertrophy in the absence of other causes of hypertrophy (i.e. hypertension, aortic stenosis, exercise training) with another affected first degree relative.

  Without hypertrophy:

Gene positive for beta-Myosin heavy chain, Myosin Binding Protein C or Troponin T mutations.

- **ATHLETES**:

  Performed 6-10 hours minimum training per week.

- **DCM:**

  Non ischaemic aetiology confirmed by either a coronary angiogram or a functional stress test. Patients must be NYHA 2 or more, established on maximum tolerated anti failure therapy and have a left ventricular ejection fraction of 40% or less.

Subjects were **excluded** if any of the following were present:

- Current smoker *OR* a history of smoking in the past 3 years.
- History of coronary artery disease (CAD), cardiac chest pain or valvular heart disease.
- In the HCM group, subjects were excluded if they had a blood pressure drop on exercise during a standard Bruce exercise tolerance test *OR* if there was a resting outflow tract gradient greater than 30mmHg.
- In the non HCM groups, subjects were excluded if they had a family history of cardiomyopathy or sudden cardiac death.
- Any contraindications to MR scanning (metal implants, pacemakers, claustrophobia, previous head or eye surgery).
- History to suspect pregnancy *OR* a positive pregnancy test *OR* breastfeeding.
- Impaired renal function,( eGFR< 30)

## 2.3 Clinical assessment

On the day of scanning, all subjects underwent a clinical assessment. This included history for:

- The presence of exclusion criteria as documented above.
- Drug history including allergies
- Weekly alcohol level (units)
- Exercise / physical activity level, documented as the number of 30 minute sessions of sweat producing exercise per week

Cardiovascular examination was also performed to assess for the presence of ventricular hypertrophy and valvular heart disease. The following measurements were carried out:

- Blood pressure measurements using a manual sphygmomanometer
- 12 lead electrocardiogram, (ECG)
- Height (cm) and weight (kg) using calibrated scales.
- Blood tests after an 8 hour fast for serum cholesterol (total cholesterol and high density lipoprotein), glucose and triglyceride.
- Creatinine check to measure glomerular filtration rate.

## 2.4 Scan Protocols

Subjects underwent a comprehensive CMR protocol which measured the following

(i) $^{31}$P MRS at rest and during leg exercise

(ii) Cardiac mass and function

(iii) Rest and adenosine stress Blood oxygen level dependent imaging (BOLD) to assess tissue oxygenation.

(iv) Rest and stress adenosine perfusion

(v) Late gadolinium enhancement (LGE) to assess patchy fibrosis.

All scanning was conducted on a Siemens 3T Trio MR system (Erlangen, Germany). Average scan time was 90 minutes; figure 2.1 shows the scan timeline.

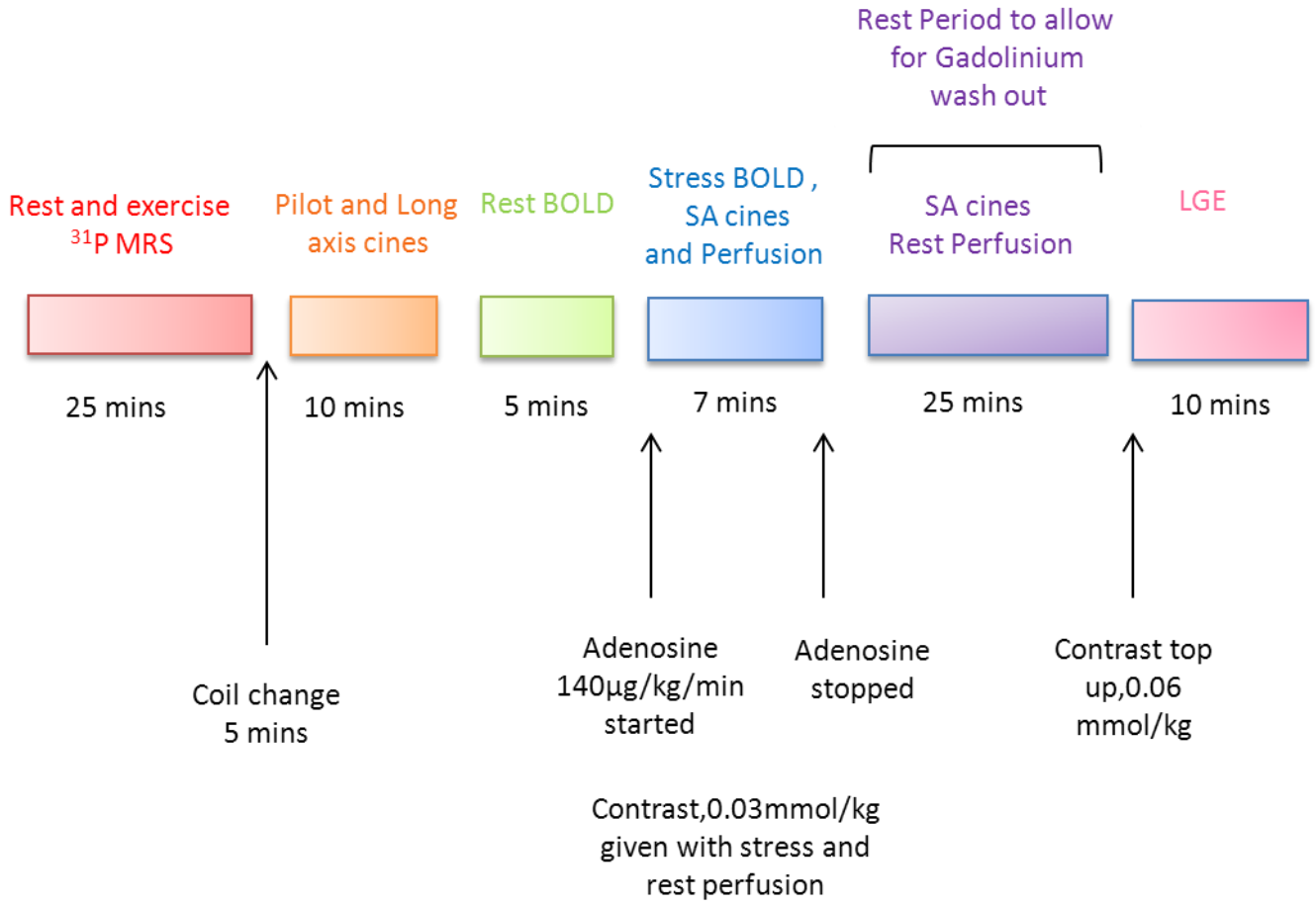



***Figure 2.1**: Timeline for the scan protocol*

### *2.4.1 $^{31}$Phosphorus Magnetic Resonance Spectroscopy*

In order to obtain cardiac exercise $^{31}$P MRS, a robust, reproducible protocol which is short enough to allow sufficient exercise in the magnet had to be developed.

This is discussed in further detail in chapters 3 and 4.

### *2.4.2 Left ventricular function and mass*

CMR is accurate, reproducible and well validated for measuring left ventricular volumes and mass[44]. Cardiac volumes were acquired using Steady State Free Precession (SSFP) imaging. Pilot, horizontal long axis, vertical long axis and short axis stack images were acquired with the patient in the supine position. Each slice was 7mm thick with a 3mm gap and is prospectively gated with echo time, 1.5 ms; repetition time, 3 ms; flip angle, 50°. The slices were obtained during a breath-hold at the end of normal expiration to minimize the effects of respiratory motion.

LV short axis epicardial and endocardial borders were manually contoured at end diastole and end systole, (figure 2.2) for determining end diastolic volume (EDV); end systolic volumes (ESV); stroke volume (SV). Ejection fraction (EF) and cardiac output (CO) are calculated (EF = SV/EDV, CO=SV x heart rate). Myocardial mass is also calculated by subtracting the endocardial volume from the epicardial volume. Left ventricular mass is calculated based on prior knowledge of myocardial specific gravity (1.05 g/cm$^3$).

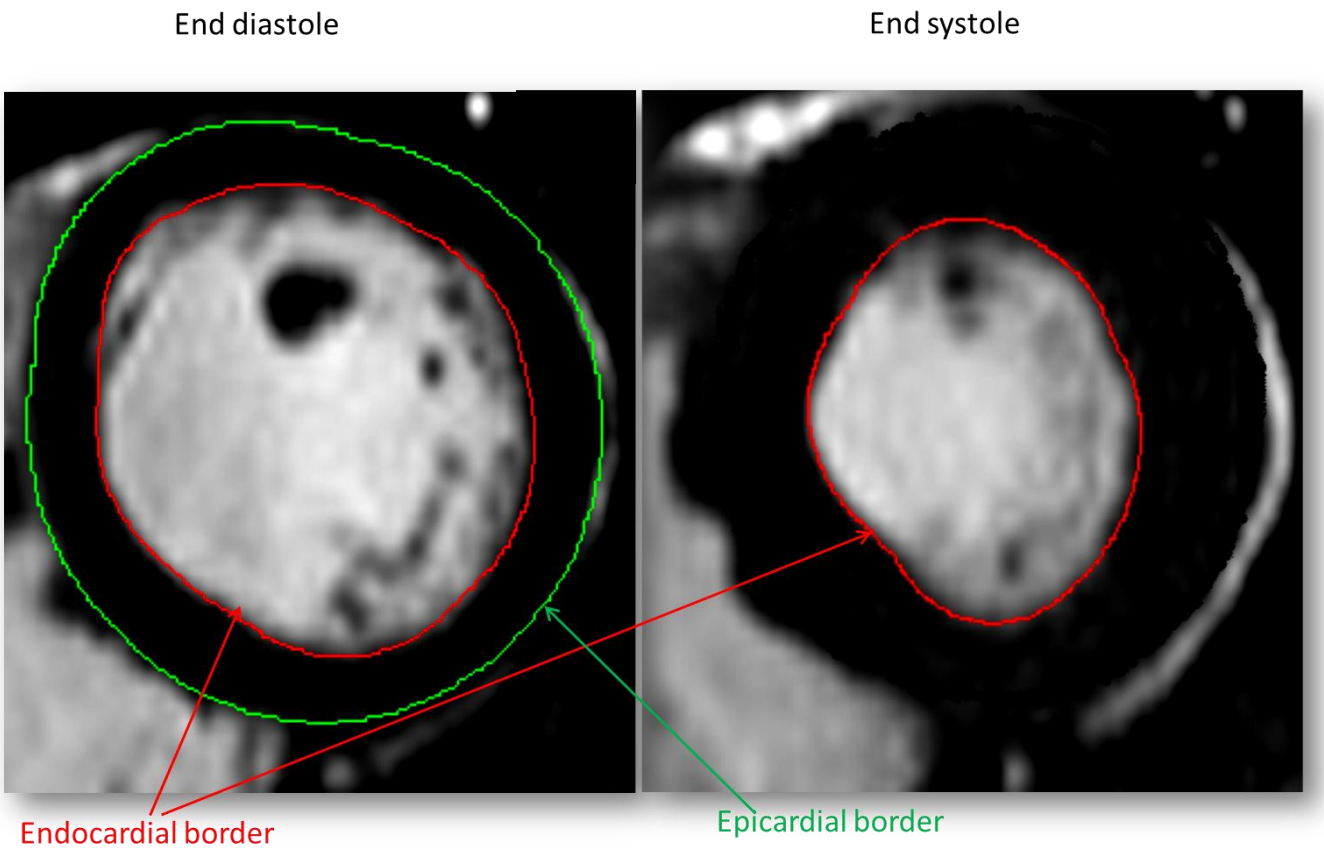



***Figure 2.2**: Epicardial and endocardial contours are drawn at end diastole and end systole*

### *2.4.3 BOLD*

BOLD-CMR was performed at three levels, basal, mid ventricular and apical. Slices were acquired at mid-diastole using a T2-prepared ECG-gated SSFP sequence with the following parameters: repetition time/echo time, 2.86/1.43 ms; T2 preparation time, 40 ms; matrix, 168_192; field of view, 340_340 mm; slice thickness, 8 mm; and flip angle, 44°. Each BOLD image was obtained during a single breath-hold over 6 heart beats. Two images of the same

slice were acquired at rest and during the infusion of adenosine (140 μg/kg/min, figure 2.3). Adenosine is traditionally used as a stressor in cardiac BOLD imaging as it causes vasodilation and a resulting reflex tachycardia[45]. The acquisition of stress BOLD images commenced at peak stress approximately 90 seconds after the initiation of adenosine infusion. If necessary, shimming and center frequency adjustments were performed before BOLD imaging to generate images free from off-resonance artefacts. Blood pressure was recorded at two minute intervals during the adenosine infusion.

For BOLD analysis, QMass software (version 6.2.3, Medis, Leiden, The Netherlands) was used. Myocardial signal intensity, (SI) was measured after manually tracing the endocardial and epicardial contours. Basal and midventricular short-axis BOLD images were divided into 6 segments (inferior septum, anterior septum, anterior, anterolateral, inferolateral, and inferior), and the apical BOLD slice was divided to 4 segments (septum, anterior, lateral and inferior) according to American Heart Association 17-segment model (excluding segment 17 – true apex).

In this cardiac gated sequence, variations of heart-rate also affect the signal intensity due to its effect on T1 relaxation and the following equation was used for correction:

$$S = S_0 \Big/ \left( 1 - \beta e^{\frac{-T_R}{T_1}} \right)$$

with T1 =1220 ms [46] and β=0.59 (determined empirically for this sequence) where $S_0$ is the measured signal intensity, S is the corrected signal intensity and TR is the image dependent

time between acquisitions of sections of k-space, governed by the heart rate. TR is replaced by the RR interval.

The relative corrected signal intensity change was calculated as follows:

$$SI\Delta\ (\%) = \frac{\text{Mean SI (stress)} - \text{mean SI (rest)}}{\text{Mean SI (rest)}} \times 100$$

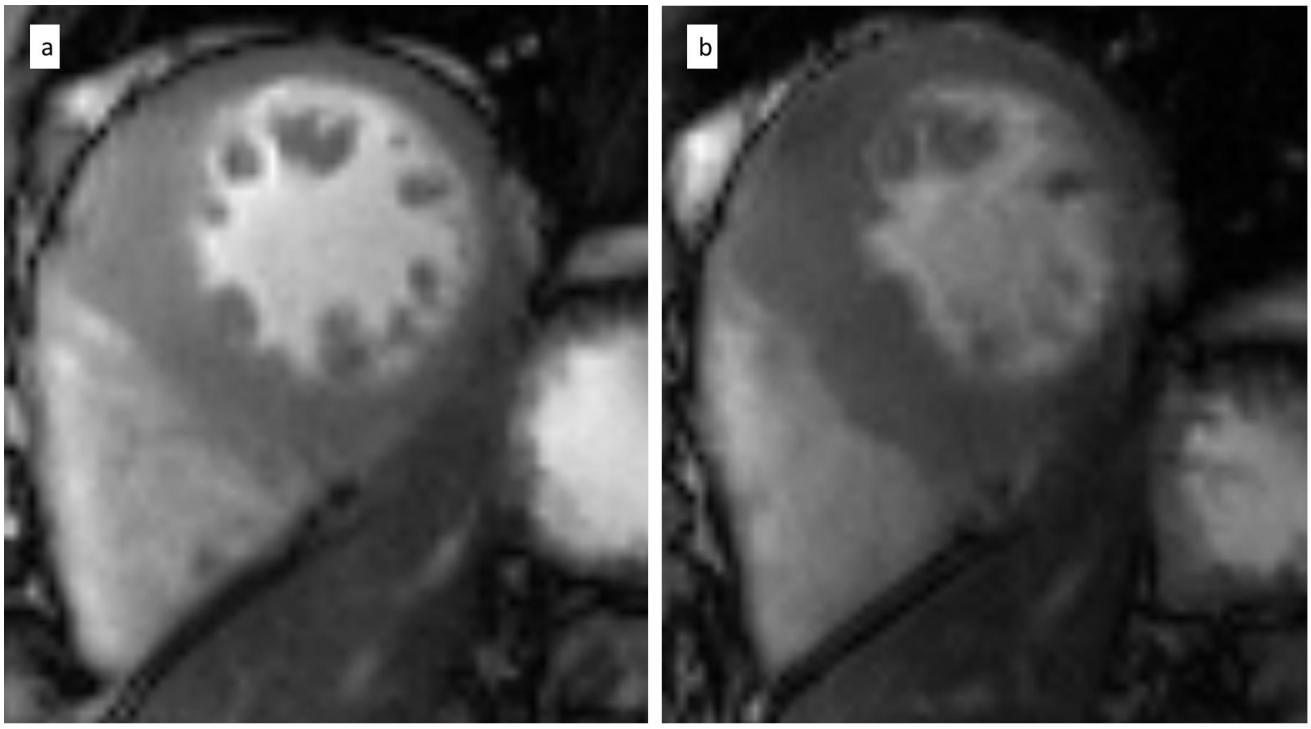



***Figure 2.3****: BOLD image a) rest and b) exercise*

## *2.4.5 Perfusion*

Three short axis cine images (base, mid-ventricular and apical) were chosen from the short axis stack, taking care to avoid the LV outflow in systole. Adenosine (140µg/kg/min) was infused through a large bore cannula in the ante-cubital fossa. Images were acquired at

peak stress after commencement of adenosine. Heart rate and blood pressure are measured before, at two minute intervals during, and after adenosine stress. To assess regional perfusion, a bolus of intravenous magnetic resonance contrast agent (0.03mmol/kg body weight of Gadodiamide, Omniscan; GE Healthcare, Amersham, United Kingdom, injection rate, 6 mL/s) was administered, followed by a saline flush of 15 mL at the same rate at the end of the adenosine infusion. Stress perfusion was measured every heartbeat during the first pass using a T1 -weighted fast (spoiled) gradient echo sequence in the 3 short-axis imaging planes. Perfusion pulse sequence parameters were as follows: repetition time (per image), 180 ms; echo time, 0.99 ms; matrix, 128x80; and slice thickness, 8 mm. All perfusion images were acquired in the 3 short-axis orientations only. Rest perfusion imaging was performed after 25 minutes and another dose of contrast (0.03mmol/kg body weight) was given, (figure 2.4).

For perfusion analysis, QMass software (version 6.2.3, Medis, Leiden, and The Netherlands) was used. The epicardial and endocaridal contours were traced. The basal and mid ventricular slices were divided into 6 equiangular segments and the apical slice into 4 segments (according to American Heart Association 17-segment model, excluding segment 17 – true apex). The signal intensity of the pixels before and during contrast injection was measured to generate signal intensity curves for each segment. The upslope or rate of change of signal intensity in the myocardium was then derived( ie the first derivative of the signal intensity curve)[47]. This rate of contrast enhancement in myocardial tissue was normalised to the rate of contrast enhancement in the LV cavity and the myocardial perfusion reserve index (MPRI) was then calculated by dividing the results at maximal

vasodilation through the results at rest[48, 49]. MPRI is a semi- quantatative method and has been widely adapted for perfusion analysis[49]. Figure 2.5 illustrated signal intensity curves at rest and during adenosine stress in a normal control as well as in HCM.

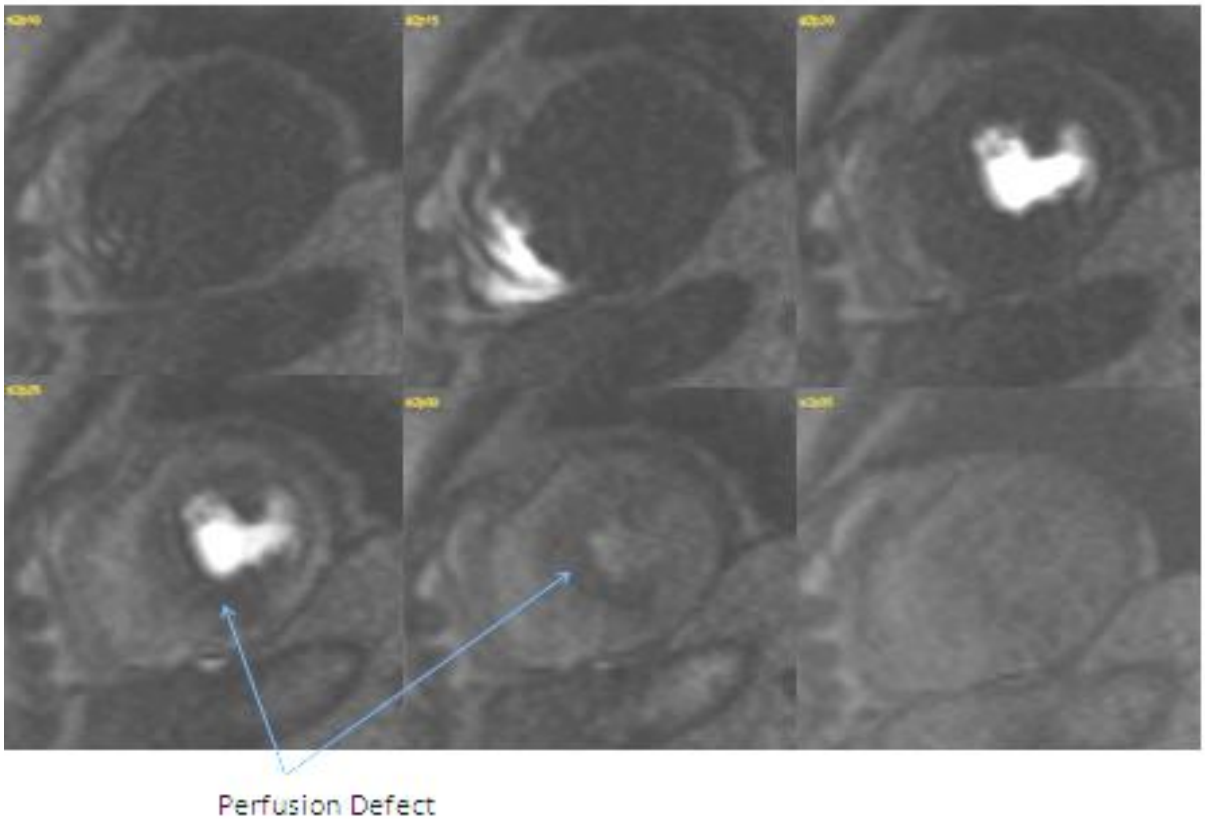



***Figure 2.4****: Sequential perfusion images during adenosine stress in a HCM patient. Note firstly there is no contrast, it then enters the right ventricle, then left ventricle and flushes through the myocardium.Note the persistent defect in the septum and inferior septum (arrows) corresponding to the areas of maximal hypertrophy.*

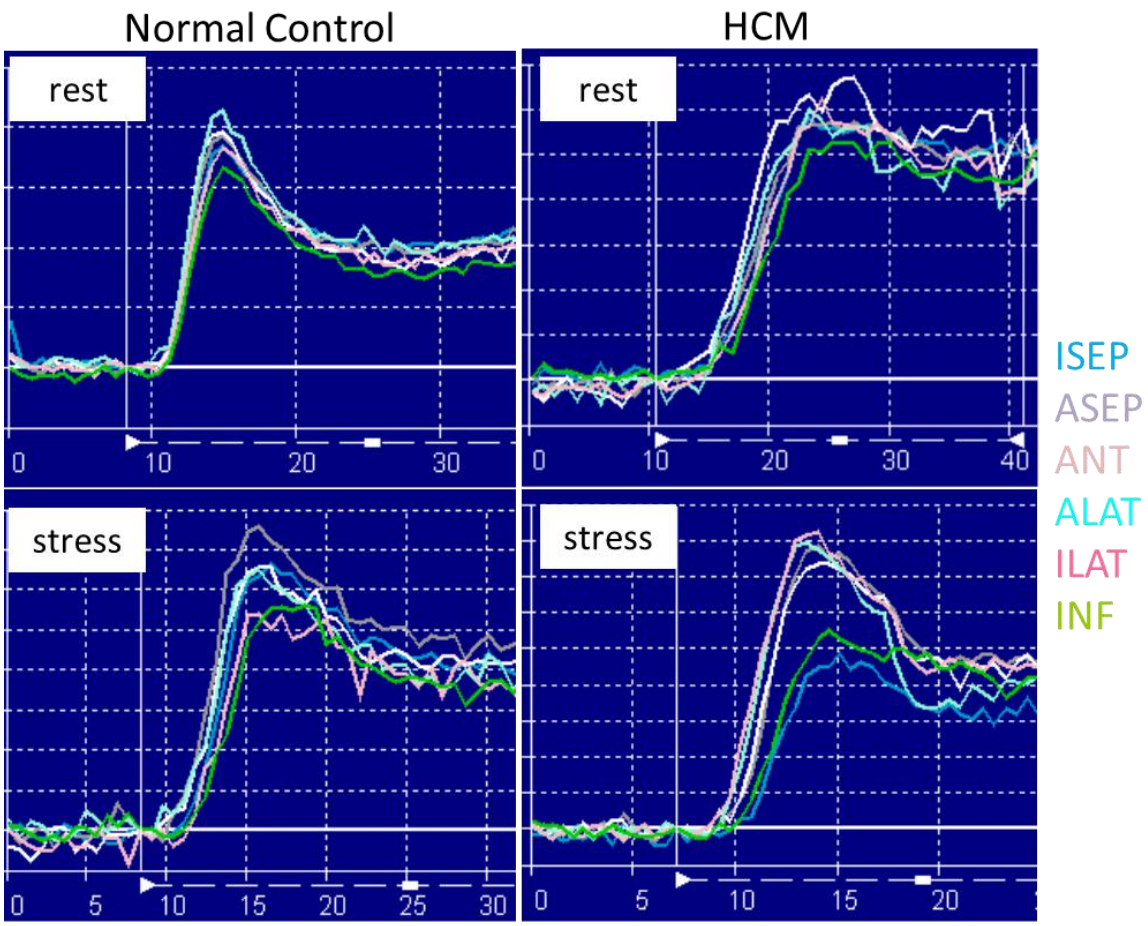



***Figure 2.5**: Myocardial intensity slope curves for normal control and HCM subject at rest and during stress, note the less steep upslope in the inferior septal and inferior segments during stress in HCM corresponding to the perfusion defect seen in figure 2.4*

### *2.4.6 Late Gadolinium Enhancement*

For late gadolinium enhancement (LGE) CMR, a top-up bolus of 0.06 mmol/kg of body weight of a gadolinium-based contrast agent (Gadodiamide, Omniscan; GE Healthcare, Amersham, United Kingdom) followed by a 10-mL saline flush were administered through an intravenous cannula inserted into the antecubital fossa. Electrocardiographically gated images were acquired after a 3 minute delay in long- and short-axis planes using a breath-

hold T1 -weighted segmented inversion-recovery turbo fast low-angle shot sequence previously described[30]. The scan parameters used were: slice thickness 8 mm, flip angle 20°, Repetition time/ Echo time =3 ms/7.5 ms.

Areas of LGE were visually scored as absent or present by consensus of 2 experienced operators. LGE was also quantified, using an in-house software MC-ROI (IDL v.6.1, www.ittvis.com), by drawing endocardial and epicardial borders as well as a region of normal intensity myocardium, figure 2.6).

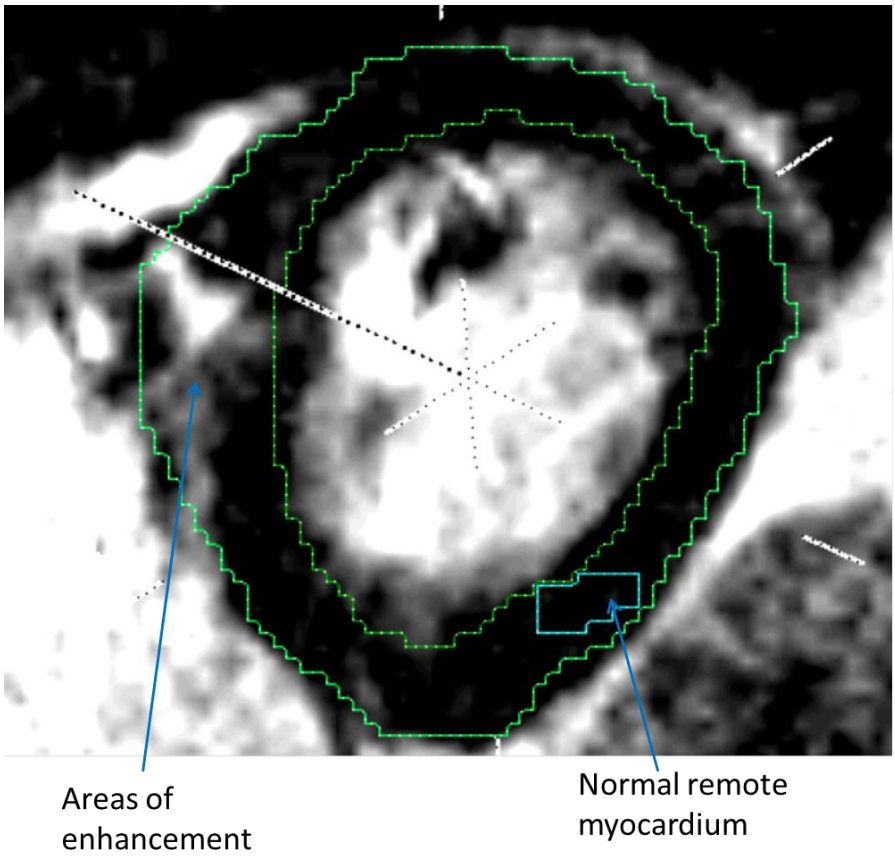



***Figure 2.6****: Epicardial and endocardial borders are drawn as well as a normal reference myocardium.*

Hyperenhanced pixels were defined as those with >2 SDs above the mean of image intensities in a remote myocardial region in the same image. Values are reported as the fraction of the segment affected i.e. the number of pixels with intensity greater than 2 standard deviations above the average intensity of the reference normal myocardium/ the total number of pixels in that segment.

Rest and stress BOLD, perfusion and LGE images were acquired on matching basal, midventricular and apical slices.

# *Chapter 3*
# *8 minute Cardiac $^{31}$P MRS acquisition protocol: application to Cardiac physiological stress testing.*

# 3.1 Introduction

Over the last two decades $^{31}$P MRS has been developed as a powerful tool for studies of tissue energetics. Thus, with increased availability of high field, broadband magnetic resonance systems, cardiac $^{31}$P MRS is becoming a recognised and increasingly published research method for non-invasive, in-vivo measurement of cardiac energetic state.

However, the technical challenges faced by persons wishing to use cardiac $^{31}$P MRS are considerable and include:

- Low magnetic resonance visibility of $^{31}$Phosphorus nuclei leading to long examination times for high quality myocardium specific information.
- Low spatial resolution and thus potential for signal contamination from neighboring tissues.
- Susceptibility to respiratory motion during acquisition
- Susceptibility to cardiac motion during acquisition

Attempts at addressing these factors to yield spectra of high quality, in a comfortable scan time, have inevitably lead to compromise between desired spatial and temporal resolution. This compromise is reflected in the wide range of published values of cardiac PCr/ATP for healthy volunteers ranging from 1.43 to 2.96; a selection of the last 10 years of published data is summarised in Table 3.1.

***Table 3.1**: Selection of published values of PCr/ATP measured in normal volunteers over the last 10 years.*

| ref | year | number of normals | age ± σ | normal PCr/ATP ± σ | technique | blood correction | muscle saturation | flip angle calibration or use of adiabatic pulses | nominal acquisition voxel volume (ml) | interpolated voxel volume (ml) | actual volume of acquired signals |
|---|---|---|---|---|---|---|---|---|---|---|---|
| Shivu et al | 2010 | 37 | 48 ± 16 | 2.11 ± 0.57 | ISIS | 17% | n/a | adiabatic pulses | 90 | 90 | 90 |
| Zhang et al | 2010 | 10 | 53 ± 3 | 2.13 ± 0.21 | 2D CSI | 15% | none | none detailed | 48 | 12 | 35 |
| Burkhard et al | 2009 | 8 | 48 ± 13 | 1.54 ± 0.24 | AW 2D CSI | none | none | none detailed | 16 | 4 | 52 |
| Esposito et al | 2009 | 19 | 41 ± 10 | 2.40 ± 0.30 | 3D ISIS | 36% | n/a | calibration + T&M | 294 | 294 | 294 |
| tyler et al | 2009 | 20 | 27 ± 6 | 2.07 ± 0.38 | AW 3D CSI | 11% | yes | flip angle calibration | 5.6 | 5.6 | 39 |
| Hudsmith et al | 2009 | 20 | 28 ± 3 | 2.02 ± 0.43 | AW 3D CSI | 11% | none | none detailed | 15 | 5.6 | 121 |
| Perseghin et al | 2009 | 11 | 25 ± 2 | 1.94 ± 0.36 | 3D ISIS | yes | n/a | adiabatic pulses + T&M | 180 | 180 | 180 |
| Perseghin et al | 2009 | 14 | 45 ± 6 | 1.83 ± 0.27 | 3D ISIS | yes | n/a | adiabatic pulses + T&M | 180 | 180 | 180 |
| Tyler et al | 2008 | 6 | 31 ± 3 | 1.76 ± 0.38 | AW 3D CSI | 11% | none | flip angle calibration | 12.5 | 12.5 | 131 |
| Tyler et al | 2008 | 6 | 31 ± 3 | 1.62 ± 0.22 | AW 3D CSI | 11% | none | flip angle calibration | 12.5 | 12.5 | 131 |
| Beer et al | 2007 | 15 | 58 ± 11 | 1.51 ± 0.32 | 3D CSI | 15% | n/a | flip angle calibration | 25 | 25 | 22 |
| Kostler et al | 2006 | 30 | 41 ± 16 | 1.90 ± 0.50 | 3D CSI | yes | yes | flip angle calibration | 25 | 25 | 25 |
| Heyne et al | 2006 | 20 | 35 ± 11 | 2.07 ± 0.17 | 2D CSI | 15% | none | none detailed | 160 | 40 | 118 |
| Chida et al | 2005 | 13 | 21 ± 1 | 2.96 ± 0.59 | AW 2D CSI | 15% | none | none detailed | 48 | 12 | 199 |
| Hansch et al | 2005 | 20 | 35 ± 11 | 2.07 ± 0.17 | 2D CSI | 15% | none | none detailed | 160 | 40 | 118 |
| Lodi et al | 2004 | 10 | 34 ± 7 | 2.34 ± 0.14 | 1D CSI | 17% | yes | manual tune and match | 512 | 512 | 268 |
| Schneider et al | 2004 | 11 | 52 ± 10 | 1.70 ± 0.30 | 3D CSI | yes | yes | flip angle calibration | 25 | 25 | 25 |
| Diamant et al | 2003 | 12 | 57 ± 7 | 1.88 ± 0.34 | ISIS | 36% | n/a | none detailed | 294 | 294 | 294 |
| Beer et al | 2002 | 10 | 59 ± 15 | 1.59 ± 0.33 | 3D CSI | yes | yes | flip angle calibration | 25 | 25 | 25 |
| Lodi et al | 2001 | 18 | 30 ± 7 | 2.39 ± 0.13 | 1D CSI | 17% | yes | manual tune and match | 512 | 512 | 268 |
| Moka et al | 2001 | 10 | 53 ± 12 | 1.74 ± 0.23 | ISIS | 26% | n/a | none detailed | 75 | 75 | 75 |
| Beer et al | 2001 | 8 | 56 ± 12 | 1.45 ± 0.29 | 3D CSI | 15% | none | none detailed | 25 | 25 | 22 |
| Beyerbach et al | 2001 | 10 | 60 ± 4 | 1.43 ± 0.14 | 2D ISIS | 36% | n/a | adiabatic pulses | 32 | 32.0 | 32 |

*Blood correction given as % of 2, 3-DPG integral representing ATP.*

Tyler et al previously developed and tested a high resolution $^{31}$P MRS acquisition protocol [50] which addresses these challenges of contamination and reproducibility. This protocol has proven reproducibility with good signal to noise when tested in healthy volunteers at rest [50], after dietary intervention [51] and subject to hypoxia [52]. However, with a total $^{31}$P MRS acquisition time of more than half an hour (depending on heart rate), this method has proved unsuitably long for children or symptomatic patients who are less able to lie prone for long periods. In addition, long acquisition times are unsuitable for acquisition during cardiac exercise stress testing, which may potentially unmask or worsen an energetic deficit due to increased physiological demand.

The aim of this study was to develop a $^{31}$P MRS acquisition which was short enough to facilitate scanning highly symptomatic patients or to acquire during exercise stress. Initial proof of principle attempts have been made to acquire data using a short protocol[53], and here a complete protocol for cardiac $^{31}$P MRS ,with improved signal to noise, which takes less than 15 minutes ($^{31}$P MRS acquisition = 8 minutes) is presented. This new protocol is the compilation of key modifications in terms of both acquisition and post processing, which minimise sources of methodological variability, and signal contamination.

The reproducibility and specificity of data acquired using this method was compared with an established high resolution method [50]. The durability and feasibility of this 8 minute cardiac $^{31}$P MRS protocol to assess cardiac exercise stress performed in the magnet is also demonstrated.

# 3.2 Methods

## *3.2.1 Study population and scan preparation*

Healthy volunteers (n = 22; age 42 ± 17 years; 13 male) were recruited for validation of the method, and a separate cohort of healthy volunteers (n = 15; age 40 ± 10 years; 10 male) were recruited for testing the method under exercise stress conditions. All recruits fulfilled the inclusion and exclusion criteria described in chapter 2.

All scans were performed on a Siemens 3 T Tim Trio system (Erlangen, Germany), using a Siemens 1.5 T heart liver coil modified for use at 3 T, consisting of a 26 x 28 cm proton/phosphorus transmit coil and a paired 12 x 15 cm loop and 23 x 12 cm butterfly phosphorus receive coil. Subjects lay prone on the coil, with their left ventricle positioned centrally and at the magnet iso-centre. Coil positioning was confirmed using proton localisation images and subject position on the coil adjusted as required.

## *3.2.2 31P-MRS acquisition protocols*

Pilot images of the vertical long axis, the horizontal long axis and a 3D stack of short axis images were initially acquired.

### *Flip angle calibration*

Eight non-localised inversion recovery spectra, consisting of a 1000 μs hard inversion pulse with inversion delay varied from 0.1 s to 3 seconds, were acquired to measure the flip angle in a phenyl phosphoric acid (PPA) reference fixed inside the radio frequency (RF) coil housing. Using home-written software in Matlab 6.5 (Mathworks, Natick, USA), the

measured flip angle achieved at the PPA reference was combined with a calculated RF field profile of the RF coil and short-axis stack of images to determine the subject specific flip angle at the selected voxel of interest.

## *Chemical Shift Imaging*

All $^{31}$P MRS data was acquired with a three dimensional acquisition weighted chemical shift imaging technique (AW-CSI) [54] with 10 averages at the centre of K-space and ultrashort TE[55] to minimise T2 effects and first order phase artefacts. An optimised RF pulse [50] centred between γ and α ATP resonance frequencies was used to ensure uniform excitation of all spectral peaks. Five Nuclear overhauser effect (NOE) pulses (2.5 ms, 222.2 V separated by 80.5 ms) were used to increase signal to noise (correction factors detailed below). Acquisition matrix was 16 x 16 x 8 for the high resolution reference protocol and 16 x 8 x 8 for the new short protocol. Field of view was 240 x 240 x 200 mm for both protocols. The high resolution acquisition was run with TR dictated by RR intervals whereas the short acquisition was run with TR of 720ms. Both protocols employed two 25 mm saturation bands placed over chest wall muscle; the short protocol included an additional 25 mm saturation band placed over liver.

In both protocols, the CSI grid was placed with a central voxel in the mid-ventricular septum on the first short axis image in which the papillary muscle was visible. The CSI grid was positioned such that the voxel(s) were orientated down the long axis of the intra-ventricular septum, and rotated to maximise coverage of the septal myocardium by either

three high resolution voxels( long protocol) or one low resolution voxel ( short protocol), figure 3.1.

### *3.2.3 Comparison of short protocol with longer, high resolution, reference protocol*

Subjects (n = 22) received both CSI protocols during the same scanning session; the total scan time was approximately 70 minutes. In addition, a subset of 10 subjects had the short, eight minute protocol repeated during the same session for the determination of inter- and intra-subject reproducibility; total scan time approximately 80 minutes.

### *3.2.4 Exercise stress protocol*

Short, 8 minute acquisitions were performed on 15 separate subjects at rest, during exercise and recovery to determine its applicability for measurement of cardiac energetics during exercise stress. Total scan time was approximately 30 minutes. A thin (~2mm), non-slip mat was positioned over the cardiac $^{31}$P coil, upon which subjects lay prone, with elastic straps across the shoulders, lower back and hamstrings to minimise body movement during exercise. A blood pressure cuff was placed on the arm with ECG electrodes on the back and lateral chest wall to improve comfort. Initially, the short protocol was run whilst subjects were at rest. This was immediately followed by repeated flexion of their legs with 2.5 kg weights attached to their ankles for the duration of a second short protocol acquisition. After finishing the exercise acquisition and ceasing exercise, a second 3D, short axis stack of images was acquired to confirm that no movement had occurred as a result of the exercise,

figure 3.3. Exercising was done at rate sufficient to raise the rate pressure product by at least 50%.

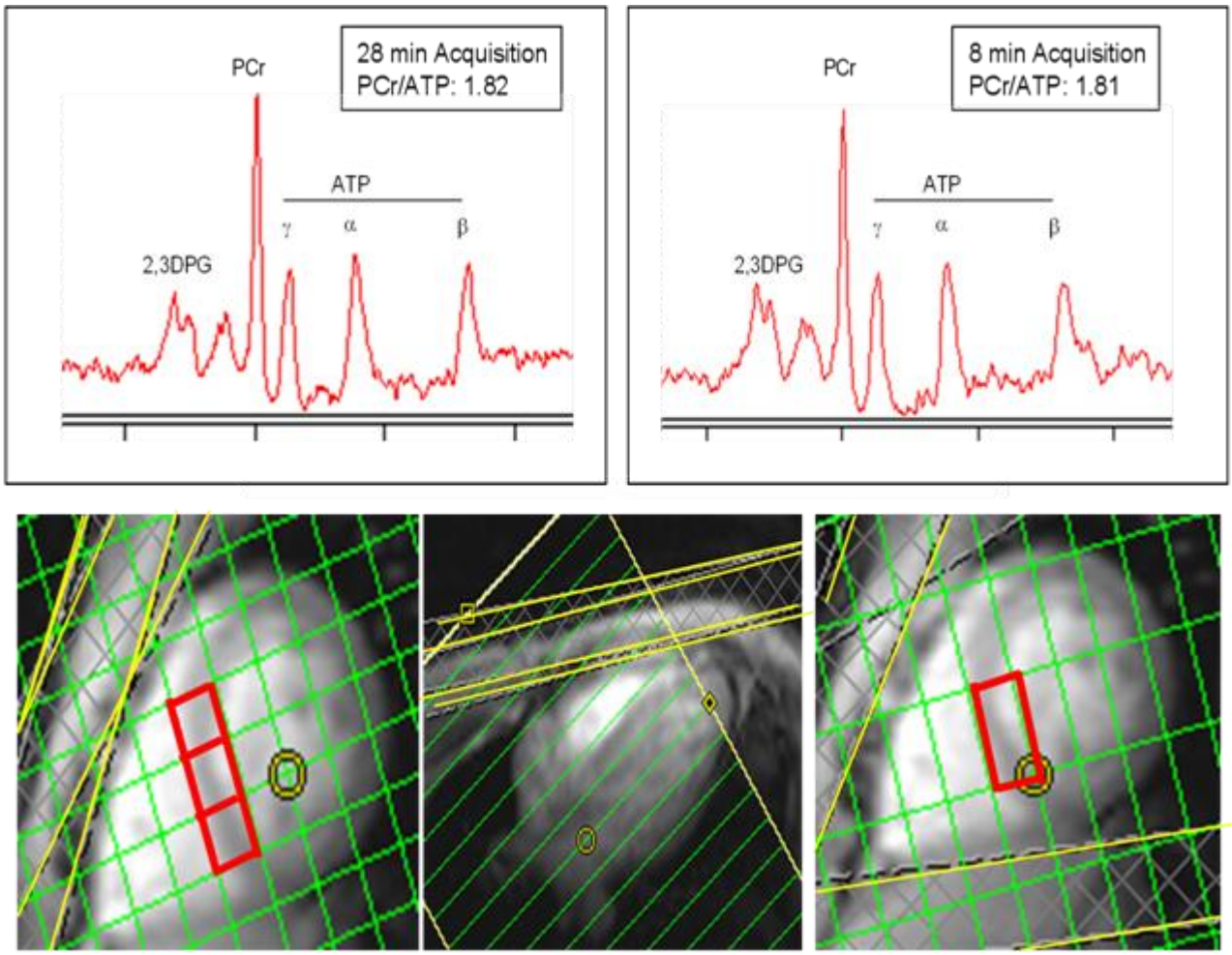



***Figure 3.1:*** *Top) Representative resting spectra from each protocol acquired in one subject at rest (heart rate 60 BPM). PCr (phosphocreatine); 2, 3 DPG (2, 3 diphosphoglycerate); ATP adenosine triphosphate) are indicated. Bottom left) anatomical placement of voxels for long protocol. Bottom right) anatomical placement of voxels for short protocol. Bottom middle) anatomical placement of voxels in long axis view.*

### *3.2.5 Data analysis*

In the longer, high resolution reference acquisition, three voxels were chosen according to the American Heart Association standardised myocardial segmentation model: inter-

ventricular septum anterior, central and inferior. In the short acquisition datasets, one equivalent inter-ventricular voxel was chosen, incorporating the middle region of the septum. Both sets of voxels were chosen from the same slice in the 3D short axis stack.

### *3.2.6 Calibrations and corrections*

Spectra were direct current (DC) corrected and baseline corrected based on the last half of acquired data points. Spectral peaks were imported into jMRUI (Java Magnetic Resonance User Interface [56]) and fitted using the AMARES algorithm (Advanced Method of Accurate, Robust and Efficient Spectroscopic fitting [57]) making use of prior knowledge relating to the relative peak frequencies, amplitudes, phases and , j-coupling patterns.

Spectral peak areas were corrected for the effects of NOE using correction factors determined by prior experiment[50]: NOE correction factors used PCr 0.80, β-ATP 0.88, α-ATP 0.88, γ-ATP 0.79, 2, 3-DPG 0.70. Correction for RF saturation were calculated for each subject using the TR and experimentally determined excitation flip angle at the chosen voxel and T1 values from literature [58]: PCr 3.8 s, γ-ATP 2.4 s, α-ATP 2.5 s, β-ATP 2.7 s, 2,3-DPG 1.39 s, and PDE 1.1 s.

The resulting peak areas of the three ATP signals were averaged and corrected for blood contamination by subtracting 11% of the 2, 3-DPG peak area[8].

### *3.2.7 Statistics*

All data are reported as mean ± standard error. Statistical significance was assessed using a significance level of $p < 0.05$. Bland- Altman analysis was used to test for agreement

between the long and new short protocol as well as for reproducibility of the short protocol. No data acquired during this study was excluded from analysis.

# 3.3 Results

## *3.3.1 Flip angle calibration*

The average flip angle measured at the inter-ventricular septum was 31.8° ± 5.4° over all subjects studied.

## *3.3.2 Comparison of short acquisition with longer, high resolution, reference acquisition*

CSI acquisitions were compared by assessing the absolute difference between PCr/ATP values measured by both CSI protocols performed on 22 healthy volunteers.

The average acquisition time for the high resolution protocol (cardiac gated) was 29 ± 0.85 minutes. The short acquisition was fixed at 8 minutes.

The average PCr/ATP value derived from the spectra acquired using the short protocol was 1.84 ± 0.07 and from the high resolution reference protocol was 1.78 ± 0.06 , demonstrating no significant difference ($p = 0.30$). Figure 3.1 shows example spectra acquired from one subject, using both protocols.

The absolute difference between PCr/ATP values acquired via each protocol for each subject was 0.22 ± 0.04 (or 11%). Bland-Altman analysis ( figure 3.2) demonstrates limits of agreement ranging from -0.64 to 0.51 and a mean difference between methods of only

0.07 indicating that these methods yield a measure of PCr/ATP within agreement of one another with little systematic bias.

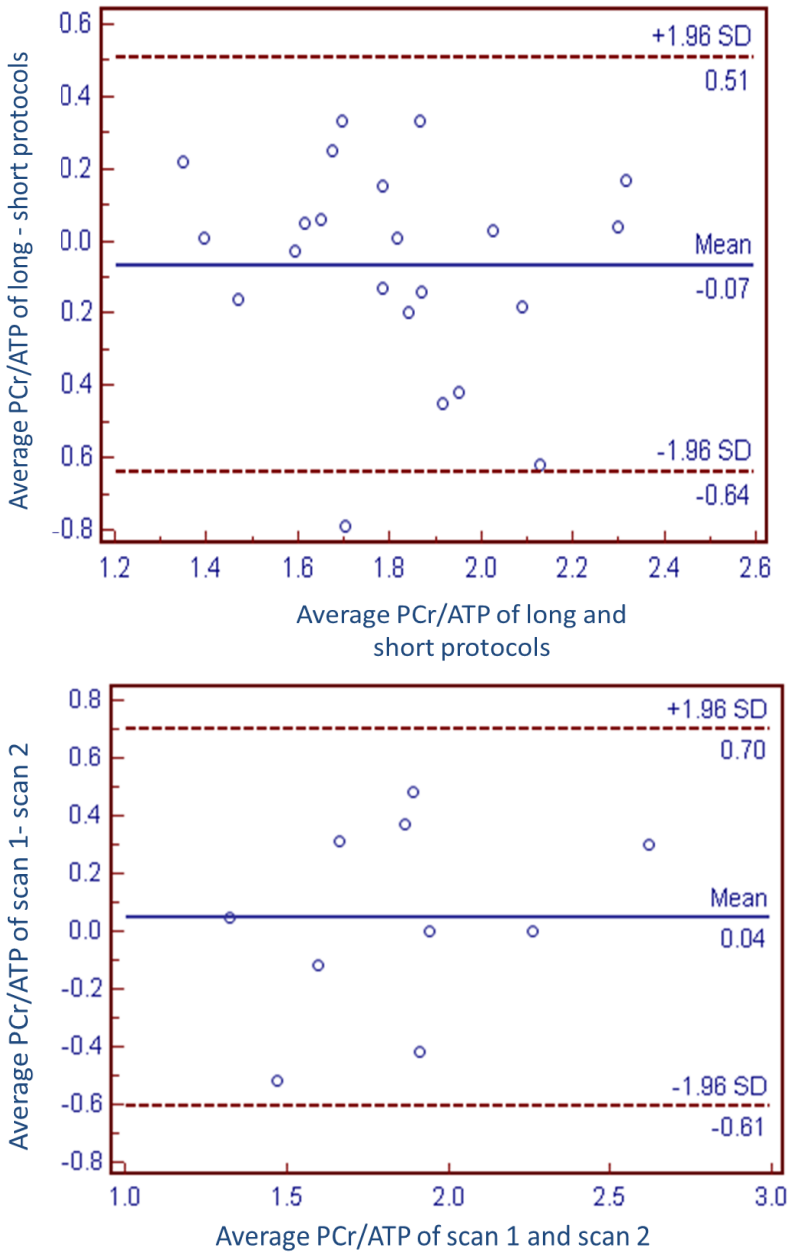



***Figure 3.2**: Top)Bland Altman plot of PCr/ATP ratio derived from data acquired with the high resolution protocol ('long') versus the 8 minute protocol ('short'). Bottom) Bland Altman plot showing the intra subject repeatability of the short acquisition method performed twice in each subject.*

### *3.3.3 Assessment of Reproducibility*

The inter-subject variability in the value PCr/ATP measured using the short protocol performed on 22 volunteers was of 17.5%, compared to 15.2% achieved using the high resolution reference protocol.

The intra-subject reproducibility of the eight minute protocol was assessed by consideration of the absolute difference between short acquisitions repeated on 10 healthy volunteers. The average PCr/ATP value measured on scan 1 was 1.88 ± 0.14 and scan 2 was 1.83 ± 0.11 ($p>0.8$). The absolute difference was 0.23 ± 0.06. A Bland-Altman plot (figure 3.2) showed a mean difference between measurements of 0.04 with levels of agreement ranging from -0.61 to 0.70.

### *3.3.4 Exercise stress*

A separate cohort of 15 healthy volunteers underwent the exercise stress protocol. A short axis image was acquired before and after exercise with a grid placed on them to determine if there had been any significant movement resulting from exercise. There was no demonstrable movement by any subject (figure 3.3), thus no data were discarded.

The average rise in rate pressure product during exercise was 80% ± 7%. The average PCr/ATP ratios were taken at rest: 1.93 ± 0.06; exercise 1.97 ± 0.08; recovery 1.96 ± 0.12. There was no significant change with exercise in this healthy population. An example is shown in figure 3.3.

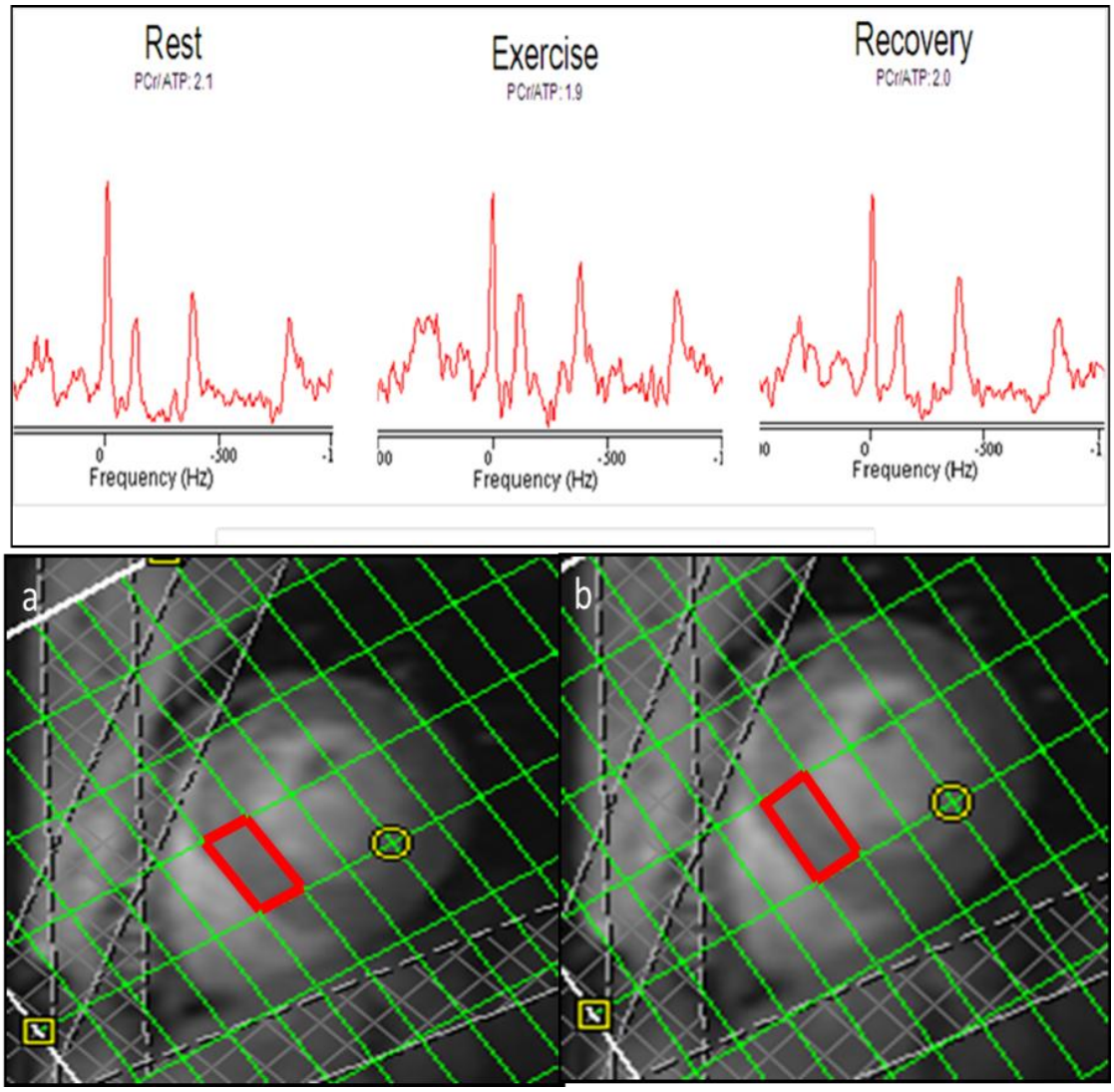



***Figure 3.3****: top) Representative spectra acquired during rest, exercise and recovery. Bottom) anatomical images with spectroscopy grid overlay used to confirm voxel position before and after exercise.*

# 3.4 Discussion

This work presents a short cardiac $^{31}$P MRS spectroscopy protocol (8 minute protocol, total scan time less than 15 minutes), which yields values of PCr/ATP matching those acquired

using a high resolution reference protocol requiring an average of 29 ± 4 minutes (total scan time approximately 40 minutes) for this cohort of volunteers.

The inherently long acquisition times associated with well resolved cardiac $^{31}$P MRS often renders the method unfeasible for studies of highly symptomatic patients, children, or for the application of cardiac exercise stress testing. This is particularly problematic for patients with low heart rates due to beta blockers.

A common approach to reducing $^{31}$P MRS acquisition times is to reduce the spatial resolution (increase voxel size). The pitfall of this approach, however, is the consequent reduction of specificity of cardiac signal acquisition, resulting in contamination from neighbouring tissues.

It is well recognised that imaging techniques can suffer significantly with signal contamination arising from adjacent voxels. The true spatial extent of information contributing to a voxel is described by the point spread function (PSF). The PSF of a standard CSI voxel is illustrated in one dimension in figure 3.4, which shows the inherent side lobes associated with the nominally selected voxel volume. These side lobes contribute information to the spectrum from distant regions extending in three dimensions around the nominal voxel location. The chest wall skeletal muscle is in the most sensitive region of the RF coil and side lobes in this area pick up signal which is correspondingly enhanced by this high receive sensitivity. Calculation of the PSF takes into account acquisition method, matrix size and field of view and the nominal voxel size is then defined as the width of this PSF at half maximum amplitude. Thus, when considering the nominal

voxel as displayed by the console, the presence of such potential for contamination is concealed.

Contamination from PSF lobes in chest muscle, which lies in the most sensitive region of a surface coil, yield an inaccurately high PCr/ATP due to the higher skeletal muscle PCr/ATP (~4:1) compared with that of myocardium. This can have the unfortunate effect of apparently improving the signal to noise (SNR) of the measurement because the contaminant skeletal muscle signal is indistinguishable from the myocardial signal. Conversely a voxel contaminated with liver will yield a low apparent PCr/ATP because liver contains no PCr.

Nominal and true voxel sizes calculated for a selection of published data from the last 10 years are summarised in Table 1, which illustrates the often wide spread discrepancy between nominal and true voxel size pointing to the need in many cases for additional measures to prevent contamination from neighbouring regions.

Acquisition Weighting (AW) [54] increases the number of acquisition averages acquired in the middle of k-space to substantially suppress the appearance of these side lobes. The effect of AW on the PSF is illustrated in figure 3.5; whilst it appears to decrease the sharpness of the edge of the voxel, thereby increasing the central volume, most importantly, it substantially improves the spatial specificity of the true voxel by removing the side lobes.

In addition the consequences of true voxel dimensions can be reduced via the use of saturation bands issued over neighbouring tissues [59] (yellow lines in figure 3.1). This essentially saturates any signal from the tissue covered by the saturation bands.

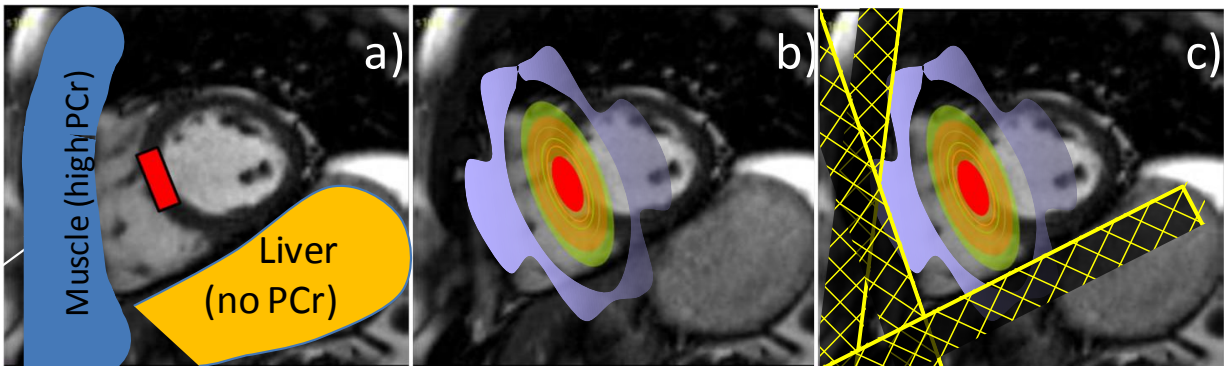



***Figure 3.4**: a) Nominal voxel is marked by the red rectangle placed in the septum. Voxel bleed potentially introducing chest wall muscle signal will increase the apparent PCr/ATP whereas liver contamination decreases PCr/ATP. (b) The true volume of a voxel, as described by the point spread function (PSF) (contours indicate signal sensitivity decreasing red to purple) is greater than that described by the nominal voxel volume calculated via matrix size and field of view alone. (c) Potential for contamination by neighbouring tissues can be minimised by careful voxel placement in combination with use of saturation bands (yellow cross hatched bars) to obliterate skeletal muscle and liver signals.*

This protocol has adopted a reduced resolution approach to achieve an acquisition time of eight minutes (nominal voxel volume 11.2 ml, true voxel volume is 93 ml) but it still maintained myocardial specificity by using acquisition weighting, and by careful placement of muscle and liver saturation bands to reduce the potential for contamination still further. The average PCr/ATP values derived from the short 8 minute spectra was 1.83 ± 0.32 which concurs with data acquired with the high resolution reference protocol, a spectral acquisition which is at least three times longer, (PCr/ATP = 1.78 ± 0.27, nominal voxel volume 5.6 ml, true voxel volume 39 ml).

This parity indicates that this combination of methods to suppress and minimise voxel contamination are sufficient to negate any elevated potential for contamination resulting from increased voxel size.

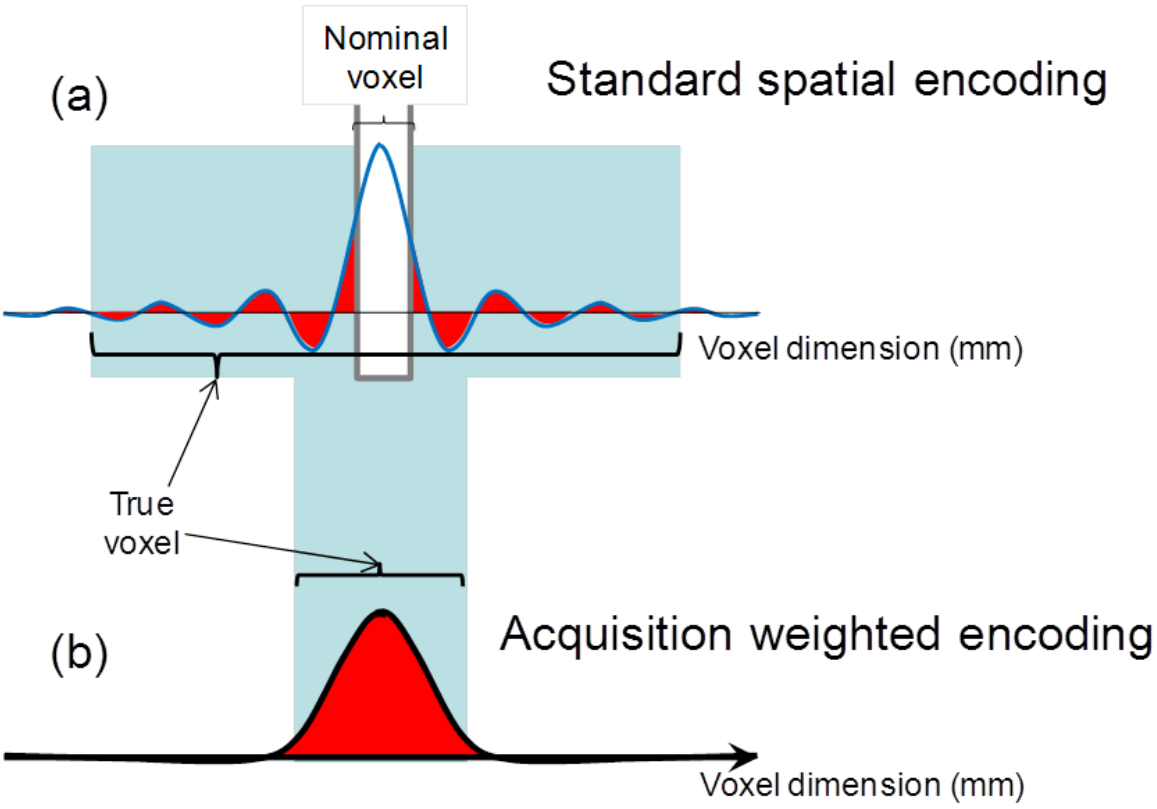



***Figure 3.5**: The point spread function (PSF) describes the signal magnitude versus distance which defines the spectroscopic voxel. (a) represents the PSF of one voxel dimension acquired using standard spatial encoding. (b) represents the PSF of the same voxel acquired using acquisition weighting: effectively suppressing the amount of distant contamination, broadening the principle lobe but improving voxel specificity.*

### *3.4.1 Assessment of reproducibility*

Information about reproducibility is necessary when making decisions about cohort sizes and for assessing the statistical power of results. However, there are surprisingly few published assessments of reproducibility in cardiac $^{31}$P MRS [50, 60]. In addition to biological

variability; variation in voxel placement and coil loading can all degrade the reproducibility of cardiac $^{31}$P MRS and hence degrade the statistical power of data.

Typically, clinical coils have fixed tune and match capacitance for maximum transmit/receive sensitivity to an average body. Larger or smaller bodies, differing BMI, muscle to fat ratio, even variations in body position will load the electrical properties of the coil differently, resulting in an attenuation of transmitted power. Surface coils are particularly susceptible to differences in coil loading by different people, body composition or position and the effect of this is illustrated in figure 3.6. Deviations from maximum transmit/receive sensitivity results in a flip angle achieved at the heart which is lower than the nominal flip angle displayed on the console. Low flip angle reduces TR related signal saturation effect, which is corrected for post-acquisition. If nominal flip angle is assumed for saturation correction any loading effects on the coil manifests as an apparently increased PCr/ATP.

In this protocol, this effect is corrected for via calculation of a subject specific flip angle at the voxel of interest. The addition of an inversion recovery scan to measure the inversion profile of the phosphorus contained in a vial of PPA fixed inside the coil housing is used to calibrate the person to person coil loading effects on flip angle. Coil loading effects may also be avoided by application of high power adiabatic pulses or the use of coils which can be tuned and matched for each scan.

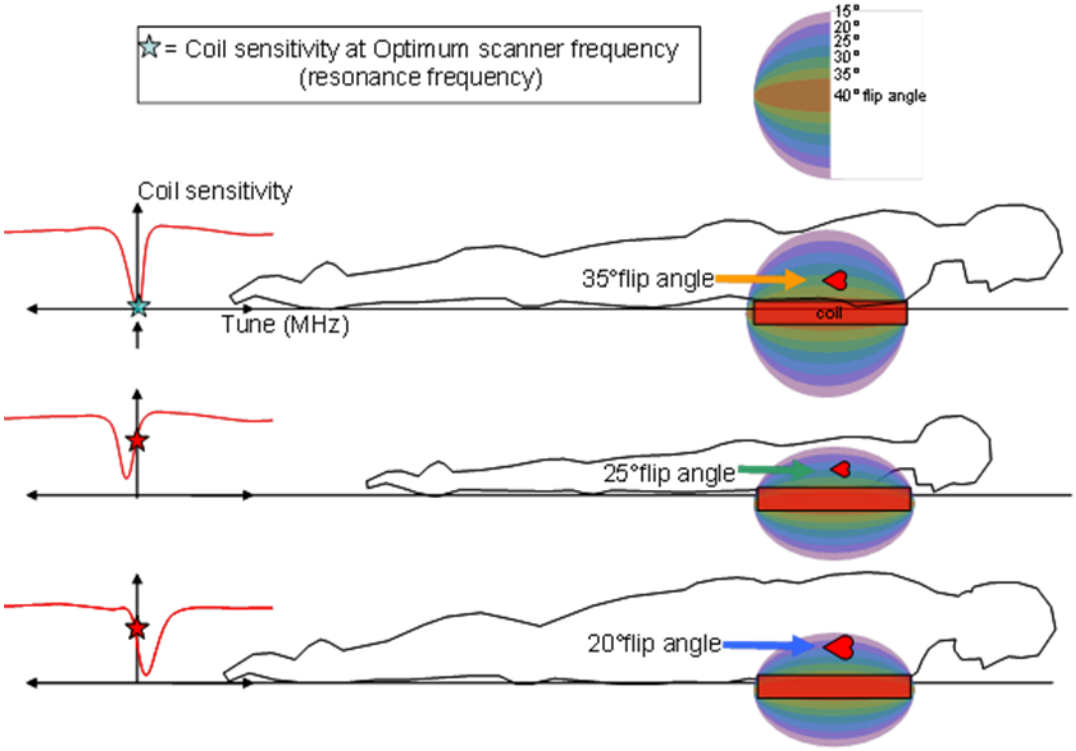



***Figure 3.6:*** *Mismatch between nominal and true flip angle is due to coil loading differences. Coils are tuned to optimum sensitivity for a typical BMI and muscle to fat ratio, subjects who are smaller or larger than this can bring about a decrease in transmitted power at the voxel of interest which reduces the actual flip angle achieved at the mid ventricular voxel. This results in a false increase in apparent PCr/ATP if the nominal flip angle is used for calculation of saturation correction. The actual flip angle can be calculated if a flip angle map is generated for each subject.*

In this study, a 17% variation in the flip angle achieved at the inter-ventricular septum is present in this group of normal volunteers with the addition of a short flip angle calibration scan to the MRS protocol. This aspect of variability is removed via the calculation of a subject specific flip angle correction and used in correction for partial saturation of the acquired metabolite signals. The inter-subject variability of the resulting PCr/ATP was 17.5% which compares favourably with previously reported variability of 18% [50] (high resolution 3D-CSI) .

### *3.4.2 Exercise protocol*

No significant change in cardiac energetics was observed as a result of physiological exercise in this group of normal volunteers; this reflects other published cardiac $^{31}$P-MRS exercise stress results generated via hand grip exercise [61-63] and leg exercise [53].

Hand grip exercise, averages a small increase in rate pressure product of 30% (rest : 9600 ± 2800 mmHg*beats/min, exercise : 12600 ± 3700 mmHg*beats/min [61]; rest : 7901 ± 1468 mmHg*beats/min, exercise: 10124 ± 2147 mmHg [63]). The effective working muscle mass is greater with lower limb versus upper limb exercise, and is better able to produce a substantial increase in RPP. Lower limb exercise is, however less popular for magnet based studies because of the increased chance of movement and corresponding introduction of noise and potential for movement of voxel location.

In this study, subjects were able to maintain an 84% increase in RPP, similar to a previous leg exercise $^{31}$P MRS protocol [53]. Non-slip surfaces combined with elastic strapping minimised chest movement which might potentially result from of the leg exercises. This was confirmed by imaging performed before and after exercise. No data required exclusion from this study for reasons of movement or SNR, and the protocol was well tolerated by all subjects.

## 3.5 Conclusion

To my knowledge, this is the shortest cardiac $^{31}$P MRS protocol that effectively addresses issues of contamination and signal distortion, for the generation of high quality,

reproducible and uncontaminated spectra. This short protocol (8 minute acquisition time, < 15 minute scan time) utilizes acquisition weighting and saturation bands over neighbouring skeletal muscle and liver to prevent signal from non-myocardial tissue from contributing to the spectrum. In addition, post processing correction for subject specific flip-angle variation and corresponding saturation effects, blood contamination, and NOE, make this a robust protocol, producing high quality, reproducible and uncontaminated spectra.

This short protocol would be useful for symptomatic patients and for $^{31}$P MRS measurements during exercise and would have widespread potential for clinical application to the study of cardiac disease.

# Chapter 4
# $^{31}$ P MRS Analysis development: Improved fitting of 2, 3 DPG

# 4.1 Introduction

$^{31}$P MRS has become increasingly important in biomedical research because of its ability to measure *in vivo* biochemical information. Accurate and efficient data post processing is essential. However, spectral analysis can be problematic due to low signal to noise. This is due primarily to the low sensitivity of MRS to the $^{31}$P nucleus (molar receptivity is 1/14 that of proton) coupled with the low natural concentration of $^{31}$ P biochemical compounds.

The content and accuracy of acquired spectra, directly corresponds with the accuracy and reliability with which the metabolite levels can be measured. The $^{31}$P MRS method described in Chapter 3 makes attempts to optimise signal to noise ratio in order to provide as accurate a measurement in a clinically appropriate time frame. The work in this chapter is centered on improving the "fit" of the spectral information during post processing.

The acquired spectra are used to determine relative concentrations of high energy phosphate metabolites in the myocardium. A metabolite concentration is estimated by the area under the curve of its spectral peak. This estimation of resonance area is related to the number of matching nuclei resonating in the volume (i.e. voxel) of interest and hence represents its molecular concentration. However, before spectral quantification, the data are imported into jMRUI (Java Magnetic Resonance User Interface[56]) for phasing and frequency alignment (PCr is set as zero Hz reference), peaks are then fitted using the AMARES (Advanced Method of Accurate, Robust and Efficient Spectroscopic fitting[57]) algorithm making use of biophysical prior knowledge relating to the relative peak

frequencies, coupling patterns, relative peak amplitudes, relative phases and assumed Lorentzian lineshapes. Corrections performed include:

1. DC correction: DC is a direct current (DC) artefact, arising from an offset voltage in the signal detection amplifiers, it manifests as a peak at zero frequency and is removed by subtracting this constant amplifier signal.

2. Baseline correction based on the last half of acquired data points: There is a time delay between nuclei excitation and the beginning of data collection; as a result the initial points of data are lost. Therefore, the transformation of the data (collected in the time domain) into the frequency domain, effectively loses the lowest frequency components. This is minimal in the sequence described in chapter 3 as it uses ultrashort echo times; however the last half of acquired data is used to estimate the missing data points.

3. Spectral peak areas are corrected for the effects of NOE using correction factors determined by prior experiment[50]: NOE correction factors used PCr 0.80, β-ATP 0.88, α-ATP 0.88, γ-ATP 0.79, 2, 3-DPG 0.70. The Nuclear Overhauser effect, describes the transfer of magnetization to the $^{31}$P nuclei by its surrounding hydrogen atoms. This transfer of nuclear spin increases the visibility of $^{31}$P nuclei; however, the magnitude of signal enhancement differs for nuclei in different molecular configurations and hence is corrected for on a per nuclei basis using results of prior experiment.

4. Peak areas are corrected for RF saturation using the TR, calculated excitation flip angle at the chosen voxel and T1 values from literature [58]: PCr 3.8 s, γ-ATP 2.4 s, α-ATP 2.5 s, β-ATP 2.7 s, 2,3-DPG 1.39 s, and PDE 1.1 s (described in chapter 3)

5. Blood correction: The resulting peak areas of the three ATP signals are averaged and corrected for blood contamination by subtracting 11% of the 2, 3-DPG peak area[8].

$^{31}$P MRS of the human heart is usually contaminated by signals that originate from the phosphate compounds in blood i.e. 2, 3 DPG and ATP. Blood has high ATP content but no PCr. Therefore, within the spectral acquisition voxel, measured ATP is a combination of ATP from blood and myocardium.

The amount of blood contamination in the voxel is estimated by the presence of 2,3 DPG[64]. It is therefore crucial to fit 2,3 DPG with highest possible accuracy, as estimating it with poor confidence i.e. large standard deviations, would lead to a propagation of errors in calculating the amount of ATP that arises from blood, ultimately affecting the confidence in the measured PCr/ATP of the myocardium.

AMARES software is used extensively in MRS for semiautomatic curve fitting. It is based on non-linear least squares fitting, figure 4.1. It applies prior knowledge about the various $^{31}$P nuclei , this include frequencies, phases, line widths and amplitudes[56] and provides a mean and coefficient of variance measure for each $^{31}$P nucleus in the sample. Incorporation of prior knowledge is useful as it guides the curve fitting process and allows for the software to measure each nucleus with more confidence and hence improved coefficient of variance

for each nucleus. However, since it reduces the number of free parameters, it must be accurate, in order to prevent the introduction of bias.

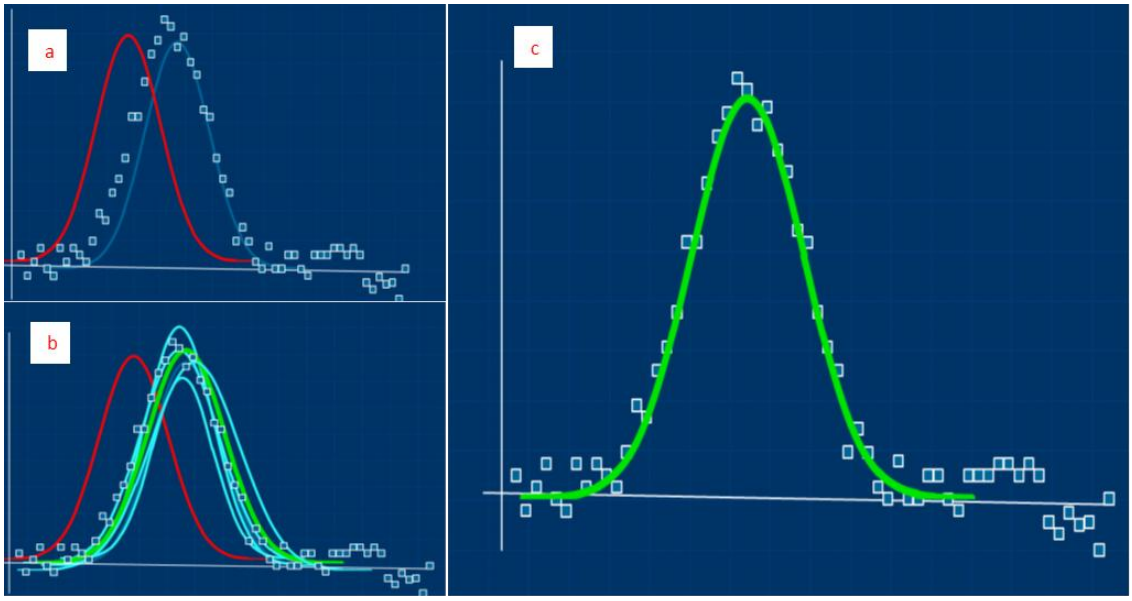



***Figure 4.1:*** *Non-linear least squares fitting to a noisy Gaussian function. Empirical, raw data are represented as blue squares, a and b show multiple curves being fitted onto the raw data based on knowledge of e.g. amplitudes, frequencies and line widths. The final fit, c, is the best fit (least sum of squares difference).*

The 2, 3 DPG molecule has 2 phosphorus atoms, figure 4.2. Information about the amplitude, line widths, relative phases and frequency are provided to AMARES for each $^{31}P$ nucleus.

Once the 2, 3 DPG resonances are integrated in AMARES, 11% of this value is deemed to represent the amount of blood ATP which is contributing to the overall ATP signal. Therefore, the total ATP resonance area is reduced by 11% of the 2, 3 DPG resonance area. This is based on experiments previously done on human blood from normal volunteers[8].

The remaining ATP is therefore arising from the myocardium and is used in the final calculation of the PCr/ ATP ratio.

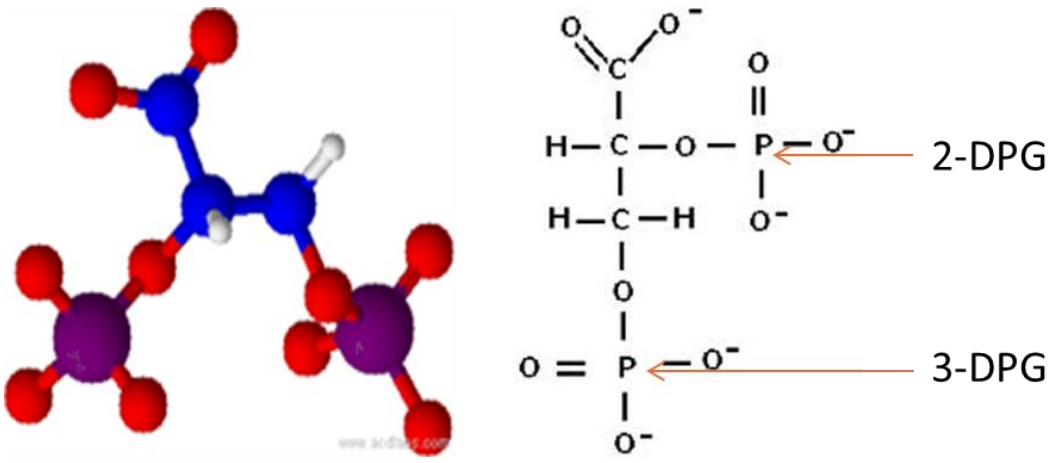



***Figure 4.2****: Molecular structure of 2, 3 DPG, (adapted from Wikipedia)*

The aim of this work was to produce a more accurate fitting of the 2, 3 DPG signal by altering the prior knowledge given to the curve fitting post processing software, AMARES.

Hence, in this study, I present an improved method for fitting the 2, 3 DPG signal in acquired cardiac phosphorus spectroscopy. The hypothesis is that this will yield particular improvements in the quality of the fitting of spectra acquired in subjects with cardiac hypertrophy where the blood signal is weak due to little blood contamination within the voxel.

# 4.2 Method

## *4.2.1 New Prior Knowledge development for 2, 3 DPG*

An extensive review of the literature for biochemical information about 2, 3 DPG was employed to guide changes to the existing prior knowledge for 2, 3 DPG.

## *4.2.2 Testing new Prior knowledge*

### *Simulated data*

Sixteen cardiac $^{31}$P spectra were created in jMRUI simulation package using the parameters in table 4.1. All simulated spectra had a PCr/ATP ratio fixed at 2.00 (PCr =2.00; ATP=1.00, after blood correction). All simulated datasets had both 20% and 40% noise added to them. The original and the new 2, 3 DPG fitting prior knowledges were applied to the each simulated dataset in both categories of noise. The 2, 3 DPG fitting is the only difference in the processing of this data.

### *Patient data*

Data from 8 HCM, 8 DCM and 8 normal controls were fitted in AMARES using both sets of 2, 3 DPG prior knowledge. All data were corrected for NOE, saturation and blood.

All data are presented as mean± standard error. In both simulated and patient data, the coefficient of variance of the 2,3 DPG fitting in AMARES as well as the eventual PCr/ATP ratio using both prior knowledges are compared.

***Table 4.1**: Values used in jMRUI simulation package to create simulated data with both 20% and 40% synthetic random noise added to each of the 16 simulations.*

| Peak number | Peak name | Amplitude | | Corrected for 0.8s TR, 27.61° flip angle, NOE | Frequency (Hz from PCr) | Line-width (Hz) |
|---|---|---|---|---|---|---|
| | | Per peak | Sum of Peaks | | | |
| 1 | β-ATP1 | 0.110 | 0.438 | 1.11 blood corrected =1.00 | -823.8 | 35 |
| 2 | β-ATP2 | 0.219 | | | -808.8 | 35 |
| 3 | β-ATP3 | 0.110 | | | -793.9 | 35 |
| 4 | α-ATP1 | 0.278 | 0.555 | 1.11 blood corrected =1.00 | -384.0 | 35 |
| 5 | α-ATP2 | 0.278 | | | -368.0 | 35 |
| 6 | γ-ATP1 | 0.254 | 0.508 | 1.11 blood corrected =1.00 | -127.7 | 35 |
| 7 | γ-ATP2 | 0.245 | | | -112.7 | 35 |
| 8 | PCr | 0.775 | 0.775 | 2.00 | 0.3 | 35 |
| 11 | 3-DPG | 0.330 | 0.55 | 0.95 (corr. to 10% blood) | 275.2 | 100 |
| 12 | 2-DPG | 0.220 | | | 319.2 | 100 |

# 4.3 Results

## *4.3.1 New Prior Knowledge for 2, 3 DPG*

The following amendments were made (table 4.2):

1. **Amplitude estimate**: The overall, integrated intensity of each of the phosphorus nuclei in 2, 3 DPG should be identical as they arise from the same molecule. However, in fitted, high resolution blood spectra it has been noted that the 3-DPG is typically 20% larger than the 2-DPG[64, 65]. This is likely due to relaxation effects. We therefore provide this information to AMARES by fixing the amplitude estimates, making 2DPG fixed to 80% of 3 DPG. Previously they were both independently estimated (figure 4.3).




***Figure 4.3****: Green arrow points to 2 DPG; blue arrow to 3 DPG. In the original fitting, note the great disparity in the sizes of these peaks even though the integration of these peaks should be roughly equal as they arise from the same molecule. Allowing AMARES to estimate these peaks particularly if there is noise in that area of the spectrum can lead to inaccuracies. With the new fit, 2 DPG=0.8x 3 DPG, AMARES can now fit these nuclei with more confidence.*

2. **Frequency Constraints**: The $^{31}P$ chemical shifts of 2, 3 DPG is sensitive to the pH of the local biochemical environment. Hence the resonance frequencies of the $^{31}P$ nuclei in 2, 3 DPG differ within a range of physiological pH. Experiments conducted on normal blood as well as sickle cell disease have determined the chemical shift of 2,3 DPG with intracellular pH changes[66, 67],figure 4.4. We have used this characteristic of 2, 3 DPG to provide AMARES with more information about the limited range of physiological resonance frequencies of 2 DPG and 3 DPG may possess.

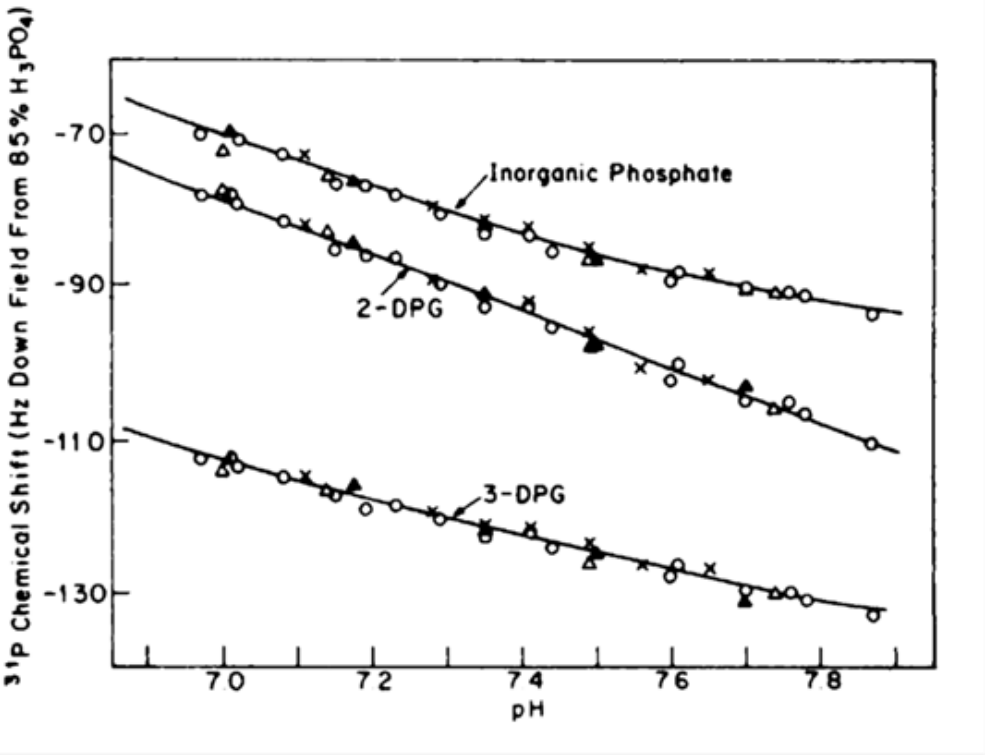



***Figure 4.4:*** *Experimental data on human blood shows that 2 DPG and 3 DPG resonant at differing frequencies but still within a narrow range at phsiological pH[67].*

3. **Linewidth**: Spectral line width represents transverse relaxation rates. The observed linewidth in vivo is largely dominated by magnetic field inhomogeneity. However, in low SNR spectra, we have noted the tendency for peaks to be fit with unfeasibly broad or narrow widths, which brings about an unphysiological outcome with exceptionally high standard deviation. For this reason, the linewidth is fitted with soft constraints encompassing the frequency range that 2- and 3-DPG nuclei possess, within a physiological pH range.

***Table 4.2:*** *A summary of the differences between the original and new prior knowledge for 2, 3 DPG.*

| | **Parameter** | **OLD Prior Knowledge** | **New Prior Knowledge** |
|---|---|---|---|
| 2 DPG | Amplitude estimate | estimate | Fixed 3DPGx0.8 |
| | Relative Phase | Fixed 0 | Fixed 0 |
| | Line Width | estimate | 20-100 |
| | Frequency | Soft constraint | 5.01-6.01 |
| | Shape | Lorentzian | Lorentzian |
| | **Parameter** | **OLD Prior Knowledge** | **New Prior Knowledge** |
| 3 DPG | Amplitude estimate | estimate | estimate |
| | Relative Phase | Fixed 0 | Fixed 0 |
| | Line Width | estimate | 2 DPGx1 |
| | Frequency | Soft constraint | 6.02-6.81 |
| | Shape | Lorentzian | Lorentzian |

### 4.3.2 Simulated Data

The PCr/ATP ratio was fixed at 2.00 for the simulated data. For the data using 20% noise, there were no differences in the mean and standard deviations of the PCr/ATP ratios calculated with the original ( 2.04±0.03) and new 2,3 DPG fit ( 2.02±0.03, P=0.4), figure 4.5. However, in the datasets with 40% noise, both the mean and standard deviations of the PCr/ATP ratios using the original 2,3 DPG fit, were significantly higher than with using the new 2,3 DPG fit, ( original fit: PCr/ATP 2.77 ± 0.25; new fit: PCr/ATP 2.33 ±0.08, P<0.05, figure 4.6). The mean difference of the measured PCr/ATP ratio and the actual ratio of 2.00 was 0.77±0.25 for the original fit and 0.33±0.11 for the new fit, P=0.02.

With 40% noise, the coefficient of variation, COV, for the 2,3 DPG fit was significantly improved with the new fitting, COV 24%, compared to the original, COV 48%, P= 0.02. There was no difference in the COV using both fits in the 20% noise category, (8% for both new and original 2, 3 DPG fit).

### 4.3.3 Patient Data

In this population, there was no significant difference in the mean PCr/ATP with the different prior knowledges (original fit: HCM 1.96±0.13, DCM 1.47±0.07, normal 2.26±0.08; new fit: HCM 1.80±0.08, DCM 1.51±0.05, normal 2.22±0.07, P>0.1). However with the new prior knowledge, there was a substantial improvement in the coefficient of variance of the 2, 3 DPG fit in all groups, (original fit vs. new fit: HCM 24% vs. 15% P<0.005; DCM 21% vs. 15% P=0.03; normal controls 23% vs. 15% P<0.0005, figure 4.7).This translated into a

reduction in the standard deviations of the PCr/ATP measurements in all 3 groups. An example of spectra in HCM is shown in figure 4.9.

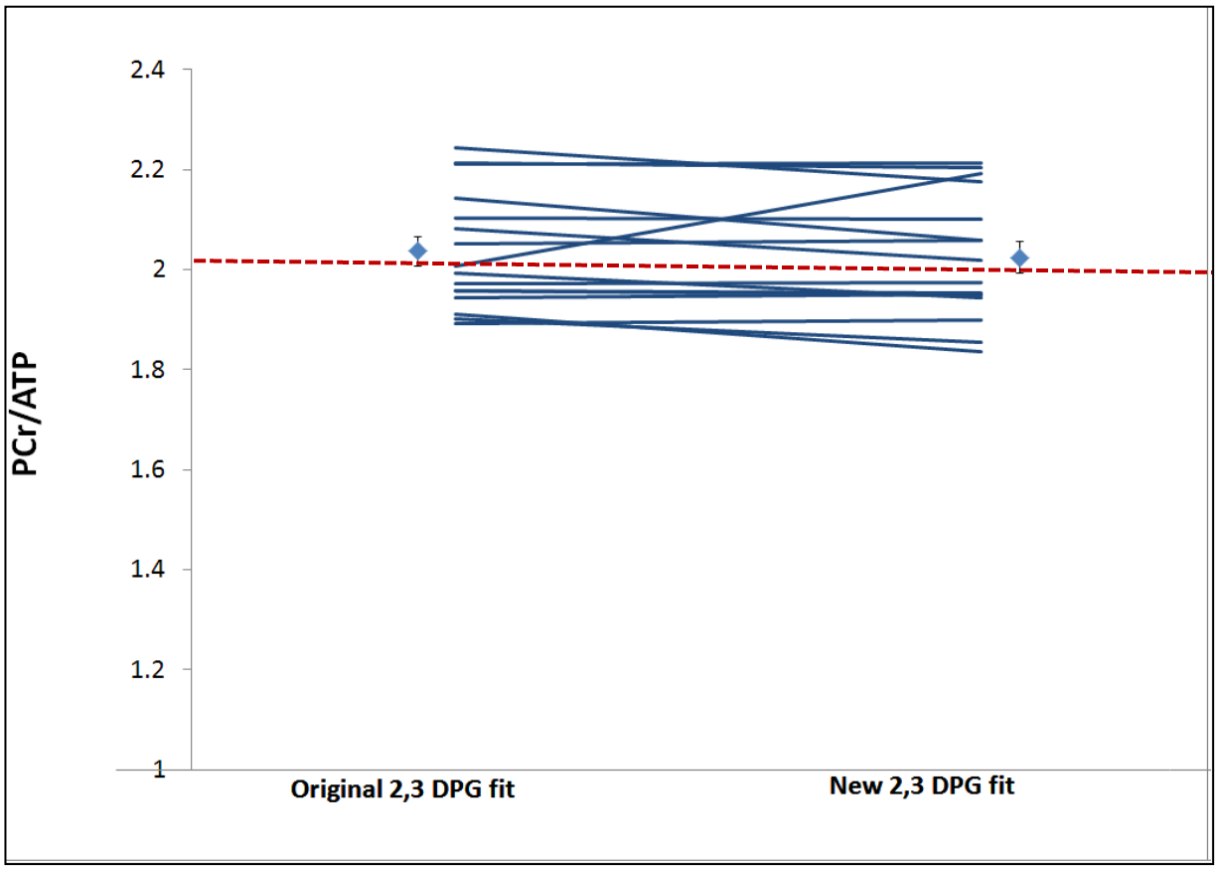



***Figure 4.5*** *Simulated data with* ***20%*** *noise using the original and new 2, 3 DPG fits. Data is mean ±standard error. Red line represents true PCr/ATP.*

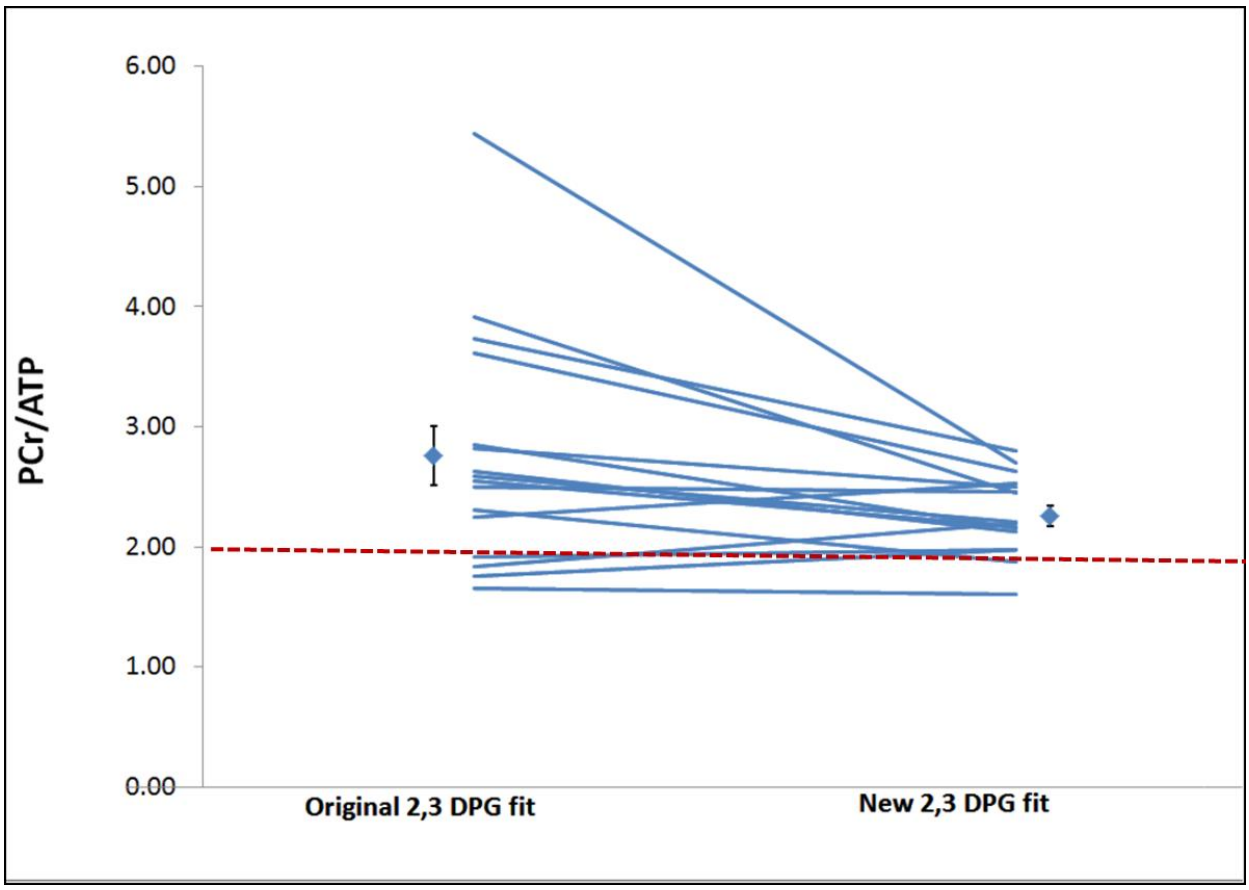
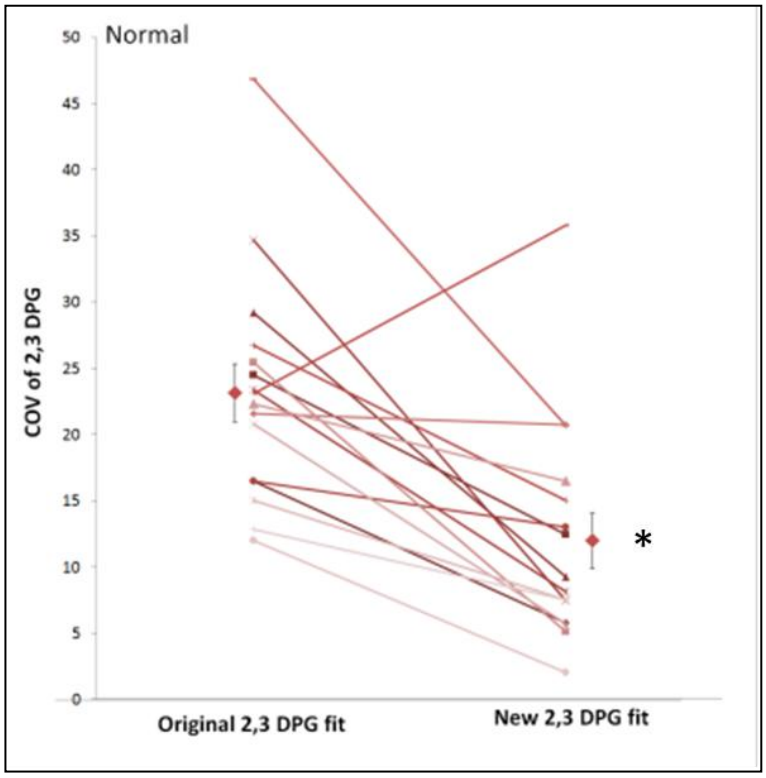
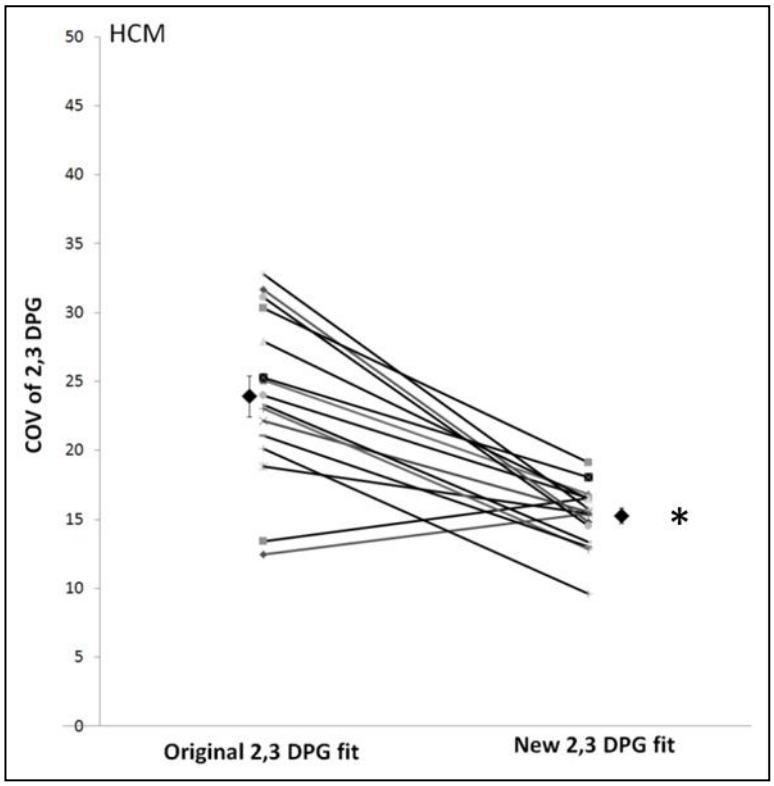



***Figure 4.6**: Simulated data with **40%** noise using the original and new 2, 3 DPG fits. Data is mean ±standard error. Red line represents true PCr/ATP.* p<0.05*


Normal
COV of 2,3 DPG
50
45
40
35
30
25
20
15
10
5
0
*
Original 2,3 DPG fit
New 2,3 DPG fit


HCM
COV of 2,3 DPG
50
45
40
35
30
25
20
15
10
5
0
*
Original 2,3 DPG fit
New 2,3 DPG fit

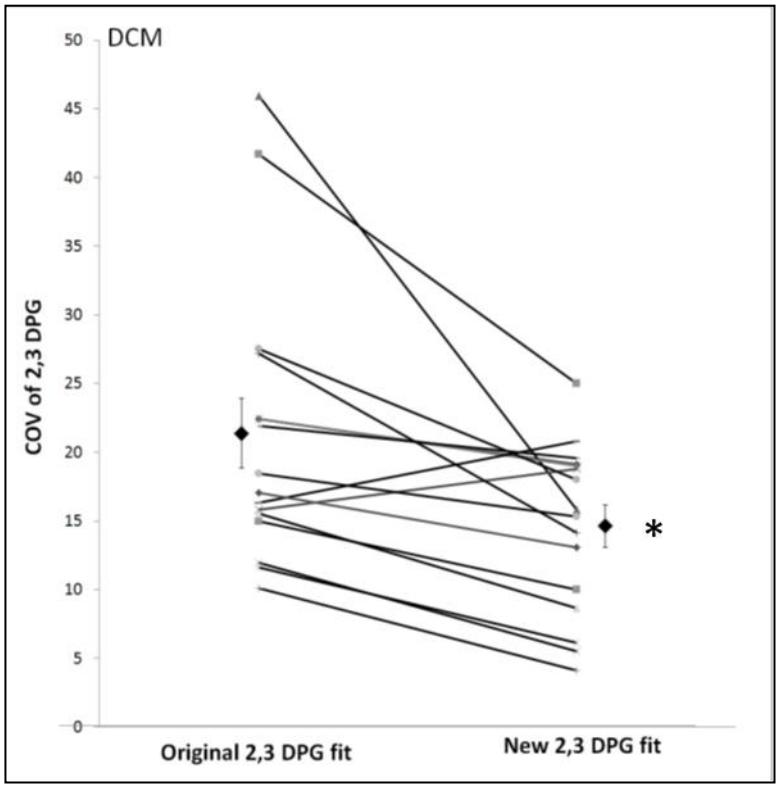



***Figure 4.7:*** *COV of 2,3 DPG from normal, HCM and DCM using the original and new 2, 3 DPG fits. Data is mean ±standard error.* p<0.05.*

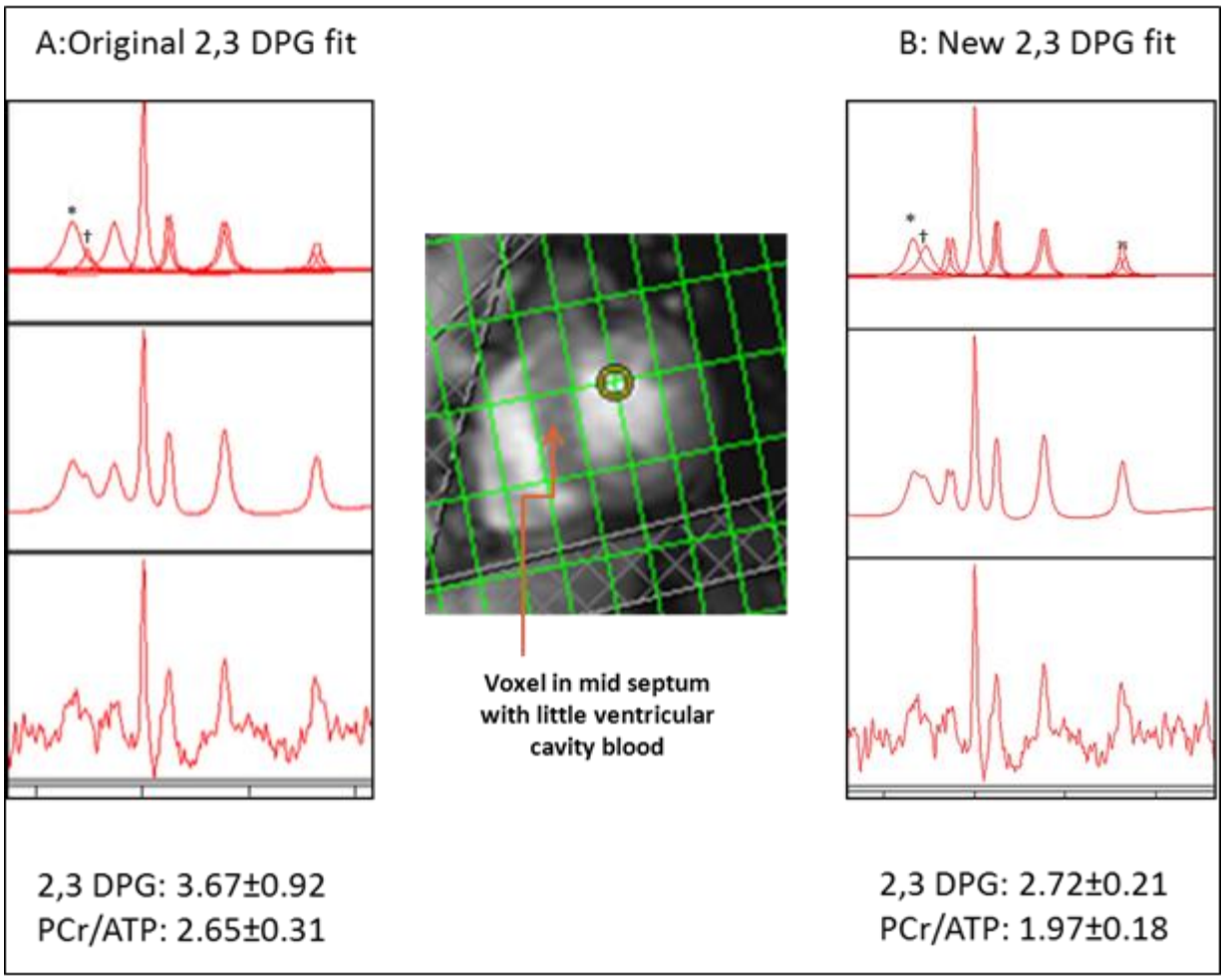



***Figure 4.8:*** *Comparison of original 2, 3 DPG fit with new fit. Values reported as mean ±sd.* represents the 2 DPG peak, † represents the 3 DPG peak.*

## 4.4 Discussion

$^{31}$P MRS is attractive as it offers a noninvasive in vivo means of measuring high energy phosphate metabolites. Given the inherent complexities of biological systems, much effort is needed to ensure a rigorous means for accurate analysis. Inclusion of biochemical prior knowledge into line shape fitting analysis allows for more reliable quantification[68].

However, one should remember that incorporating prior knowledge is only beneficial when it is sufficiently close to reality.

In the simulated data, a more accurate measurement (i.e. closer to the fixed PCr/ATP of 2.0) was achieved in the 40% noise data with the new prior knowledge whereas the new fit made no difference to the final measurement in the less noisy 20% noise data. Hence, this simulated data clearly shows that improving the 2, 3 DPG fit gives a more accurate final PCr/ATP ratio, particularly in noisy or low signal data.

The use of biophysical prior knowledge therefore better guides the spectral fitting algorithm on the fitting of difficult in-vivo data as there is a range of signal to noise in human data governed by factors such as body habitus, movement during scanning and underlying cardiac pathology. In DCM, due to the thinned myocardium, the 2, 3 DPG signal from cavity blood is adequate. Conversely, in the hypertrophied myocardium there is little blood within the voxel (figure 4.9). We postulate that particularly in cardiac hypertrophy, the spectral voxel of interest has too little cavity blood contamination and hence the signal from 2, 3 DPG is weak. The AMARES algorithm therefore struggles to fit 2, 3 DPG and this error is unavoidably propagated to the final calculation of PCr/ATP. With clearer, biological instructions given to AMARES for the fitting of 2, 3 DPG, the algorithm was able to fit true signal with more confidence and ultimately reflect a more accurate PCr/ ATP ratio. In the 16 HCM datasets, the COV of measured 2, 3 DPG dropped from 22% with the original fit to 17% with the new fit. However, the COV of the 2,3 DPG fit also improved in the DCM and the normal groups suggesting that the poor confidence of fit with the original prior

knowledge is not only due to poor signal from blood ( as in hypertrophy), but also the inherent noise of the method and MR invisibility of $^{31}P$. Hence this refinement of the measure would prove useful in measuring subtle changes in PCr/ATP ratios which would otherwise be lost in the standard deviations of the measure.

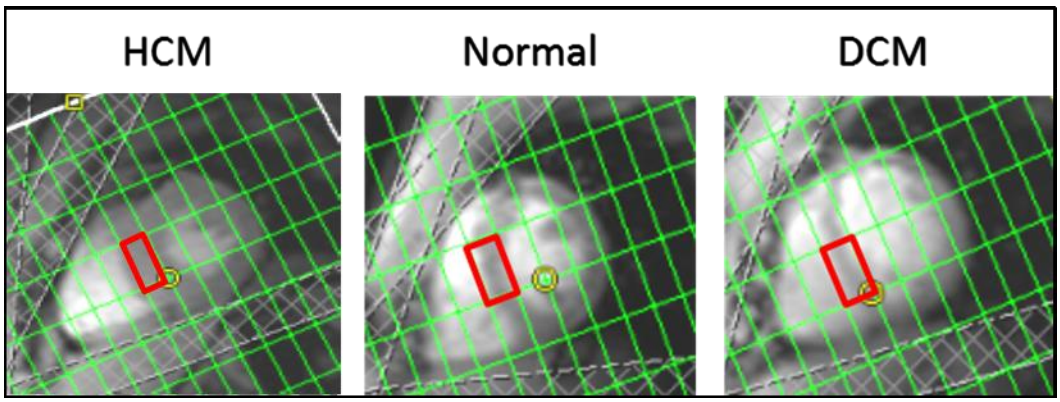



***Figure 4.9**: Examples of voxel content in HCM, DCM and normal controls. In HCM with significant septal hypertrophy, there is very little blood contamination conversely, in DCM with thinned myocardium there is significant left and right ventricular cavity blood within the voxel.*

Within HCM, DCM and normal controls, no significant change in the average value of PCr/ATP has been brought about by the improved data fitting but a considerable improvement in the confidence of fitting is illustrated by a narrowing of the group average standard deviation. This is due solely to the improved COV of the 2, 3 DPG fit in all groups. The lack of change in the group average supports the assumption that the imposed prior knowledge has not brought about any systematic bias to this data but has instead reduced the occurrence of erroneous, outlying fits to noisy data associated with unrealistic linewidths, non-physiological frequencies and non-chemical amplitude ratios.

The improved standard deviation indicates that the number of subjects needed to power $^{31}$P MRS experiments would be less. In HCM and DCM, based on this pilot data, in order to detect a 10% change in PCr/ATP with an intervention, (α 0.05, power 80%) half the number of subjects need to be scanned if the new 2, 3 DPG prior knowledge is applied, table 4.3

| | **Using Original 2,3 DPG fit** | | **Using New 2,3 DPG fit** | |
|---|---|---|---|---|
| | PCr/ATP (mean± SE) | Sample size | PCr/ATP (mean± SE) | Sample size |
| **HCM** | 1.96±0.13 | 59 | 1.80±0.08 | 27 |
| **DCM** | 1.47±0.07 | 28 | 1.15±0.05 | 14 |
| **Normal** | 2.26±0.08 | 16 | 2.22±0.07 | 13 |

***Table 4.3:*** *Sample size needed to detect a 10% change, α 0.05, power 80% ,using the mean and standard error of the PCr/ATP using the original and the new 2,3 DPG fit in the pilot patient data above. Power calculations were performed using mean of the difference (based on a 10% change with an intervention) and the standard deviation of the difference. These are a priori power calculations using G* Power 3.2.1 software and based on the use of paired T test to compare the effect of the intervention if an experiment was designed using these power calculations.*

## 4.5 Conclusion

$^{31}$P MRS is a valuable tool for assessment of myocardial metabolism. Post processing corrects for blood contamination. In hypertrophied hearts poor fit of 2, 3 DPG was exacerbated by the little blood contamination within the voxel of interest. This lead to a propagation of this error to the final calculated myocardial PCr/ ATP ratio. This work developed an improved fit for 2, 3 DPG and tested it with both simulated and patient data, including hypertrophied and thinned myocardium. The quality of this outcome is reflected in the power calculations which illustrate an almost 50% reduction of sample size required to statistically demonstrate a physiological change in PCr/ATP with an intervention in HCM and DCM.

# *Chapter 5*
# *Effect of exercise on cardiac energy metabolism in Hypertrophic Cardiomyopathy*

# 5.1 Introduction

Original predictions based on data from in vitro studies of recombinant proteins, supported by evidence from animal models and patients strongly support the energy depletion hypothesis, ( discussed in chapter 1), as a unifying mechanism causing disease in HCM.

HCM phenocopies (i.e. an HCM-like phenotype) exist in several diseases associated with compromised energy metabolism secondary to defects in ATP generation, e.g. Friedreich ataxia[69, 70], mitochondrial tRNA mutations[71], CD36 deficiency[72], very-long-chain acyl-CoA dehydrogenase deficiency[73]. In further support of the link to energetic abnormalities, mutations in the γ2-subunit of AMP-activated kinase (AMPK), a key energy-regulating enzyme, have been described in patients with morphological features of HCM in combination with Wolff-Parkinson-White syndrome and progressive conduction disease[74-76].

Impaired energetics (decreased PCr/ATP using cardiac $^{31}$P MRS) has been documented in genetically modified animal models of HCM [77,78]; in asymptomatic patients with clinical features of HCM[79]; in genotyped, phenotypically affected and phenotypically unaffected (gene carrier), HCM patients[4]. In support of a potentially reversible abnormality in energy metabolism in HCM, Abozguia et al demonstrated that the metabolic modulator, perhexiline, improves cardiac energetics and diastolic dysfunction in HCM. Table 5.1 summaries the published PCr/ATP data in HCM patients using $^{31}$P MRS[4, 7, 79-83].

While all previous studies of cardiac energetics HCM have been conducted at rest, in many situations an energetic deficit would worsen or would only become unmasked when hearts are stressed, e.g. during exercise. The high incidence of exercise-related death in HCM may be explained by a possible acute further impairment of myocardial energetics. However, cardiac energetics during stress conditions has previously not been examined in patients with HCM.

As a proof-of-principle study, this chapter explores the hypothesis that cardiac energetics are further impaired during exercise in HCM, compared to normal subjects or physiological hypertrophy in athletes, where no changes would be expected.

***Table 5.1****: Summary of data published on PCr/ATP measurements in HCM. All values are mean ±SD apart from Abozguia et al values are mean ± SE, * P<0.05.*

| Author | Year | HCM Sample size | Field | Rest PCr/ATP in HCM | Rest PCr/ATP in normal | Additional findings in HCM |
|---|---|---|---|---|---|---|
| de Roos et al | 1992 | 9 | 1.5 T | 1.32±0.29* | 1.65±0.26 | ↑Pi /PCR Decreased pH |
| Sieverding et al | 1997 | 13 | 1.5T | 1.95±0.72 | 2.17±0.51 | ↑Pi/PCr |
| Jung et al | 1997 | 14 | 1.5T | 1.98±0.37* | 2.46±0.53 | ↑PME/PCR ↑Pi/PCr |
| Crilley et al | 2003 | 31 | 2T | 1.70±0.43* | 2.44±0.3 | Abnormal PCr/ATP in HCM with no LVH |
| Shivu et al | 2008 | 26 | 3T | 1.42±0.51* | 2.11±0.57 | |
| Esposito et al | 2008 | 19 | 1.5T | 2.18±0.41* | 2.41±0.30 | |
| Abozguia et al | 2010 | 46 | | 1.28±0.01 | 2.26±0.02 | Perhexiline improved PCr/ATP |

# 5.2 Method

## *5.2.1 Ethics and Study Cohort*

Sixty seven subjects (35 HCM, 12 Athletes and 20 normal controls) were included in this study. All subjects were screened for inclusion and exclusion criteria as described in Chapter 2.

## *5.2.2 31P MRS acquisition and analysis*

This is as described in chapter 3 and 4. The exercise protocol is also described in chapter 3.

## *5.2.3 Cardiac Mass and LGE assessment*

These are described in chapter 2.

## *5.2.4 Haemodynamic assessment*

Rest and exercise pulse rates were monitored via 3 lead ECG and blood pressure was recorded using an automatic sphygmomanometer whilst in the scanner. Pulse and blood pressures were measured at two minute intervals during exercise. An adequate exercise response was defined as a 50% increase in rate pressure product.

## *5.2.5 Statistical analysis*

Paired student *t* tests were used to test for differences between rest and exercise. Two way ANOVA was used to test differences between the groups. Data are presented as mean ± standard error. A p value of $<0.05$ was considered to be significant. All data passed tests of normality.

# 5.3 Results

## 5.3.1 Study Population

In the studied cohorts, there were no differences in age between normal, 39±2 years, and athletes, 32±3 years, (ANOVA p =0.28); and normal and HCM 45±2 years (ANOVA p =0.10). There was also no gender difference, with the percentage of males being: normal 55%; athletes 58%; HCM 50%. None of the athletes or normal controls was diabetic or hypertensive. Two individuals in the HCM subgroup were hypertensive and one was diabetic.

## *5.3.2 Measure of Hypertrophy*

The LV mass and LV mass indexed to body surface area and normalized to end diastolic volumes were significantly higher in HCM and athletes compared to normal controls (table 5.2).

## *5.3.3 Measure of exercise*

Adequate physiological exercise was achieved in all groups with percentage increases in RPP being: normal 72± 9%; HCM 73± 6%; Athlete 75±14%.

***Table 5.2:*** *A comparisons of left ventricular mass in normal; primary pathological hypertrophy, HCM; physiological hypertrophy, Athletes.*

| | **Normal (n= 21)** | **HCM (n=35)** | **Athlete (n=12)** |
|---|---|---|---|
| Mass (g) | 121± 6 | 166± 10* | 176± 14* |
| Mass index (g/m$^2$) | 65± 2 | 90± 7* | 92± 5† |
| Mass/ EDV (g/ml) | 0.9± 0.1 | 1.5±0.1* | 1.1± 0.1† |

*=p<0.005 vs. normal; †=p<0.05 vs. normal

### *5.3.4 Rest and exercise energetics*

There was no difference in resting PCr/ATP between normal controls (2.14 ± 0.08) and athletes (2.07 ± 0.05, ANOVA P = 0.90). However, resting PCr/ATP was significantly reduced in HCM, (1.71± 0.06, ANOVA P<0.0001).

During exercise there was a further reduction in PCr/ATP in HCM (1.56±0.05, P=0.02) but no change in normal controls (2.16±0.07, P=0.98), and athletes (2.11±0.07, P=0.73, figure 5.1). The change of PCr/ATP during exercise in HCM (-0.14±0.06) was significantly different (P<0.05) from the change in controls (+0.05±0.06), figure 5.1. There was a significant negative correlation between change in energectics with exercise and resting PCr/ ATP, figure 5.2( r=-0.65, P<0.0001). Figure 5.3 demonstrates examples of spectra at rest and during exercise in normals and HCM.

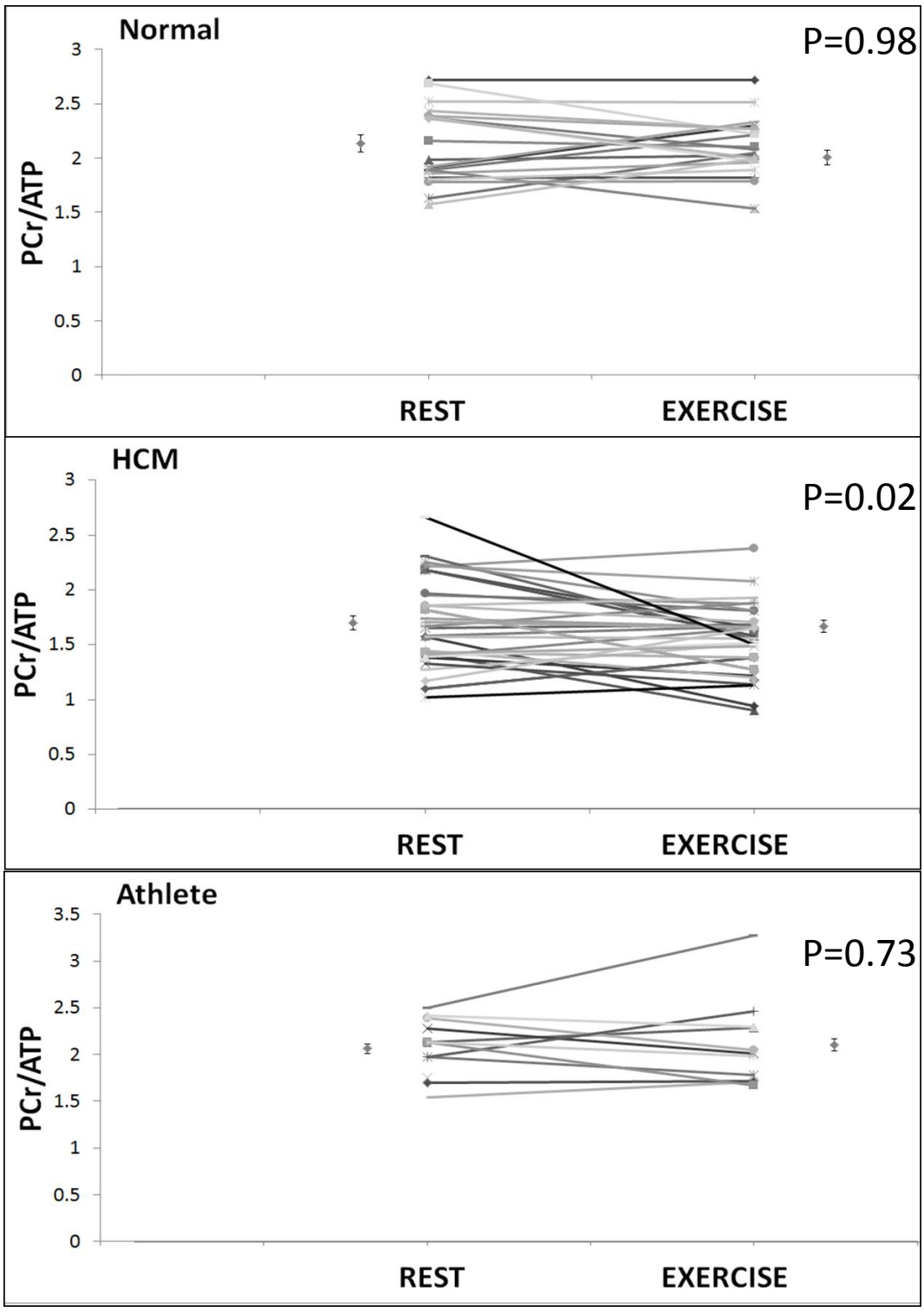



***Figure 5.1:*** *The effect of exercise on PCr/ATP in normal controls, HCM, and Athletes, showing a reduction in the HCM group, but no change in athletes or normal*.

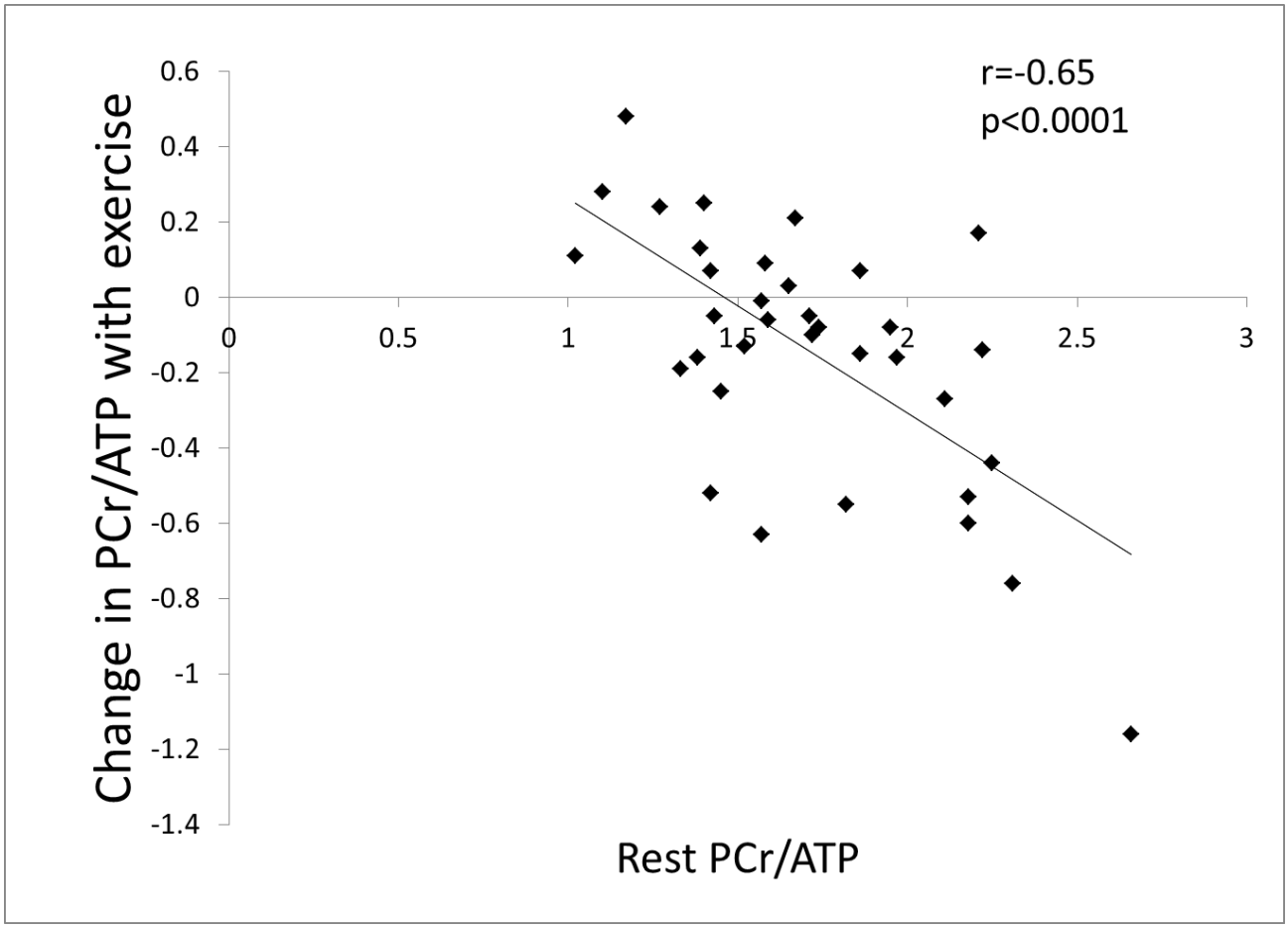



***Figure 5.2****: Correlation between change in energetics with exercise and resting PCr/ATP*.

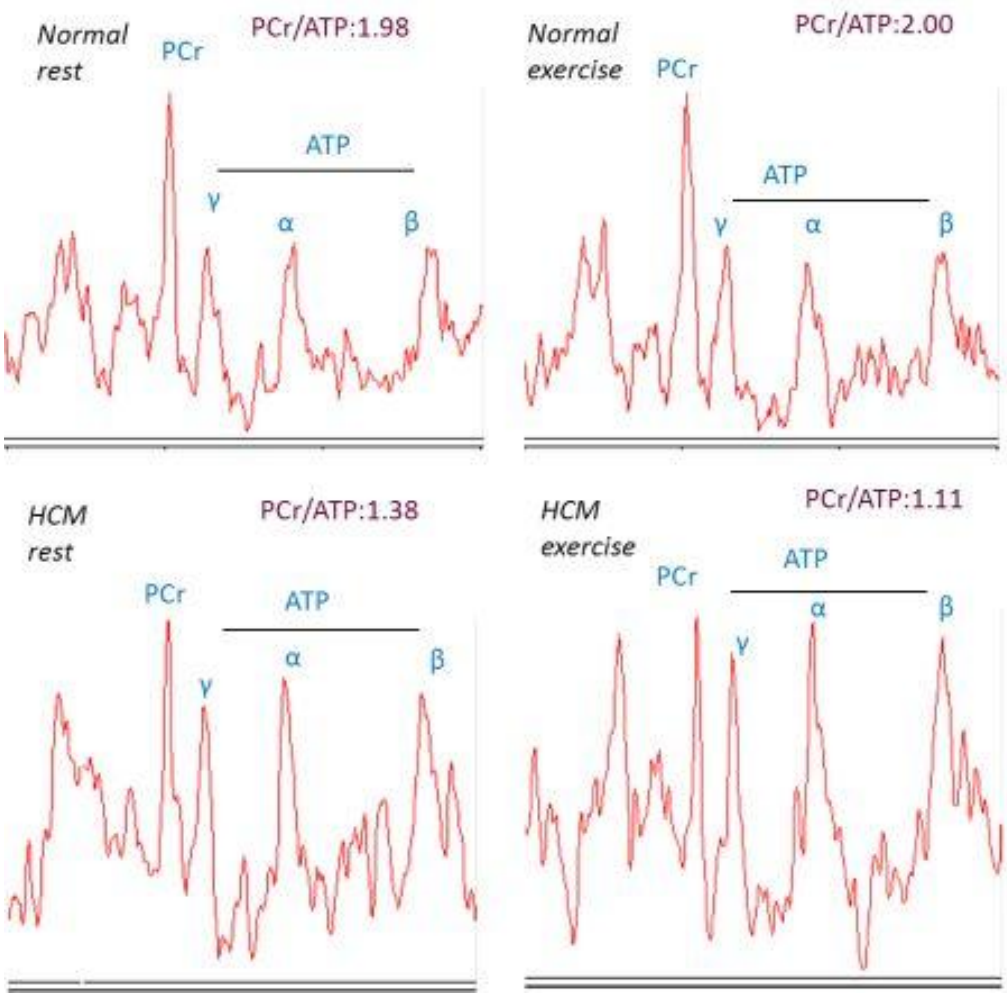



***Figure 5.3*** *Examples of rest and exercise energetics in normal and HCM*.

## *5.3.5 Relationship between energetics and hypertrophy*

Cardiac mass index and rest PCr/ATP ratios did not correlate with either physiological hypertrophy in athletes or pathological hypertrophy in HCM, (HCM: R=0.01, P=0.95; athletes: R=0.22 P=0.49, figure 5.4). Similarly, cardiac mass normalized to end diastolic volume did not correlate with resting PCr/ATP, (HCM R=0.21, P=0.22; Athletes R=0.28, P=0.40). Change in energetics with exercise also did not correlate with mass index, (HCM

R=0.02, P=0.91; athletes: R=0.01 P=0.97, figure 5.3) or mass normalized to end diastolic volume, (HCM R=0.20, P=0.25; Athletes R=0.01, P=0.97).

In HCM, average wall thickness at the sight of voxel placement for PCR/ATP measurement was 17.6± 0.10 (range 7.8-28.8 mm). There was no correlate with wall thickness and resting PCr/ ATP (R=0.02, P=0.90) or change in energetics with exercise (R=0.18, P=0.30) in the HCM cohort.

Wall thicknesses were normal in the athlete group, 8.7±0.5mm.

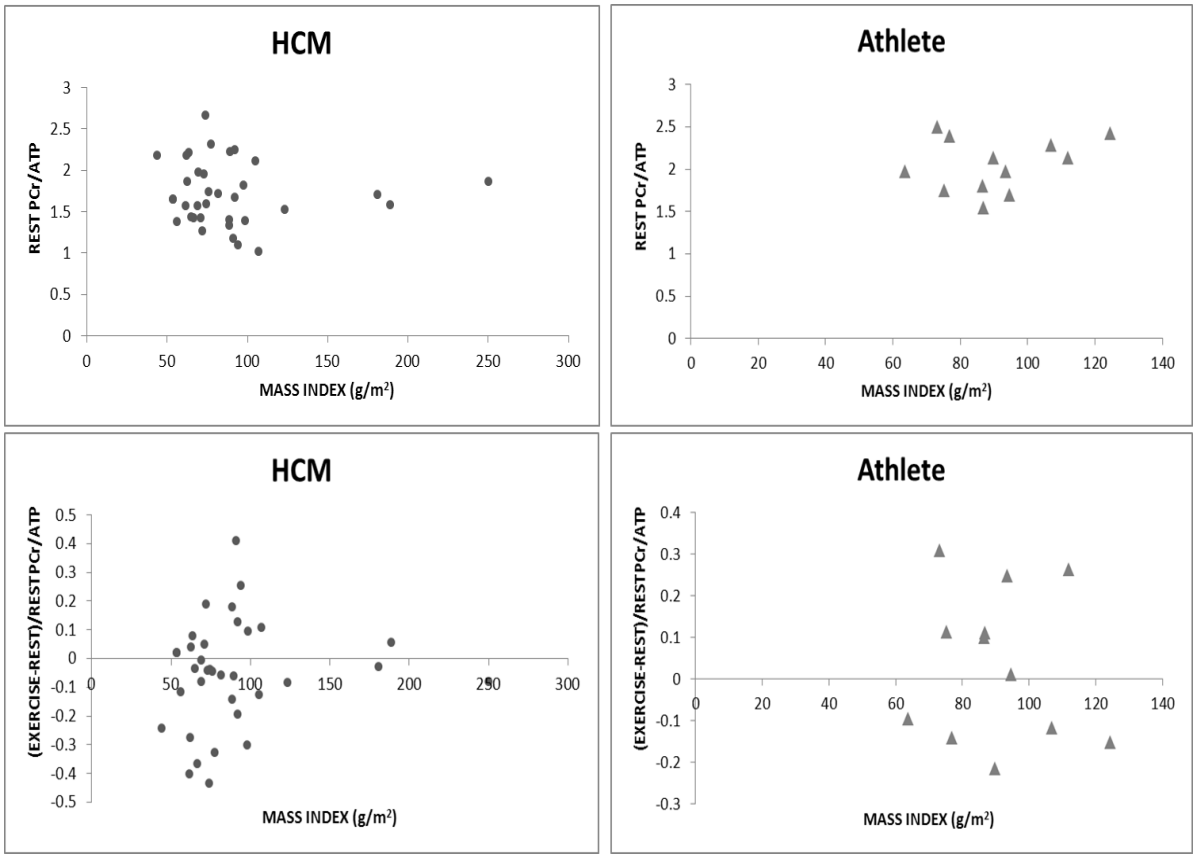



***Figure 5.4****: This figure illustrates the lack of relationship between resting energetics and change in energetic with exercise and hypertrophy, both physiological (athletes) and pathological (HCM).*

### 5.3.6 Relationship between energetics and LGE

LGE burden was defined as the fraction of myocardial signal intensity > 2 standard deviations above remote normal myocardium. PCr/ATP was compared to LGE burden of the mid septum in the mid ventricular slice (same position for the energetics measurement).

The normal controls and athletes had no LGE. In HCM, the average segment fraction of LGE >2SD in the mid ventricular septum was 0.24± 0.15. On a per subject basis, LGE correlated weakly with resting PCr/ATP ratio (R= - 0.345, P=0.04), but did not correlate with change in PCr/ATP with exercise.

## 5.4 Discussion

The main demonstration of the present study was the further impairment of PCr/ATP in HCM during exercise. At similar levels of exercise, this did not occur in normal controls or athletes with physiological hypertrophy. To my knowledge, this is the first report of exercise energetics in HCM.

### 5.4.1 Rest and exercise PCr/ATP in normal controls and athletes

In previous reports for normal volunteers, there was no change in PCr/ATP ratios during physiological exercise either via hand grip exercise [61-63] or leg exercise[53]. However, normal volunteers [84], and athletes[85], have been shown to have a reduction in PCr/ATP after exhaustive pharmacological exercise stimulation using atropine and dobutamine [84-86]. During pharmacological stimulation, there were extreme rises in RPP; of greater than 300%,

suggesting extreme physiological stimulus may be required to see alteration in PCr/ATP in these subgroups. Lamb et al[84] found a close relation between myocardial PCr/ATP and the level of cardiac workload. Reduction in cardiac energetics even in normal hearts during extreme work may be partly explained by ATP utilisation that is not completely matched by ATP synthesis possibly because of limited coronary reserve at these extreme levels of exercise. However, in this report, the maintenance of resting levels of PCr/ATP during moderate physiological exercise in normal controls and athletes, (~ 70% raise in RPP), suggests an adequate adaptation of oxidative phosphorylation to increased energy demands in these cohorts under modest changes in RPP.

### *5.4.2 Rest and exercise PCr/ATP in HCM*

Depressed resting PCr/ATP in HCM, and further reduction during similar levels of exercise observed in only the HCM cohort firstly suggest an inefficient resting metabolic profile and secondly an inability to adapt to the increased energy demand of exercise. Inefficient resting energy profile as measured by PCr/ATP in HCM is a consistent finding in the literature, (table 5.1) and is perhaps not surprising that this is exacerbated during exercise.

Energy demand and supply pathways are tightly linked in the normal heart, such that even large changes in energy expenditure will not lead to gross changes in the concentrations of PCr or ATP. However, in HCM an imbalance exists between energy demand and supply at rest with further impairment during exercise. I postulate that this is multifactorial and can be attributed to increased energy demand coupled with a decreased energy supply and physical properties of the myocardium potentially affecting supply and demand.

Furthermore, the negative correlation between change in energetics with exercise and resting energetic profile highlights that exercise is able to unmask energy abnormalities in the HCM hearts which at rest appear to be normal or near normal. It is observed from this correlation that the hearts with already low resting PCr/ATP did not necessarily have a further drop with exercise. I postulate that perhaps there is a minimum physiologic level of PCr/ATP and it is perhaps these individuals who are nearing this threshold who are most at risk. However, larger studies with longitudinal follow up would be needed to explore this correlation further.

## *Increased energy demand*

The primary sarcomeric mutation increases the energy cost of contraction (discussed in chapter 1). Well studied examples include HCM mutations in β Myosin Heavy chain and thin filament regulatory proteins and troponin T.

Recent studies of β Myosin Heavy chain mutations have demonstrated altered cycling rates of the mutant heads forcing wild type heads to detach before completion of their power stroke[25].

Thin filament regulatory proteins mutations cause an increased calcium sensitivity resulting in increasing crossbridge formation at submaximal calcium concentrations. This results in an excess consumption of ATP without producing a proportionally greater stroke volume[28, 87]. Furthermore, this increased calcium sensitivity would lead to prolonged contraction, as

the calcium transient falls in diastole, using yet more ATP and possibly being one mechanism contributing to diastolic dysfunction.

Troponin T mutations result in accelerated cross bridge detachment. This effectively shortens the power stroke for each ATP hydrolyzed[29].

Hence increased energy demand at rest and exercise in HCM is likely due to the intrinsic metabolic abnormalities caused by the sarcomeric mutations.

## *Decreased energy supply*

Decreased supply of substrate and oxygen may result from microvascular dysfunction which is a recognised feature of HCM[30, 31 32] . Angina and symptoms suggesting myocardial ischemia are frequent features in the natural history of HCM. The direct link between microvascular dysfunction and tissue deoxygenating in HCM is yet to be demonstrated (this is explored further in chapter 6).

In addition to impaired perfusion, ineffective oxidative phosphorylation will also affect energy supply. Mitochondrial morphological disorganization and impaired function has been demonstrated in HCM both in human tissue[88] as well as mouse genetic models of HCM[89]. These abnormalities of electron transport chain would lead to inefficient oxidative phosphorylation and ATP production.

Defects in PCr formation and transfer are yet another factor potentially affecting energy supply in HCM. Decreased total creatine has been shown in explanted hearts of HCM with end stage heart failure[90] as well as HCM mouse models[78]. This would directly reduce

phosphocreatine concentration, as the ratio of PCr to total creatine remains constant unless there is acute ischaemia[91]. In addition, decreased creatine kinase activity has been demonstrated by Ingwall et al[92] in cardiac hypertrophy. This was a pressure overload cohort, in contrast, Spindler et al[78] demonstrated no change in creatine kinase activity in transgenic HCM mice.

## *Physical properties of the myocardium potentially affecting cardiac energetics*

It has been postulated that hypertrophy itself can affect cardiac energetics. This report showed that resting and exercise energetic profiles were not related to cardiac mass either due to physiological mass increases as in athletes or the pathological hypertrophy of HCM, neither was there a relation with wall thickness in HCM. This is further supported by Crilley et al[4] who has shown abnormal resting PCr/ATP ratios in HCM without hypertrophy. However, Jung et al[79] demonstrated a positive correlation between PCr/ATP and hypertrophy, of note, their cohort, (n=15) had end diastolic interventricular wall thickness ranging from 14 to 33mm. Therefore, they were unable to comment on energetics in pre hypertrophied HCM hearts.

Late gadolinium burden has also been thought to be related to energetics. Esposito et al[83] observed a correlation between PCr/ATP and fibrosis in HCM, they concluded that altered energetics might be secondary to myocardial alterations causing LGE. Importantly, I also demonstrate that LGE is not related to the change in energetics with exercise. This is logical as fibrosis is metabolically inactive and myocardial scar has been shown to contain

negligible amounts of ATP[93] . Therefore, the presence of LGE, per se, should not affect measured PCr/ATP.

### *5.4.2 Effect of deranged exercise energetics in HCM*

Irrespective of their aetiologies, the metabolic abnormalities found in this study raise the question of their clinical relevance. I propose that this demonstration of further impairment of cardiac energetics during exercise in HCM provide possible explanations for exercise systolic and diastolic dysfunction and for the high incidence of exercise-related death in HCM.

During exercise, in addition to the increased energy demand coupled with decreased supply as discussed above, the free energy release of ATP hydrolysis is reduced. As PCr levels fall acutely during exercise, free ADP levels also increase acutely. This reduces the free energy change of ATP hydrolysis (figure 5.5) and hence contributes to the measured derangement in exercise energetics reported in this chapter.

$$\Delta G_{\sim ATP} = \Delta G^{o}_{\sim ATP} - RT \, ln \, [ATP]/[ADP][Pi]$$

***Figure 5.5****: Equation for calculating free energy change of ATP hydrolysis, $\Delta G_{\sim ATP}$. $\Delta G^{o}_{\sim ATP}$ is the standard free energy change of ATP hydrolysis (-30.5kJ/mol under standard conditions; R is the gas constant (8.3J/mol.K) and T is temperature in degrees Kelvin. (Adapted from ATP and the Heart, J Ingwall)*

Hence less free energy is available to drive ATP utilizing reactions such as moving ions against their concentration gradients (eg.SERCA) or changing the conformation of proteins such as myosin.

Studies have shown that a limited exercise capacity is common in patients with HCM and is related to the development of diastolic dysfunction during peak exercise[94, 95]. Okeie et al [96] also demonstrated LV systolic impairment and regional wall motion abnormalities during dobutamine stress echocardiography in HCM. The authors concluded that the mechanisms responsible for these abnormal responses remain unclear. However, both myocardial contraction and relaxation are energy dependent processes. ATP is required in systole for the power stoke of the actin-myosin cross bridges leading to muscle contraction and indeed ATP is required to pump free calcium back into the sarcoplasmic reticulum to allow for diastole. I postulate that this chapter's report of abnormal myocardial energetic further attenuated by exercise, contribute to this observed exercise systolic and diastolic dysfunction in HCM. In addition, further impaired function of SERCA during exercise, could potentially cause Ca++ overload with resulting increased rate of membrane depolarisation and subsequent VT and VF.

## 5.5 Limitations

Exercising in the magnet to a degree that is comfortable and does not produce chest wall movement significantly limits the intensity of exercise. We report modest increases in RPP as compared to pharmacological stimulation with dobutamine and atropine. It is possible that changes are more pronounced with extreme exertion, however, there were safety

concerns about giving positive inotropic agents in HCM in an MRI environment. Also, the level of exercise as measured by increases in RPP does not necessarily reflect similar exercise intensity, measurements such as maximum oxygen consumption would have been more comparable.

## 5.6 Conclusion

During exercise, the pre-existing energetic deficit in HCM is further exacerbated. This may underlie acute derangement of energy-dependent ion homeostasis, triggering calcium overload and ventricular arrhythmias. These findings offer a possible explanation for the high incidence of exercise-related death in HCM and suggest that treatments that optimize energetics may be protective.

# *Chapter 6*
# *Myocardial Tissue Oxygenation in Hypertrophy assessed with Blood-Oxygenation-Level-Dependent (BOLD) MRI*

# 6.1 Introduction

The interplay between myocardial perfusion, oxygenation and regional function in the setting of epicardial coronary artery stenosis, although complex, has been increasingly explored[45, 97] . It is known that myocardium subtended by a stenosed coronary artery may not become ischaemic due to chronic formation of collaterals[97, 98], and, vice versa, myocardium subtended by an angiographically normal coronary artery may show severe exercise-induced myocardial ischemia due to micro-vascular dysfunction[99]. However, little is known about myocardial tissue oxygenation in patients with pathological LV hypertrophy (i.e. HCM) or physiological hypertrophy (e.g. elite athletes). Importantly, myocardial tissue hypoxia may play a significant pathophysiological role in patients with HCM, being potentially responsible for arrhythmia and sudden death.

Microvascular function in HCM has been investigated using a variety of imaging modalities that assess myocardial perfusion including CMR[30, 31], positron emission tomography (PET) [32] and thallium scanning[33]. In a recent study using CMR, our group showed that patients with HCM demonstrate a reduced myocardial perfusion reserve as measured by hyperaemic myocardial blood flow following adenosine infusion, particularly in the endocardium, and in proportion to the magnitude of hypertrophy[30]. However, whether de-oxygenation occurs at rest and/or stress in hypertrophied myocardium is unknown, and the simultaneous measurement of both myocardial perfusion and oxygenation in this setting has not previously been possible in clinical studies. Such a measurement would answer the important pathophysiological question whether microvascular dysfunction in

hypertrophied and non-hypertrophied myocardium in hypertrophic cardiomyopathy is severe enough to result in ischaemia, particularly at stress. Another report using catheter measurements in the great cardiac vein showed myocardial oxygen consumption and coronary blood flow increasing during cardiac pacing in HCM[100]. Not only is this method invasive, it reflects global change, the averaging effect of which may mask subtle or regional disease.

The work in this chapter explores the interplay between tissue oxygenation and microvascular dysfunction on a paired per segment basis and its effect on myocardial energy metabolism in HCM and athletes with physiological, adaptive hypertrophy. In these experiments, myocardial tissue oxygenation was measured using the Blood Oxygen Level-Dependent CMR (BOLD) technique. BOLD imaging capitalises on the fact that deoxygenated hemoglobin in blood can act as an intrinsic contrast agent, changing proton signals in a fashion that can be imaged to reflect the level of blood oxygenation. Increases in $O_2$ saturation increase the BOLD imaging signal ($T_2$ or $T_2$*), whereas decreases diminish it[101, 102]. BOLD is well established in functional Brain MRI[103-107] and skeletal muscle studies[108, 109]. The BOLD technique has proven to show excellent correlation with coronary venous sampling[110] and has been applied in coronary artery setting [45, 102, 111-114] as well as in hypertensive cardiomyopathy [115]. At 3T, the blood and extravascular tissue $T_2$ is much more sensitive to its oxygenation level than at 1.5 T, consequently contrast will be increased [116]. This boost in contrast is accompanied by the increased signal to noise ratio at 3T, which makes cardiac BOLD imaging considerably more robust.

I hypothesise that tissue oxygenation during stress is impaired in HCM in the presence of hypertrophy and also in pre-hypertrophied mutation carriers and that this does not occur in physiological hypertrophy of athletes.

## 6.2 Methods

Sixty nine subjects were recruited into this study (26 HCM with left ventricular hypertrophy; 11 HCM pre hypertrophy; 12 athletes; 20 normal controls). Inclusion and exclusion criteria are described in chapter 2.

Subjects underwent CMR scanning at 3T to access:

1. left ventricular function , mass and volumes
2. Rest and adenosine stress BOLD signal intensity.
3. Rest and adenosine stress perfusion to measure myocardial perfusion reserve index.

These methods and analysis are described in chapter 2.

### *6.2.1 Statistical analysis*

Data analysis was performed with commercially available software packages (IBM SPSS Statistics, version 19.0 and Medcalc version 9.6.4.0 for Windows. ANOVA with post hoc Bonferroni comparisons were used to compare the hemodynamic response to stress between the 4 groups. Statistical tests were two tailed, and a P value of less than 0.05 was considered to indicate a statistically significant difference. Correlations were done using bivariate Pearson's method. To determine independent predictors of BOLD SI change

multiple linear regression was used. ). All continuous variables were normally distributed (Kolmogorov-Smirnov test). Furthermore the differences between age, sex and body surface area between the 4 groups were taken into account for the perfusion and oxygenation comparisons. Only variables with significant association with BOLD SI change on bivariate analysis ($p<0.05$) were entered into the multivariate model. Receiver-operating characteristic (ROC) curve analyses were used to explore the diagnostic ability of BOLD-CMR to detect patients with HCM. The criterion value was set at the maximum Youden index.The Youden Index is a frequently used summary measure of the ROC curve. It both, measures the effectiveness of a diagnostic marker and enables the selection of an optimal threshold value (cutoff point) for the marker. Youden Index is = $\max[SE_i + SP_i - 1]$where $SE_i$ and $SP_i$ are the sensitivity and specificity over all possible threshold values. This value corresponds with the point on the ROC curve farthest from the diagonal line.

# 6.3 Results

## *6.3.1 Study population and Hemodynamic measurements*

Subject characteristics are described in table 6.1 and table 6.2. There were differences in age, sex and body surface area between the 4 groups of subjects which were taken into account for perfusion and oxygenation analyses. As expected, subjects with overt HCM had significantly increased maximum wall thickness and LV mass index, and smaller LV volumes, than normal controls. HCM mutation carriers without hypertrophy had normal cardiac dimensions and LV mass but equally high-normal ejection fraction as subjects with overt HCM. The athletes had increased LV mass and larger end-diastolic LV volumes than

controls but similar ejection fractions. Overall, the HCM cohort was considered low risk according to clinical risk stratification (Table 2). During adenosine stress there were equivalent rises in rate pressure product in all groups, (normals 78±28%, athletes 65±29%, overt HCM 57±34%, HCM gene carriers 66±28 P=0.18).

***Table 6.1****: Baseline Characteristics of Study Groups*.

| | **Normal Controls (n=20)** | **Elite Athletes (n=12)** | **HCM gene carriers (no LVH) (n=10)** | **HCM patients (with LVH) (n=27)** |
|---|---|---|---|---|
| **Age** | 39.6±2.2 | 31.5±2.7 | 36.2±4.5 | 48.2±1.8 |
| **Male n (%)** | 13 (65%) | 8(73%) | 4 (40%) | 19 (70%) |
| **BSA ($m^2$)** | 1.9±0.04 | 1.88±0.06 | 1.7±0.06 | 2.0±0.04 |
| **LV end-diastolic volume index, $ml/m^2$** | 78.5±3.4 | 92.2±5.7 | 63.3±2.8* | 58.6±2.3* |
| **LV end systolic volume, $ml/m^2$** | 30.0±1.6 | 33.8±3.7 | 17.4±2.0* | 16.2±1.0* |
| **LV ejection fraction, %** | 61.1±0.9 | 64.9±1.8 | 72.9±2.5* | 73.6±1.0* |
| **LV mass index $g/m^2$** | 64.7±2.2 | 92.8±4.6* | 60.4±3.1 | 95.5±7.7* |
| **LV Wall thickness** | 10.2±0.3 | 12.3±0.2 | 9.6±0.04 | 19.3±1.0 |

HCM, hypertrophic cardiomyopathy; LVH, left ventricular hypertrophy;*Values are means± SE unless otherwise stated. *P<0.05 vs. normal controls*

***Table 6.2**: Clinical Risk Stratification and Medications in HCM cohort*.

| | **HCM gene carriers without LVH (n= 10)** | **HCM patients with LVH (n= 27)** |
|---|---|---|
| **No. of SCD risk factors (0/1/2/3 risk factors), % (n)** | 82,9,9 (8, 1,1,0) | 54,31,15,0 (15,8,4,0) |
| **Family history of SCD, % (n)** | 18 (2) | 42 (11) |
| **Unexplained syncope, % (n)** | 0 (0) | 4 (1) |
| **NSVT on Holter monitor, % (n)** | 9 (1) | 12 (3) |
| **Abnormal exercise blood pressure response, % (n)** | 0 (0) | 0 (0) |
| **Maximum LV wall thickness ≥ 30mm, % (n)** | 0 (0) | 4 (1) |
| **LV outflow tract gradient, % (n)** | 0 (0) | 0(0) |
| **β-Blockers, % (n)** | 36 (4) | 69 (18) |
| **Calcium Channel Inhibitors, % (n)** | 0 (0) | 6 (23) |

HCM, hypertrophic cardiomyopathy; LV, left ventricular; LVH, left ventricular hypertrophy; NSVT, non-sustained ventricular tachycardia; SCD, sudden cardiac death. **P<0.05 vs. normal controls*

## *6.3.2 Changes in BOLD signal intensity*

During adenosine stress, the percentage increase in BOLD signal intensity (BOLD SIΔ) was similar in athletes and normal volunteers (19.0% [95% CI: 15.6-22.4] in normal controls and 18.7% [95% CI: 15.9-21.6] in athletes, P=0.9). Interestingly, with the same degree of stress,

there was a significantly reduced BOLD SIΔ response in both pre hypertrophied and hypertrophied HCM compared to normal controls (BOLD SIΔ: 10.5% [95% CI: 6.9-22.37]in HCM pre hypertrophy; 7.2% [95% CI: 4.6-9.8]in HCM with hypertrophy P<0.0001..vs. normal, figure 6.1).

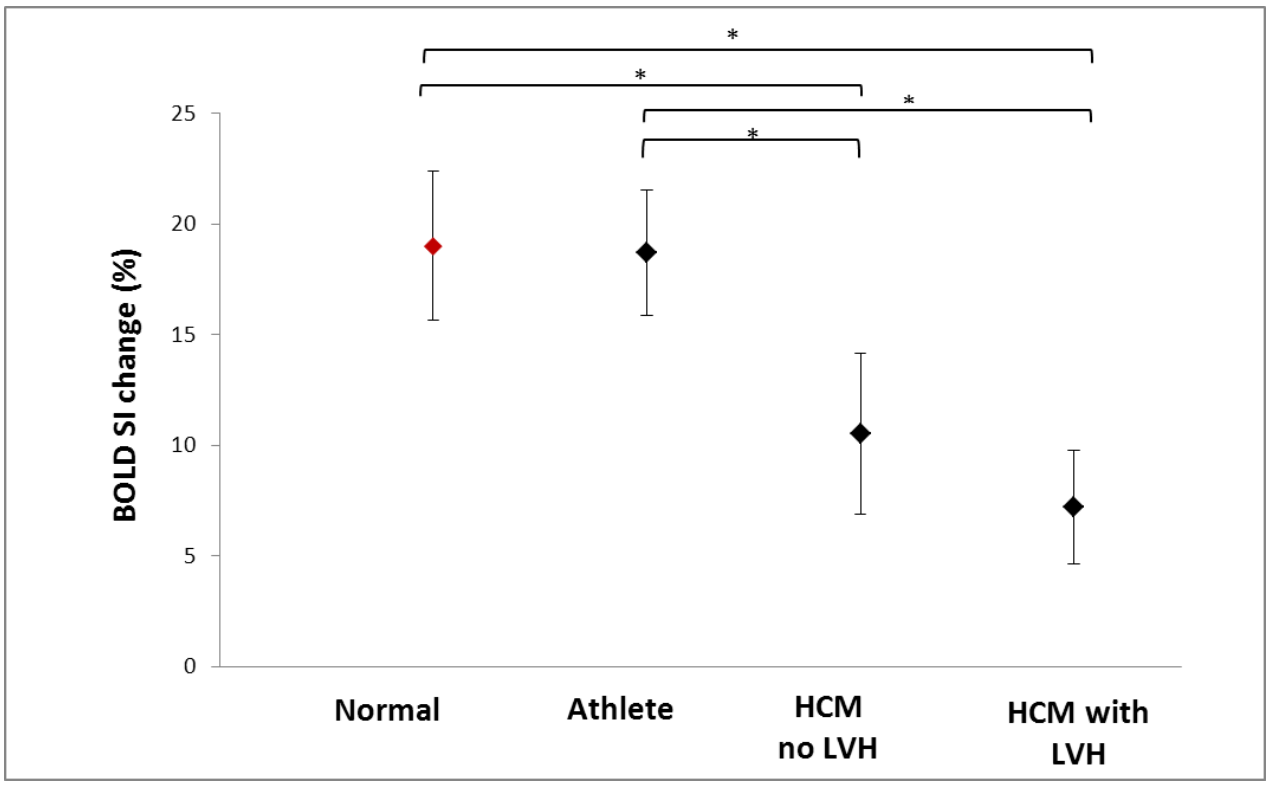



***Figure 6.1****: The mean and standard error of BOLD SIΔ% with adenosine stress in normal, athletes, and HCM patients with and without hypertrophy. * P<0.001 compared to normal; †P<0.001 compared to athletes*.

### *6.3.3 Relationship between BOLD, MPRI and Wall thickness.*

MPRI was significantly reduced in HCM with hypertrophy and conversely, increased in athletes, (normal controls: 1.8 [95% CI: 1.7-2.0]; athletes: 2.0 [95% CI: 1.6-2.5], P=0.29 vs

normal; HCM with hypertrophy: 1.3 [95% CI: 1.1-1.5] P<0.0001 vs. normal controls. However there was no difference in HCM with no hypertrophy: 1.7 [95% CI: 1.4-2.0] P<0.0001 vs. normal controls, figure 6.2.

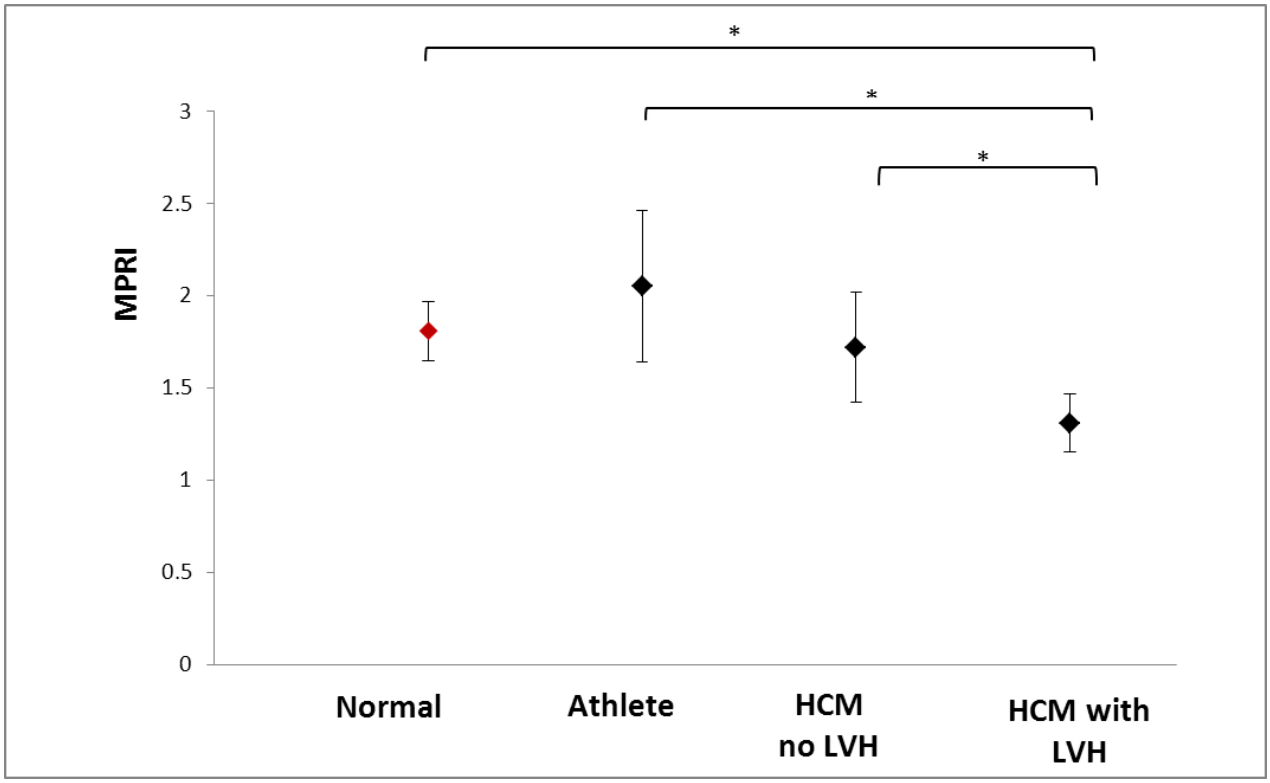



**Figure 6.2**: The mean and standard error of *MPRI with adenosine stress in normal, athlete, HCM with and without hypertrophy. * P<0.001 compared to normal; †P<0.001 compared to athletes; γ P<0.05 compared to HCM with no hypertrophy.*

In all groups, there was a weak but significant correlation between BOLD SIΔ and MPRI per segment, (R=0.27, P<0.0001) and between BOLD SIΔ and end diastolic wall thickness per segment, (R= 0.24, P< 0.001).

Multiple linear regression analysis showed that both MPRI (β 0.2, P<0.001) and wall thickness (β-0.2, P<0.001) are independent predictors of BOLD SI change.

### 6.3.4 Relationship between BOLD, MPRI and energetics in HCM

In HCM, all 35 of the 37 subjects had rest and exercise PCr/ATP (data presented in chapter 5). Using the BOLD SIΔ and MPRI of the mid ventricular septum only (matched to myocardium where the voxel was placed for PCr/ATP measurement), there was no relationship between the percentage change in PCr/ATP during leg exercise and either BOLD SIΔ during adenosine stress (R=0.10, P= NS) or MPRI during adenosine stress, ( R=0.01, P= NS).

Further analysis was performed on those HCM patients (n= 23, 66%) with an identified HCM mutation. In the subgroup with Beta myosin heavy chain mutation (n=12), there was a moderate correlation between percentage change in PCr/ATP with leg exercise and BOLD SIΔ with adenosine exercise (R=0.5, P=0.05). There was no correlation in the myosin binding protein C mutation sub group, (R=0.3, P=NS).MPRI did not correlate with energetic change in either genotyped group.

### 6.3.5 BOLD- CMR as a Diagnostic tool

Although this was not the primary endpoint of this study, I explored the diagnostic performance of BOLD-CMR and whether changes in the BOLD signal during adenosine stress can identify HCM patients. For this analysis the average BOLD signal per heart per subject was used. Receiver operating characteristic (ROC) analysis (figure 6.3) showed that BOLD can predict HCM with excellent sensitivity (94.6%) and modest specificity (58.1) with an area under the ROC curve of 0.765 ± 0.06, P<0.0001 (figure 6.3).In contrast, the

averaged MPRI per heart can predict HCM with 43.2% sensitivity and 87.1% specificity (AUC 0.639±0.07, P=0.04, figure 6.3).

### *6.3.6 BOLD Image quality and inter observer Variability*

No scan was graded as non-analysable. 12% of the segments were excluded from analysis due mainly to off- resonance or breathing artifacts. These artifacts occurred mainly at the anterior and lateral walls at the heart lung interface.

To examine interobserver variability, 5 datasets were randomly selected and analyzed by a second, experienced, blinded operator. There was excellent correlation between the BOLD SIΔ values between the 2 operators, R=0.910, P<0.0001. There was 100% agreement between the two operators on the segments that were to be removed due to artefact (6 segments in this subgroup).

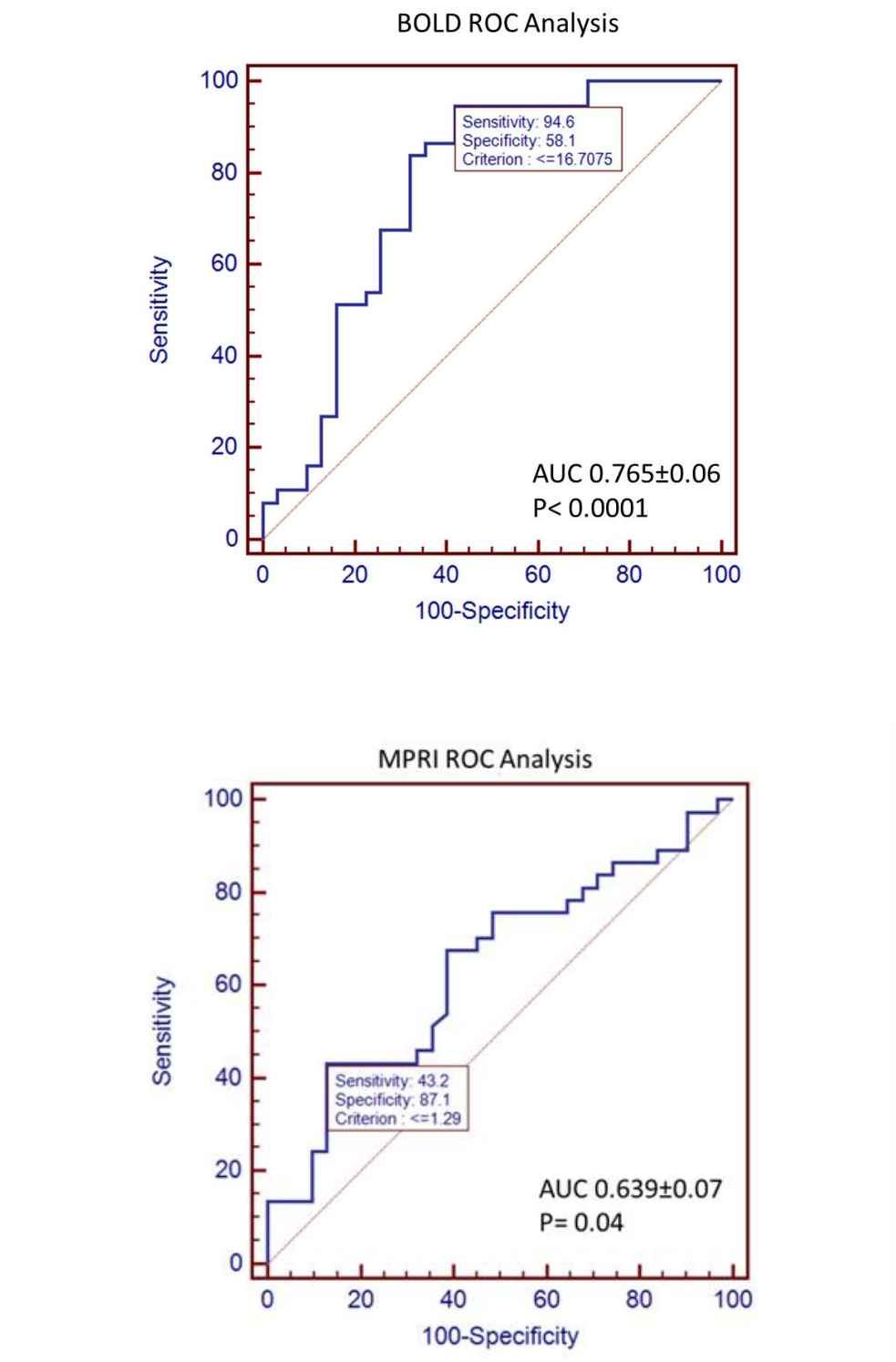



***Figure 6.3:*** *ROC curves for BOLD and MPRI for identifying Normal and athletes vs. HCM.*

# 6.4 Discussion

The main demonstration of this study is the blunted increase in myocardial tissue oxygenation in response to adenosine stress in HCM. Interestingly, this is evident in both HCM with hypertrophy and in pre hypertrophied HCM mutation carriers and does not occur in physiological hypertrophy of athletes. The BOLD SIΔ in this normal population (18.3%) is consistent with previously published values of 17.02% [45] using the same technique , whereas the BOLD changes in HCM (7.9% for patients with LVH,9.8% patients without LVH) are intermediate between normal values and values published for coronary artery stenosis of 3.4%[45]) . Importantly, the average SI change in this HCM population is similar with the BOLD SI values in remote to ischaemia segments in patients with coronary artery disease which are well known to have microvascular dysfunction[45, 117].

The impaired ability to increase and/ or maintain intravascular myocardial oxygenation during vasodilatory stress in HCM is either secondary to a decreased supply or increased demand for oxygen.

## *6.4.1 Decreased Oxygen supply*

This data show two possible mechanisms for decreased oxygen supply in HCM i.e. either microvascular dysfunction or mechanical factors affecting oxygen diffusion.

### *Microvascular dysfunction*

This is a well described phenomenon in HCM[30] and is a strong, independent predictor of clinical deterioration and death[31]. In addition to abnormal BOLD SIΔ, this chapter reports

abnormal perfusion reserve both in the pre hypertrophied and hypertrophied HCM cohorts. It is therefore tempting to link microvascular dysfunction to impaired oxygen supply. To some extent, this is true as this data presented, on a per segment basis, shows a modest but significant correlation between perfusion reserve during stress and oxygenation response to stress. Conversely, in athletes there was an augmented flow response to stress (also described In PET and echocardiographic studies)[118]; however, this did not translate to enhanced oxygenation. In fact, Karamitsos et al described that some degree of dissociation exists between flow and oxygenation, in the setting of coronary artery disease with pronounced epicardial flow disturbances[45]. It is therefore likely that perfusion is not the only determinant of oxygenation in HCM.

### *Mechanical factors affecting oxygen diffusion*

These results demonstrate a reduced BOLD SIΔ with increasing wall thickness.

Myocyte disarray, increased interstitial space and inadequate growth of capillaries as occurs in HCM could potentially affect transfer of oxygen from the capillary to the plasmalemma by increasing diffusion distance.

In the myocardium, the dominating vessels are the capillaries with a volume fraction of more than 90% of the intramyocardial blood volume[119]. Actual loss of myocardial capillaries and defective capillary growth has been demonstrated in HCM in the setting of hypertrophy[120, 121]. Thus the effect of decreased capillary density is increased diffusion

distance. Diffusion in the extracellular space is relatively slow as this compartment lacks an oxygen carrier[122]. Hence with increased diffusion distance, increased demand for oxygen during exercise in an already inefficient energetic system could potentially lead to an increased oxygen extraction fraction from the capillary bed. This potentially accounts for relationship of increasing wall thickness causing a reduced BOLD measure and the finding that wall thickness is an independent predictor of BOLD SIΔ.

### *6.4.2 Increased Oxygen Demand*

The measured blunted increase in oxygenation in HCM may in fact be due to an increase in oxygen demand above that expected for the same level of exercise in a normal heart.

The augmented oxygen demand in HCM during exercise is likely due to the increased energy cost of contraction. It has been proposed that sarcomeric HCM mutations lead to inefficient energy metabolism. *In vitro* and mouse models have shown increased contractility of the mutant myofilaments due to altered myosin kinetics, increased thin filament calcium sensitivity or changes in myosin binding regulation[3, 24] (chapter1). This is further supported by the findings of abnormal resting PCr/ATP ratios in HCM. I report for the first time that this abnormal resting metabolism is further attenuated during physiological exercise (chapter 5). It is therefore possible that this exaggerated increase in ATP demand during exercise explains the augmented increase in oxygen extraction and hence the reduced BOLD signal. The finding of reduced BOLD SIΔ response in even the pre hypertrophied HCM mutation carriers gives further support to this increase oxygen demand

being due to the underlying HCM causing mutation and resulting increased energy cost of contraction.

However, as a group, the data do not show a correlation between the blunted BOLD response and the percentage change in PCr/ATP. This is somewhat surprising as both measures independently show significant reductions in HCM with and without hypertrophy. I believe this is a reflection of the heterogeneity of HCM causing mutations and their differing effects on energy metabolism. This potentially explains why, at this level of stress, in the subgroup with Beta myosin heavy chain mutation, there was a demonstrable relation between oxygen supply and energy demand but not in the myosin binding protein C. In Beta myosin heavy chain mutations, there is generally faster cross bridge turnover rate and apparent gain of protein function[23] ,whereas in myosin binding protein C there is enhanced calcium sensitivity and reduced maximal force-generating capacity of myocytes [123].It is possible that the Beta myosin heavy chain mutations have even more energy wastage during contraction . It is tempting to speculate that perhaps more strenuous exercise may be needed to unmask the energy inefficiency and increased oxygen requirement in myosin binding protein C mutations. However, one must be cautious as the diversity of mutations within genes is great and their energy consequence as well as their clinical translation is varied. Larger studies with both moderate as well as more strenuous exercise are needed to unravel this interesting correlation found in this dataset.

On balance, the blunted BOLD response in HCM is likely due to an intricate interplay between supply and demand rather than exclusively one or the other. There is no doubt

that the energy cost of contraction is increased in HCM regardless of the phenotype. This increased energy demand together with the potential barriers to oxygen supply due to the impaired perfusion and abnormal histology result in an impaired BOLD SI change with exercise.

### *6.4.3 BOLD- CMR as a Diagnostic tool*

This data show that the BOLD technique has the potential to distinguish changes in tissue oxygenation during stress between 1.normal, athletes and 2.HCM. It is a particularly attractive test as it is noninvasive and does not involve radioactive materials or even gadolinium contrast.

BOLD can distinguish between normal controls or athletes and HCM with a sensitivity of 94.6% and specificity of 58.1%. Furthermore, within the HCM cohort, changes are demonstrated in BOLD signal in individuals who have inherited the genetic mutation but have no hypertrophy.

The differential diagnosis between hypertrophy in HCM and Athlete's Heart remains problematic, and often one can only distinguish between these diagnoses by recommending a period of de-training, which most athletes are resistant to. Furthermore, in HCM, with current genetic testing, a mutation cannot be identified in as much as 40% of patients. In these families, it is difficult to conclusively exclude disease in a first degree relative despite a normal looking heart. These individuals are usually offered lifetime clinical follow up. These results propose that by the BOLD stress test, patients with

apparently normal hearts can potentially be diagnosed as having or not having inherited HCM.

All available imaging modalities have been used to find a clear measure to differentiate physiological from pathological hypertrophy. Initial studies focused on geometric differences; however, more recent studies have focused on established and novel functional, metabolic and tissue characteristics[124]. Figure 6.4 schematically details the relative contribution of differing imaging modalities toward a more complete understanding of the physiology in athlete's heart syndrome and figure 6.5 summarizes the differences between HCM and the athlete's heart.

I propose that the oxygenation response of the heart to adenosine stress may provide further insight into the differential diagnosis.

The high sensitivity (94.6%) of the BOLD stress test suggests that a negative result i.e. a normal oxygen response to stress would suggest the absence of disease. However, the test has moderate specificity (58.1%), therefore a positive result i.e. a blunted BOLD response, may suggest the presence of disease but does not confirm the diagnosis. As with any test, the result needs to be interpreted within the clinical context.

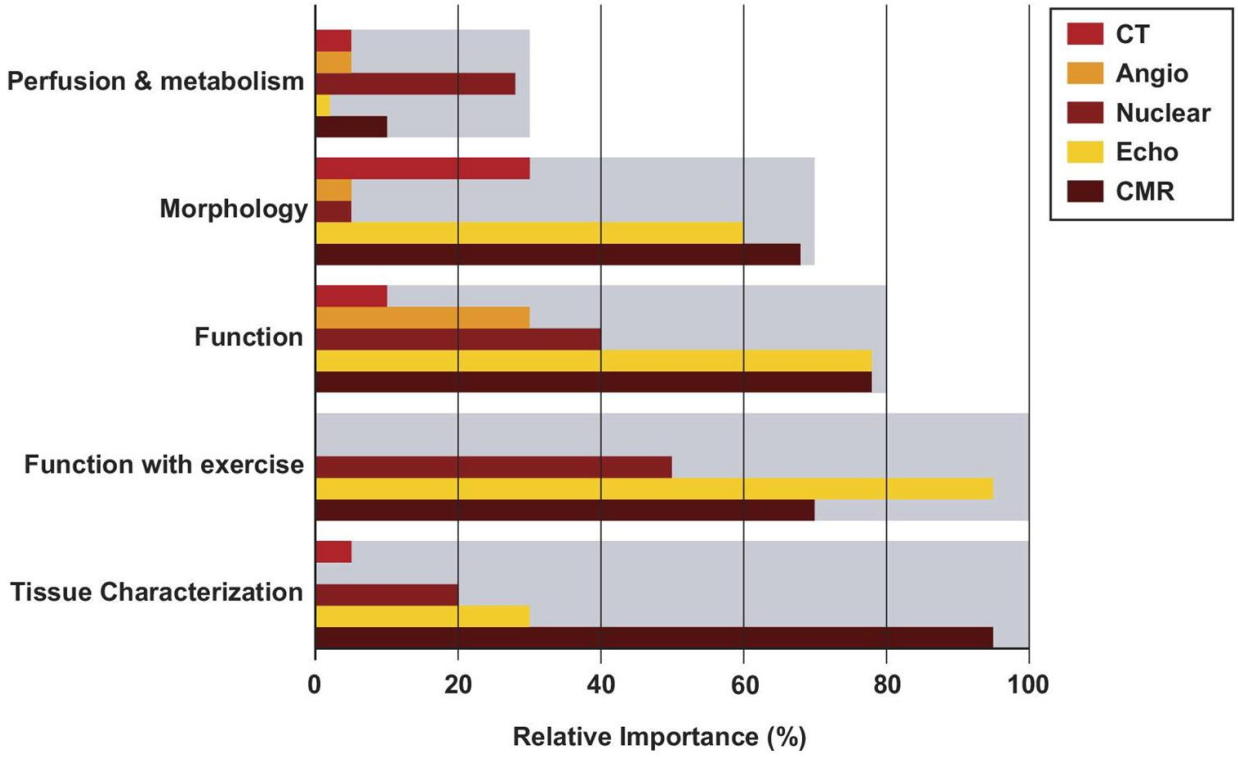



***Figure 6.4***: Demonstrating the progressive importance of function, exercise studies and tissue characterization and detailing the potential for each imaging modality to progress current understanding. Angio :angiography; CMR :cardiac magnetic resonance; CT :computed tomography; Echo: echocardiography (adapted from La Gerche et al[124]).

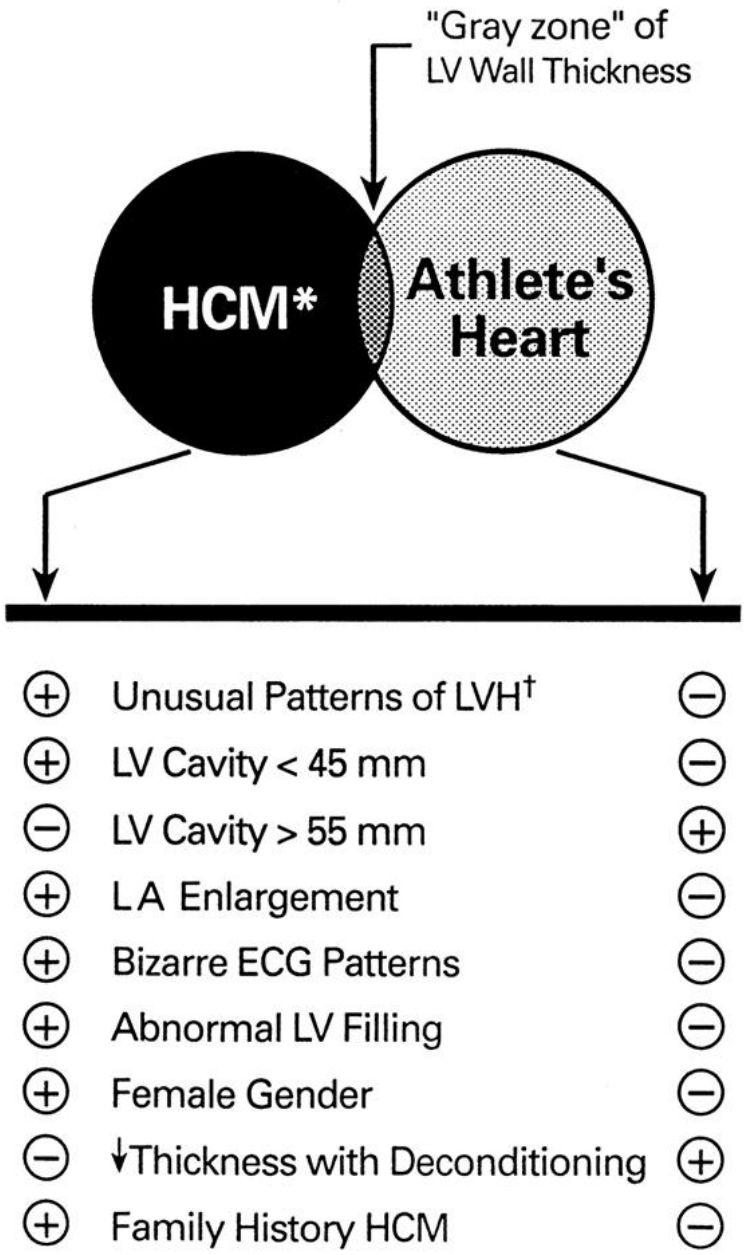



***Figure 6.5*** Criteria for distinguishing an athlete's heart from HCM ( adapted from Maron et al[125]).

However, this is a preliminary analysis of sensitivity and specificity, and larger follow-up studies are needed to fully address the diagnostic performance of BOLD and compare it to

the sensitivity and specificity of other traditional parameters such as wall thickness and diastolic impairment

## 6.5 Conclusion

To my knowledge, this is the first report of myocardial perfusion and oxygenation on a paired segmental basis in HCM. Furthermore, this is the first report of oxygen and cardiac energy change during exercise in HCM.

These results demonstrate a striking blunted oxygenation response of the HCM heart to adenosine stress. This is likely due to an intricate imbalance between oxygen supply and demand and occurs even in the pre hypertrophied HCM mutation carrier. The BOLD test can potentially be a useful addition to the clinician's armamentarium for distinguishing between hypertrophy in the athletes and pathological hypertrophy in HCM and for distinguishing HCM mutation carriers' pre hypertrophy and the normal heart.

## 6.6 Future work

Now that a technique for acquiring and processing exercise spectra has been developed (chapter 3 and 4) and as genetic testing is becoming more common place in clinical practice, it would be interesting to further explore the relationship between specific HCM causing mutations, energy change with exercise and BOLD response. Longitudinal follow-up would provide information about the role of myocardial energetics and BOLD response to risk of sudden death. It is tempting to speculate that increased energy demand coupled

with tissue deoxygenation may trigger cellular pump failure, abnormal calcium handling and ultimately lethal arrhythmias. This is work which our group is currently planning.

# *Chapter 7*
# *Effect of Short Term Exercise Training on Cardiac Function and Cardiac Energy Metabolism in Dilated Cardiomyopathy*

# 7.1 Introduction

Deprivation of cardiac energy has a major role in heart failure. In this condition, changes have been demonstrated in substrate utilisation [90], oxidative phosphorylation[11, 40], and high energy phosphate metabolism[11] ( see chapter 1) . Moreover, myocardial PCr/ATP has been shown to be a predictor of both total and cardiovascular mortality in patients with DCM [10]. As such, energy sparing treatments such as angiotensin converting enzyme inhibitors or beta-blockers[126-128] improve prognosis in heart failure and energy-requiring treatments with catecholamine[129] or phosphodiesterase inhibitors[130] increase mortality. In addition, patients with ischaemic and non-ischaemic cardiomyopathies show a 33% improvement in PCr/ATP ratios with trimetazidine, a substrate modulator which switches energy metabolism from fatty acid to glucose oxidation[131] .

Exercise training regimens are also well established therapies for heart failure patients, which results in reduced heart failure symptoms, improved cardiac function[132, 133],exercise tolerance , perceived quality of life[134] and daily activity levels[135]. Importantly, the composite endpoint of mortality and adverse events may be reduced in exercising subjects compared with sedentary controls[136, 137]. Beer et al demonstrated that exercise training improves cardiac function without adversely affecting metabolism[138] and hence this would suggest that exercise training is an energy-sparing treatment.

Exercise training not only improves peripheral adaptations of haemodynamic, ventilation and autonomic function[139]; it also has direct effects on the myocardium by improving diastolic [140] and systolic function[138].

However, to my knowledge, information oncardiac energetics and function both at rest and during exercise pre and post training has not been examined. These measurements could potentially provide insight into the metabolic response of the failing heart to exercise training and its functional significance. The work in this chapter aims to address this.

# 7.2 Methods

## *7.2.1 Subjects and Protocol*

Seventeen patients with DCM were recruited from outpatient cardiology clinics. Inclusion and exclusion criteria are discussed in chapter 2.

All patients were on maximal tolerated medical therapy, as determined by their cardiologist. NYHA class was determined by their treating team.

Subjects were studied before and after 8 weeks of exercise training (Figure 7.1). One 49 year old male subject with NYHA class IV heart failure withdrew from the trial after one week, stating severe fatigue causing an inability to comply with the exercise regimen. A further male subject aged 52 years old, with NHYA class III heart failure, withdrew after two weeks because of a recurrence of a back injury preventing exercise training. Therefore, 15 subjects were included in the final analyses.

### 7.2.2 Exercise program

Subjects were given an exercise bike for the duration of the study and were instructed to exercise for 30 minutes per day, 5 days per week, aiming to maintain a heart rate commensurate with an 80% of maximal VO2. All exercise was performed as an outpatient on an electrically braked bike ergometer in addition to their usual daily exercise. Warm-up and cool-down periods preceded and followed each exercise session, respectively. Exercise intensity was targeted to maintain a level commensurate with a predetermined heart rate, which was recorded during the exercise. Exercise intensity was progressively increased throughout the 8 week exercise period, on an individualized basis as tolerated.

### 7.2.3 Body weight and composition

The subjects were weighed on arrival at OCMR and their heights were recorded for BMI calculations. Body fat percentages, water percentages, and lean body weights were measured by using a bioimpedance analyser (Bodystat, Douglas, Isle of Man).

### 7.2.4 Measurement of cardiac volumes, mass and function and LGE

Cardiac volumes and function ( chapter 2) were measured using cine SSFP imaging at 3T during rest and after 8 minute of leg raising exercises in the magnet (alternating straight leg flexion at the hip while lying supine). Late gadolinium enhancement CMR was also performed as described in chapter 2.

### 7.2.5 Magnetic resonance spectroscopy of the heart

31P-MRS was used to measure cardiac PCr/ATP. The method, including the exercise protocol is described in chapter 3; the post processing method can be found in chapter 4.

### 7.2.6 Quality of Life Score

Quality of life scores were calculated using the Minnesota Heart Failure Questionnaire (appendix 1), with 21 questions assessing symptoms from heart failure over the previous 4 week period, with scores ranging from 0 (no effect) to 5 (very much affected).

### 7.2.7 6 Minute Walk test

6 minute walk tests were used to determine exercise capacity, with subjects asked to walk a maximum distance during 6 minutes and Borg scores ( appendix 2) were used to assess perceived dyspnea before and at the completion of the 6-minute walk test.
All assessments were repeated after the 8 week training period.

### 7.2.8 Statistics

Statistical analysis was performed by using SPSS (SPSS Inc, Chicago, IL). Values are presented as means + standard errors. Shapiro–Wilk test was used to determine if data were normally distributed. All tested variables were found to be normally distributed. Comparisons were made between pre- and post-exercise regimens using paired student T-tests. Differences were considered significant at $P < 0.05$. A sample size of 14 was chosen to detect a 10% difference in PCr/ATP with an 80% power and an alpha significance of 0.05 (chapter 4.4).

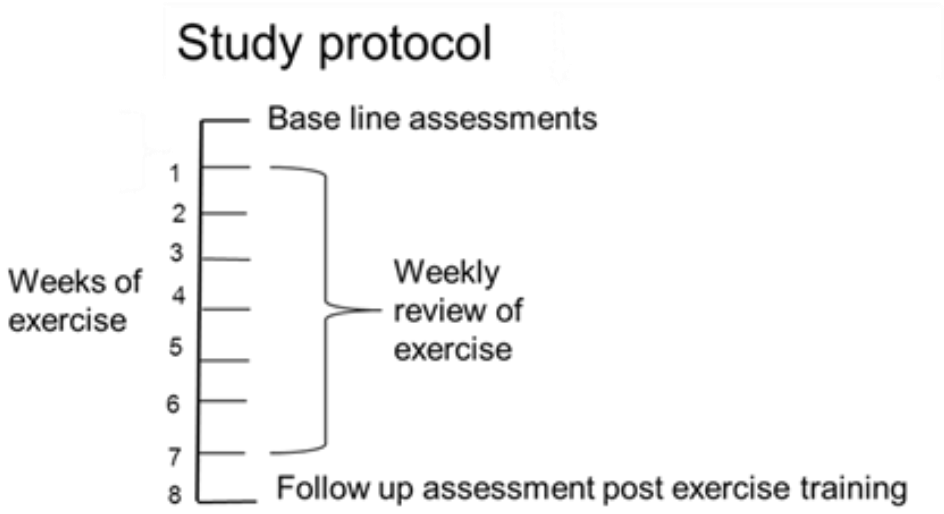



***Figure 7.1**: Time line describing study protocol.*

# 7.3 Results

All subjects remained medically stable over the trial, without any symptoms or signs of worsening heart failure. There were no changes in cardiac medications during the trial. Baseline characteristics for the subjects are presented in Table 7.1.

## *7.3.1 Weight and body composition*

Over the 8 weeks there was no change in total body weight or fat and water composition (Table 7.2).

***Table 7.1:*** *Baseline characteristics of subjects (n = 15)*

| **Baseline characteristics** | |
|---|---|
| Sex | M=8, F=7 |
| Age (years) | 59 ± 2 |
| Weight (kg) | 83 ± 3 |
| BMI | 28 ± 1 |
| NYHA Class 1(n)<br>Class 2(n)<br>Class 3(n)<br>Class 4(n) | 4<br>7<br>4<br>0 |
| Heart Rate (bpm) | 64 ± 4 |
| Blood pressure<br>Systolic (mmHg)<br>Diastolic (mmHg) | <br>135 ± 5<br>67 ± 3 |
| Medications<br>ACE/ARB<br>B-blockers<br>Spironolactone<br>Digoxin<br>Loop diuretic | <br>15 (100%)<br>15 (100%)<br>2 (13%)<br>2 (13%)<br>8 (53%) |

*NYHA; New York Heart Association Class. Bpm; beats per minute. ACE; Angiotensin Converting Enzyme inhibitors, ARB; Angiotensin receptor blocker.*

**Table 7.2:** *Body weight and composition measurements in subjects before and after exercise training*

| | Pre training | Post Training |
|---|---|---|
| Total body weight (kg) | 83 ± 4 | 81 ± 5 |
| Body mass index (kg/m$^2$) | 28 ± 1 | 28 ± 1 |
| Lean body weight (kg) | 56 ± 4 | 54 ± 4 |
| Fat weight (kg) | 28 ± 2 | 27 ± 2 |
| Fat (% of body weight) | 34 ± 2 | 34 ± 2 |
| Water weight (L) | 42 ± 3 | 42 ± 2 |
| Water (% of body weight) | 47 ± 3 | 47 ± 3 |

*Data are means ± SEM, there was no statistical difference between the paired measurements*

## *7.3.2 Haemodynamics*

There was no difference in resting heart rates before and after 8 weeks of exercise training

(61 ± 3 versus 63 ±3 beats per minute, Table 7.3). Moreover, heart rates increased to 84

and 88 beats per minutes with leg raising exercises, before and after the 8 weeks of training, respectively. Rate pressure product increased with leg rising before and after the exercise training, without any effect of exercise training (Table 7.3).

***Table 7.3**: Cardiac parameters before and after training. Cardiac function and ventricular volumes were measured using cardiac magnetic resonance imaging. Cardiac high energy phosphates were measured using cardiac 31P-MR spectroscopy. Diastolic function was measured using transthoracic echocardiography.*

| | Pre-training | | Post-training | |
|---|---|---|---|---|
| | **Rest** | **Leg Raising** | **Rest** | **Leg Raising** |
| *Haemodynamics* | | | | |
| **Heart Rate (bpm)** | 63 ± 3 | 84 ± 3 ††† | 61 ± 3 | 88 ± 5 ††† |
| **Systolic Blood Pressure (mmHg)** | 116 ± 6 | 128 ± 5 | 122 ± 4 | 120 ± 7 |
| **Diastolic Blood Pressure (mmHg)** | 70 ± 3 | 74 ± 3 | 65 ± 3 | 68 ± 3 |
| **Rate Pressure Product (mmHg/min)** | 7510 ± 734 | 10890 ± 753††† | 7325 ± 479 | 10492 ± 770†† |
| **Ejection Fraction (%)** | 39 ± 3 | 41 ± 3 | 44 ± 3** | 49 ± 3† |
| **End diastolic volume (ml)** | 211 ± 26 | 207 ± 25 | 210 ± 26 | 221 ± 31 |
| **End systolic volume (ml)** | 137 ± 23 | 129 ± 22 | 126 ± 22* | 120 ± 23 |
| **Stroke volume (ml)** | 74 ± 4 | 77 ± 4 | 89 ± 7** | 103 ± 9†† |
| **Cardiac Output (L/min)** | 4.6 ± 0.3 | 6.3 ± 0.4 ††† | 5.4 ± 0.5* | 9.0 ± 0.9 ††† |
| **PCr/ATP** | 1.7 ± 0.1 | 1.7 ± 0.1 | 1.7 ± 0.1 | 1.6 ± 0.1 |

*Data are means ± SEM. *p < 0.05, **p < 0.01, †††< 0.001 compared with corresponding pre trial value. Bpm: beats per minute*.

### *7.3.3 Cardiac volumes and function*

Prior to training, leg raising did not significantly alter cardiac volumes or ejection fraction (Table 7.3). After 8 weeks of exercise training, 13 of the 15 subjects had an improvement in resting left ventricular ejection fraction. On average, left ventricular ejection fraction increased from 39% pre-exercise training to 44% after 8 weeks of exercise bike training, (figure 7.2). Interestingly, the 2 patients who did not improve had a relatively high level of baseline physical activity prior to entering the study.

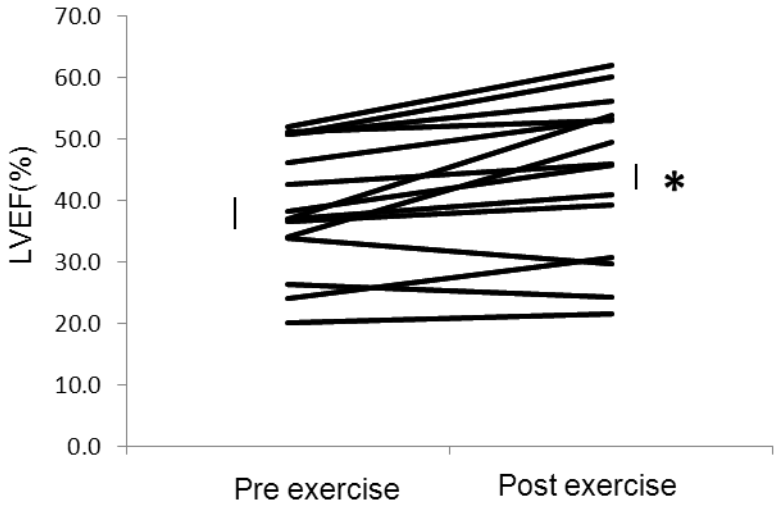



***Figure 7.2****: resting LVEF pre and post exercise training*

Whilst there was no relationship to baseline NYHA class or 6 minute walk test, there was a negative correlation with the amount of exercise performed before entering the trial ($r = -0.62$, $p < 0.05$), indicating more sedentary subjects had the greatest improvement in cardiac function. Moreover, whilst left ventricular ejection fraction did not improve with leg raising at the initial visit (LVEF at rest 39 ± 3% and exercise 41 ± 3%, P= 0.56), after the 8 week training period, global systolic function significantly improved ( LVEF 44 ± 3% to 49 ± 3%, $P < 0.05$), suggesting recruitment of inotropic reserve.

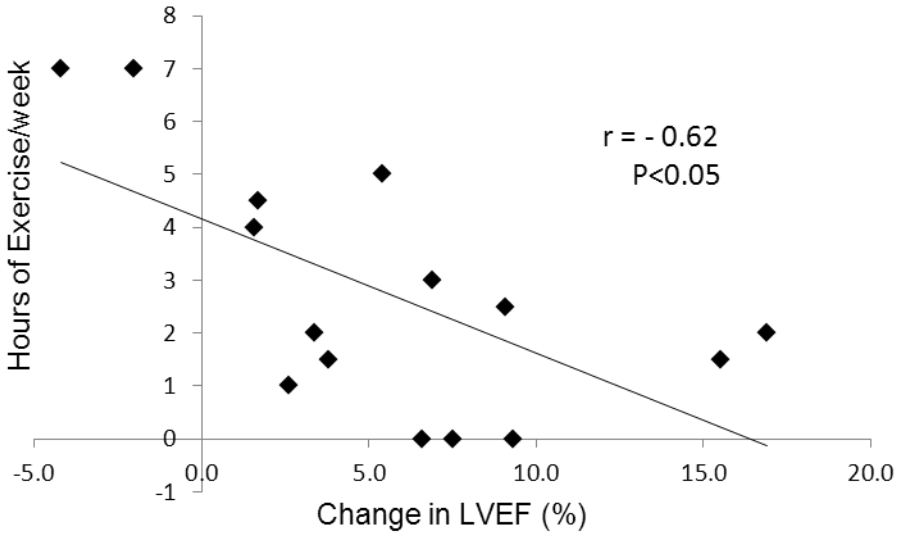



**Figure 7.3:** *Relationship between hours of weekly exercise before starting training and change in resting LVEF pre and post training.*

## *7.3.4 Cardiac Energetics*

Cardiac high energy phosphate metabolism was impaired in all subjects pre-trial, with an average PCr/ATP of 1.71 ± 0.13. Prior to the exercise training, there was no difference in

cardiac PCr/ATP during leg raising (PCr/ATP of 1.7±0.1 during leg raising, P= NS). After the 8 weeks of exercise training, there was again no difference in cardiac PCr/ATP at rest or during leg raising exercises (PCr/ATP 1.7±0.1 and 1.6±0.1, respectively, Table 7.3). Figure 7.4 shows examples of the cardiac spectra in one participant.

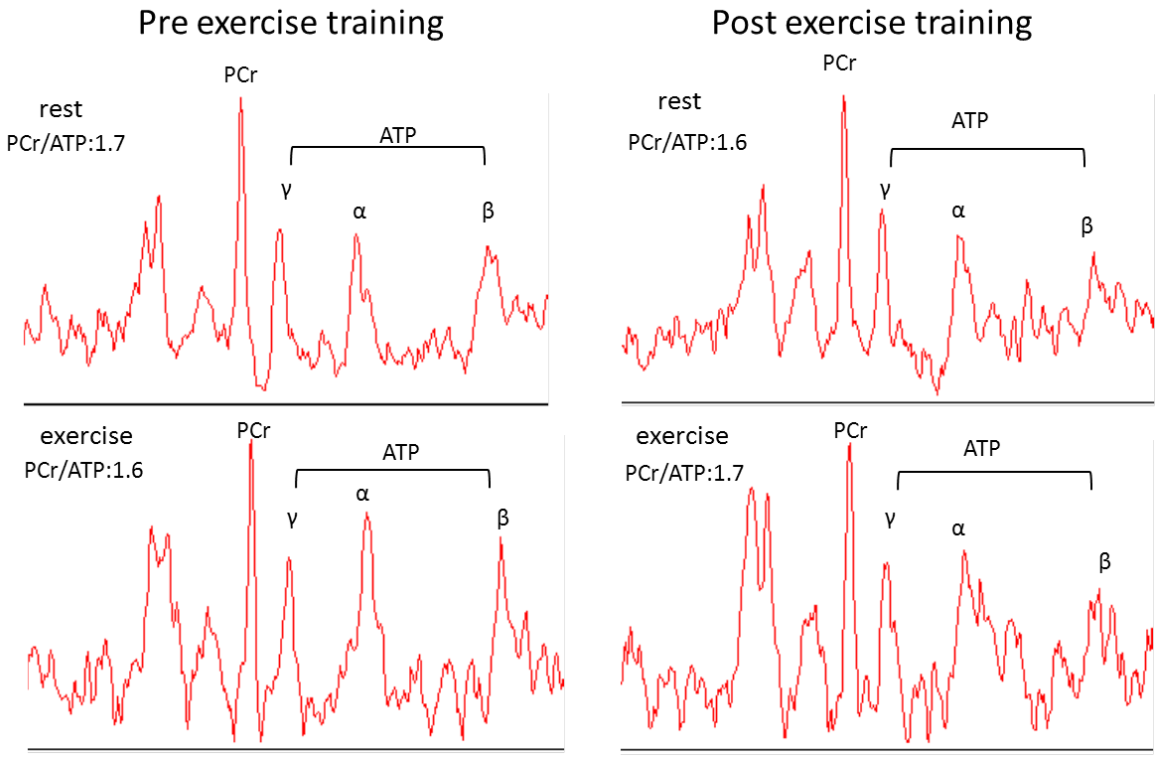



***Figure 7.4**: Spectra measured at rest and during 8 min leg exercise pre and post 8 week exercise training.*

## *7.3.5 Late Gadolinium Enhancement*

In total, 120 slices of LGE images were acquired, (8 per subject from base to apex). Six slices were rejected due to outflow artefacts. Each remaining slice was divided into 6 segments. Thirty percent of the segments were scored as visually having LGE. Figure 7.5 shows some examples of LGE patterns.

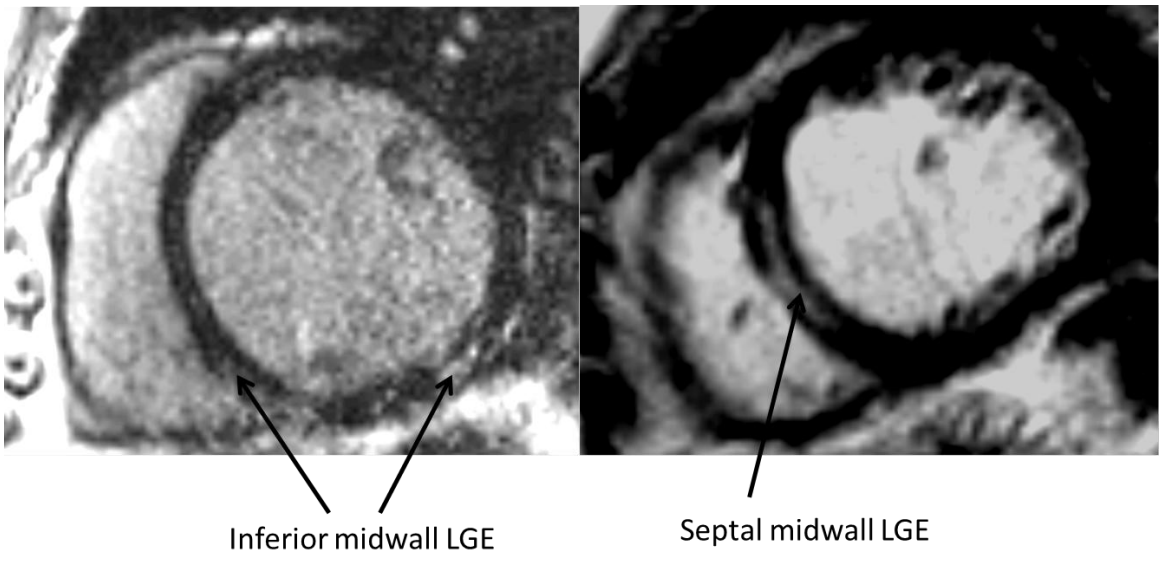



***Figure 7.5****: Examples of LGE patterns observed.*

80% of subjects had LGE, with the range of burden from 6% to 31%. The mean LGE volume fraction of the affected segments per heart was 0.10 ± 0.11. There was no relationship between the LGE burden with resting EF(r=0.05), percentage change in rest EF after training (r = 0.4), or cardiac PCr/ATP(r=0.4).

### *7.3.6 Quality of Life Score*

At baseline subjects had a Minnesota heart failure questionnaire scores averaging 26 ± 5, which did not correlate to NYHA class, 6 minute walk test distance or resting ejection fraction. After the exercise training there was a 28% improvement in the Minnesota heart failure questionnaire, with an average post training score of 17 ± 3 ($p < 0.01$).

### *7.3.7 6 Minute Walk test*

Baseline 6 minute walk tests were mildly impaired, with an average baseline distance of 469 ± 21 m before the exercise training and an 8% improvement to 508 ± 25 m after the 8 weeks of exercise training.

## 7.4 Discussion

This report has shown that patients with DCM pre-training have impaired resting cardiac PCr/ATP; however, this does not decrease further with leg-raising exercises. Whilst there was no improvement in left ventricular ejection fraction with leg raising exercises pre-training, after 8 weeks of exercise training there were significant improvements in both resting and exercise left ventricular function, but no concomitant alterations in cardiac PCr/ATP at rest or during leg-raising. The most sedentary patients had the greatest improvement in resting and exercise left ventricular ejection fraction, suggesting that the improvement in resting function and inotropic reserve may be secondary to reconditioning with no additional energy cost.

The improvement in resting left ventricular ejection fraction is consistent with previous studies showing improved systolic function after 5 and 8 months of training, [132] [133] but this report shows for the first time that significant improvement is expected after only 8 weeks of training. In addition, this report also demonstrates for the first time that not only does resting systolic function improve with training but that ejection fraction during leg raising exercises also improves. This is commensurate with the improvements seen with 6-minute

walk tests and improvement in symptoms, measured by the Minnesota heart failure questionnaire.

It is important to note that left ventricular size, measured by end-diastolic volume, remained unchanged, while end-systolic volume, stroke volumes and ejection fractions all improved. This suggests exercise does not lead to regression of dilation, but may improve conditioning of the diseased myocardium leading to improved function. In fact, there may be a contribution of disuse atrophy in cardiac muscle of patients with health failure. This is supported by the negative correlation seen with the amount of exercise performed at the start of the training period with the change in ejection fraction after the 8 weeks of exercise training. Two subjects who performed 7 hours of exercise per week did not have an improvement in their ejection fractions, whilst sedentary subjects had the greatest improvement. This either suggests that the active subjects had already gained benefit from a high amount of baseline exercise, or sedentary subjects were generally more deconditioned. In line with the latter, it has been long known that the cardiovascular system rapidly adapts to prolonged rest with a reduction in muscle mass, myocardial function and alterations in haemodynamics which can take 8 weeks of training to restore[141].

Perhaps surprisingly, there was no change in cardiac PCr/ATP during exercise pre training. In addition, there was no improvement in rest or exercise myocardial PCr/ATP after the training period. This is consistent with a recent study by Beer et al who investigated the effects of exercise training on resting myocardial function and energetics in dilated

cardiomyopathy and found improvement in left ventricular end-systolic volume and ejection fraction, however no change in resting cardiac energetics. The authors concluded that the absence of deterioration in myocardial energetics suggested that the exercise training was not energy-costly to the myocardium, supporting exercise therapy in dilated cardiomyopathy.

One possible explanation for the observed lack of change in PCr/ATP during exercise in our cohort is the substandard degree of exercise achieved. The average RPP increase was 45% compared with the ≈70% increase achieved in the HCM, athlete and normal cohorts reported in chapter 5. Generally this was a more symptomatic group with low exercise capacity in the MRI. Nevertheless, this level of exercise likely reflects their realistic daily exercise tolerance.

## 7.5 Conclusion

Short-term exercising training in patients with mild to moderate heart failure from DCM, irrespective of the presence of myocardial fibrosis, led to improvements in resting and exercise left ventricular function. Leg raising did not augment left ventricular function before training, but did after 8 weeks of cycle training, suggesting a recruitment of inotropic reserve. Resting and exercise PCr/ATP did not worsen after exercise training. Hence, these results suggest that exercise training has early functional improvements for patients with heart failure with no additional energy cost, and the most sedentary patients may see the greatest improvements.

# *Chapter 8*
# *Summary*

Cardiac $^{31}$P MRS is the only non-invasive in vivo technique for the determination of cardiac high energy phosphate metabolism. Long acquisition times (20 minutes or more, depending on heart rate) required to achieve sufficient signal to noise ratios for reliable interpretation have limited the utility of $^{31}$P MRS studies during exercise or in patients with symptomatic cardiac disease. This work reported on the development of an 8 minute $^{31}$P MRS protocol and demonstrates the validity of this 'short' acquisition by comparison with a 'long' (at least 20 minutes) method of published reproducibility[50]. The reproducibility and application to exercise testing of this novel method were also demonstrated.

Post processing of acquired $^{31}$ P MRS corrects for blood contamination amongst other factors. It was noticed that particularly in hypertrophied hearts there was little blood contamination within the voxel of interest. This lead to a poor fit of 2, 3 DPG and a propagation of this error to the final calculated myocardial PCr/ ATP ratio. This work developed an improved fit for 2, 3 DPG and tested it with both simulated and patient data, including hypertrophied and thinned myocardium. The quality of this outcome was reflected in the power calculations which illustrate an almost 50% reduction of sample size required to statistically demonstrate a physiological change in PCr/ATP with an intervention in HCM and DCM. This new method then explored cardiac energy metabolism at rest and during exercise in both HCM and DCM.

In HCM, the increased cost of energy contraction, due to the effects of the underlying sarcomeric mutation, is well established at rest. This thesis is the first to report on the further worsening of cardiac energetics as measured by PCr/ATP during exercise in HCM.

This is independent of mass or wall thickness or LGE burden. Given these results, it is tempting to speculate that an explanation for the high incidence of exercise-related death in HCM is an acute impairment of myocardial energetics, leading to acute contractile failure, and derangement of ion homeostasis with Ca++ overload and subsequent ventricular fibrillation.

As the determinants of cardiac energetics are multifactorial i.e. apart from the increase in energy demand due to the HCM sarcomeric mutations, it is possible that decrease energy supply may coexist. This thesis explored the relationship between microvascular dysfunction and tissue oxygenation (measured using the BOLD technique) in HCM. To my knowledge, this is the first report of myocardial perfusion and oxygenation on a paired segmental basis in HCM. A modest correlation between these parameters suggested that some degree of dissociation exists between flow and oxygenation.

However, the most striking finding was the blunted increase in myocardial tissue oxygenation in response to adenosine stress in HCM. Interestingly, this is evident in both HCM with hypertrophy and in pre hypertrophied HCM mutation carriers and does not occur in physiological hypertrophy of athletes. Hence, an intricate interplay between oxygen supply and demand must exist in HCM even in the pre hypertrophied mutation carriers and should logically affect cardiac energy supply. This was demonstrated in the Beta myosin heavy chain mutation group where stress oxygenation correlated with change in PCr/ATP during exercise. Furthermore, this thesis proposes that the BOLD test can potentially be a useful tool for distinguishing between hypertrophy in the athletes and pathological

hypertrophy in HCM and for distinguishing HCM mutation carriers' pre hypertrophy and the normal heart. Further large scale studies will be needed to test this hypothesis.

In DCM, the effect of short term exercise training is further clarified i.e. short-term exercising training in patients with mild to moderate heart failure from DCM, irrespective of the presence of myocardial fibrosis, led to improvements in resting and exercise left ventricular function. This suggests a recruitment of inotropic reserve. Resting and exercise PCr/ATP did not worsen after exercise training. Hence, these results suggest that exercise training has early functional improvements for patients with heart failure with no additional energy cost, and the most sedentary patients may see the greatest improvements.

Science has advanced significantly in its understanding of disease mechanisms in both HCM and DCM. This thesis provides further insight into the role of energetics, perfusion and oxygenation in HCM; and energetics and exercise training in DCM. Nonetheless, in search of improved treatments and a possible cure for these conditions, the road ahead still promises to be long.

The answers provided by this body of work stimulate further questions. Perhaps the most compelling of which are the role of BOLD imaging as a diagnostic tool and the use of cardiac energetics at rest and during exercise as a predictor of mortality and morbidity in DCM and HCM. Larger studies are required to investigate BOLD as a tool for differentiating athletes' heart from HCM or normal heart from HCM pre hypertrophy, and these are currently ongoing in our group. Longitudinal follow up is needed to further clarify rest and exercise

PCr/ATP as a means of predicting risk of sudden death, and overall morbidity and mortality in both HCM and DCM.

This work has interrogated aspects of disease pathogenesis in HCM and DCM and has proposed further areas of study. The primary aim of these efforts is to advance our understanding of these cardiomyopathies as we continue to search for a cure for both HCM and DCM.

# Bibliography


1. Watkins H, Ashrafian H, Redwood C. Inherited cardiomyopathies. *N Engl J Med*. 2011;364:1643-1656
2. Towbin JA, Bowles NE. The failing heart. *Nature*. 2002;415:227-233
3. Seidman JG, Seidman C. The genetic basis for cardiomyopathy: From mutation identification to mechanistic paradigms. *Cell*. 2001;104:557-567
4. Crilley JG, Boehm EA, Blair E, Rajagopalan B, Blamire AM, Styles P, McKenna WJ, Ostman-Smith I, Clarke K, Watkins H. Hypertrophic cardiomyopathy due to sarcomeric gene mutations is characterized by impaired energy metabolism irrespective of the degree of hypertrophy. *J Am Coll Cardiol*. 2003;41:1776-1782
5. Jung WI, Sieverding L, Breuer J, Schmidt O, Widmaier S, Bunse M, van Erckelens F, Apitz J, Dietze GJ, Lutz O. Detection of phosphomonoester signals in proton-decoupled 31p nmr spectra of the myocardium of patients with myocardial hypertrophy. *J Magn Reson*. 1998;133:232-235
6. Jung WI, Hoess T, Bunse M, Widmaier S, Sieverding L, Breuer J, Apitz J, Schmidt O, van Erckelens F, Dietze GJ, Lutz O. Differences in cardiac energetics between patients with familial and nonfamilial hypertrophic cardiomyopathy. *Circulation*. 2000;101:E121
7. Shivu GN, Abozguia K, Phan TT, Ahmed I, Henning A, Frenneaux M. (31)p magnetic resonance spectroscopy to measure in vivo cardiac energetics in normal myocardium and hypertrophic cardiomyopathy: European Journal of Radiology. 2010;73:255-259
8. Neubauer S, Krahe T, Schindler R, Horn M, Hillenbrand H, Entzeroth C, Mader H, Kromer EP, Riegger GA, Lackner K, et al. 31p magnetic resonance spectroscopy in dilated cardiomyopathy and coronary artery disease. Altered cardiac high-energy phosphate metabolism in heart failure. *Circulation*. 1992;86:1810-1818
9. Neubauer S, Horn M, Pabst T, Godde M, Lubke D, Jilling B, Hahn D, Ertl G. Contributions of 31p-magnetic resonance spectroscopy to the understanding of dilated heart muscle disease. *Eur Heart J*. 1995;16 Suppl O:115-118
10. Neubauer S, Horn M, Cramer M, Harre K, Newell JB, Peters W, Pabst T, Ertl G, Hahn D, Ingwall JS, Kochsiek K. Myocardial phosphocreatine-to-atp ratio is a predictor of mortality in patients with dilated cardiomyopathy. *Circulation*. 1997;96:2190-2196
11. Neubauer S. The failing heart--an engine out of fuel. *N Engl J Med*. 2007;356:1140-1151
12. Neubauer S, Horn M, Pabst T, Harre K, Stromer H, Bertsch G, Sandstede J, Ertl G, Hahn D, Kochsiek K. Cardiac high-energy phosphate metabolism in patients with aortic valve disease assessed by 31p-magnetic resonance spectroscopy. *J Investig Med*. 1997;45:453-462
13. Sardanelli F, Zandrino F, Molinari G, Cordone S, Delfino L, Levrero F. Magnetic resonance spectroscopy of ischemic heart disease. *Rays*. 1999;24:149-164
14. Okada M, K. M, Inubushi T, Kinoshita M. Influence of aging or left ventricular hypertrophy on the human heart: Contents of phosphorus metabolites measured by 31p mrs. *MRM*. 1998;39:772-782
15. Beer M, Sandstede J, Landschütz W, Seyfarth T, Lipke C, Köstler H, Pabst T, Kenn W, Meininger M, von Kienlin M, Horn M, Harre K, Hahn D, Neubauer S. Absolute concentrations of myocardial high-energy phosphate metabolites in normal, hypertrophied

and failing human myocardium, measured non-invasively with 31p-sloop-magnetic resonance spectroscopy. *J Am Coll Cardiol*. 2002;40:1267-1274

16. Conway MA, Allis J, Ouwerkerk R, Niioka T, Rajagopalan B, Radda GK. Detection of low phosphocreatine to atp ratio in failing hypertrophied human myocardium by 31p magnetic resonance spectroscopy. *Lancet*. 1991;338:973-976
17. Ho CY, Seidman CE. A contemporary approach to hypertrophic cardiomyopathy. *Circulation*. 2006;113:e858-862
18. Maron BJ, Gardin JM, Flack JM, Gidding SS, Kurosaki TT, Bild DE. Prevalence of hypertrophic cardiomyopathy in a general population of young adults. Echocardiographic analysis of 4111 subjects in the cardia study. Coronary artery risk development in (young) adults. *Circulation*. 1995;92:785-789
19. McKenna WJ, Mogensen J, Elliott PM. Role of genotyping in risk factor assessment for sudden death in hypertrophic cardiomyopathy. *J Am Coll Cardiol*. 2002;39:2049-2051
20. Ashrafian H, McKenna WJ, Watkins H. Disease pathways and novel therapeutic targets in hypertrophic cardiomyopathy. *Circ Res*. 2011;109:86-96
21. Van Driest SL, Ellsworth EG, Ommen SR, Tajik AJ, Gersh BJ, Ackerman MJ. Prevalence and spectrum of thin filament mutations in an outpatient referral population with hypertrophic cardiomyopathy. *Circulation*. 2003;108:445-451
22. Ashrafian H, Redwood C, Blair E, Watkins H. Hypertrophic cardiomyopathy:A paradigm for myocardial energy depletion. *Trends Genet*. 2003;19:263-268
23. Ferrantini C, Belus A, Piroddi N, Scellini B, Tesi C, Poggesi C. Mechanical and energetic consequences of hcm-causing mutations. *J Cardiovasc Transl Res*. 2009;2:441-451
24. Redwood CS, Moolman-Smook JC, Watkins H. Properties of mutant contractile proteins that cause hypertrophic cardiomyopathy. *Cardiovasc Res*. 1999;44:20-36
25. Lowey S. Functional consequences of mutations in the myosin heavy chain at sites implicated in familial hypertrophic cardiomyopathy. *Trends Cardiovasc Med*. 2002;12:348-354
26. Bottinelli R, Coviello DA, Redwood CS, Pellegrino MA, Maron BJ, Spirito P, Watkins H, Reggiani C. A mutant tropomyosin that causes hypertrophic cardiomyopathy is expressed in vivo and associated with an increased calcium sensitivity. *Circ Res*. 1998;82:106-115
27. Morimoto S, Nakaura H, Yanaga F, Ohtsuki I. Functional consequences of a carboxyl terminal missense mutation arg278cys in human cardiac troponin t. *Biochem Biophys Res Commun*. 1999;261:79-82
28. Elliott K, Watkins H, Redwood CS. Altered regulatory properties of human cardiac troponin i mutants that cause hypertrophic cardiomyopathy. *J Biol Chem*. 2000;275:22069-22074
29. Sweeney HL, Feng HS, Yang Z, Watkins H. Functional analyses of troponin t mutations that cause hypertrophic cardiomyopathy: Insights into disease pathogenesis and troponin function. *Proc Natl Acad Sci U S A*. 1998;95:14406-14410
30. Petersen SE, Jerosch-Herold M, Hudsmith LE, Robson MD, Francis JM, Doll HA, Selvanayagam JB, Neubauer S, Watkins H. Evidence for microvascular dysfunction in hypertrophic cardiomyopathy: New insights from multiparametric magnetic resonance imaging. *Circulation*. 2007;115:2418-2425
31. Cecchi F, Olivotto I, Gistri R, Lorenzoni R, Chiriatti G, Camici PG. Coronary microvascular dysfunction and prognosis in hypertrophic cardiomyopathy. *N Engl J Med*. 2003;349:1027-1035
32. Camici P, Chiriatti G, Lorenzoni R, Bellina RC, Gistri R, Italiani G, Parodi O, Salvadori PA, Nista N, Papi L, et al. Coronary vasodilation is impaired in both hypertrophied and

nonhypertrophied myocardium of patients with hypertrophic cardiomyopathy: A study with nitrogen-13 ammonia and positron emission tomography. *J Am Coll Cardiol*. 1991;17:879-886

33. Perrone-Filardi P, Bacharach SL, Dilsizian V, Panza JA, Maurea S, Bonow RO. Regional systolic function, myocardial blood flow and glucose uptake at rest in hypertrophic cardiomyopathy. *Am J Cardiol*. 1993;72:199-204
34. Basso C, Thiene G, Corrado D, Buja G, Melacini P, Nava A. Hypertrophic cardiomyopathy and sudden death in the young: Pathologic evidence of myocardial ischemia. *Hum Pathol*. 2000;31:988-998
35. Varnava AM, Elliott PM, Sharma S, McKenna WJ, Davies MJ. Hypertrophic cardiomyopathy: The interrelation of disarray, fibrosis, and small vessel disease. *Heart*. 2000;84:476-482
36. Marcus ML, Harrison DG, Chilian WM, Koyanagi S, Inou T, Tomanek RJ, Martins JB, Eastham CL, Hiratzka LF. Alterations in the coronary circulation in hypertrophied ventricles. *Circulation*. 1987;75:I19-25
37. National heart failure audit. 2010
38. Assomull RG, Prasad SK, Lyne J, Smith G, Burman ED, Khan M, Sheppard MN, Poole-Wilson PA, Pennell DJ. Cardiovascular magnetic resonance, fibrosis, and prognosis in dilated cardiomyopathy. *J Am Coll Cardiol*. 2006;48:1977-1985
39. Jefferies JL, Towbin JA. Dilated cardiomyopathy. *Lancet*. 2010;375:752-762
40. Ide T, Tsutsui H, Hayashidani S, Kang D, Suematsu N, Nakamura K, Utsumi H, Hamasaki N, Takeshita A. Mitochondrial DNA damage and dysfunction associated with oxidative stress in failing hearts after myocardial infarction. *Circ Res*. 2001;88:529-535
41. Bottomley PA, Ouwerkerk R, Lee RF, Weiss RG. Four-angle saturation transfer (fast) method for measuring creatine kinase reaction rates in vivo. *Magn Reson Med*. 2002;47:850-863
42. Grove TH, Ackerman JJ, Radda GK, Bore PJ. Analysis of rat heart in vivo by phosphorus nuclear magnetic resonance. *Proc Natl Acad Sci U S A*. 1980;77:299-302
43. Bottomley PA. Noninvasive study of high-energy phosphate metabolism in human heart by depth-resolved 31p nmr spectroscopy. *Science*. 1985;229:769-772
44. Pennell DJ, Sechtem UP, Higgins CB, Manning WJ, Pohost GM, Rademakers FE, van Rossum AC, Shaw LJ, Yucel EK. Clinical indications for cardiovascular magnetic resonance (cmr): Consensus panel report. *J Cardiovasc Magn Reson*. 2004;6:727-765
45. Karamitsos TD, Leccisotti L, Arnold JR, Recio-Mayoral A, Bhamra-Ariza P, Howells RK, Searle N, Robson MD, Rimoldi OE, Camici PG, Neubauer S, Selvanayagam JB. Relationship between regional myocardial oxygenation and perfusion in patients with coronary artery disease: Insights from cardiovascular magnetic resonance and positron emission tomography. *Circ Cardiovasc Imaging*. 2010;3:32-40
46. Sharma P, Socolow J, Patel S, Pettigrew RI, Oshinski JN. Effect of gd-dtpa-bma on blood and myocardial t1 at 1.5t and 3t in humans. *J Magn Reson Imaging*. 2006;23:323-330
47. Jerosch-Herold M, Seethamraju RT, Swingen CM, Wilke NM, Stillman AE. Analysis of myocardial perfusion mri. *J Magn Reson Imaging*. 2004;19:758-770
48. Nagel E, Klein C, Paetsch I, Hettwer S, Schnackenburg B, Wegscheider K, Fleck E. Magnetic resonance perfusion measurements for the noninvasive detection of coronary artery disease. *Circulation*. 2003;108:432-437
49. Al-Saadi N, Nagel E, Gross M, Bornstedt A, Schnackenburg B, Klein C, Klimek W, Oswald H, Fleck E. Noninvasive detection of myocardial ischemia from perfusion reserve based on cardiovascular magnetic resonance. *Circulation*. 2000;101:1379-1383

50. Tyler DJ, Emmanuel Y, Cochlin LE, Hudsmith LE, Holloway CJ, Neubauer S, Clarke K, Robson MD. Reproducibility of 31p cardiac magnetic resonance spectroscopy at 3 t. *NMR Biomed*. 2009;22:405-413
51. Holloway CJ, Cochlin LE, Emmanuel Y, Murray A, Codreanu I, Edwards LM, Szmigielski C, Tyler DJ, Knight NS, Saxby BK, Lambert B, Thompson C, Neubauer S, Clarke K. A high-fat diet impairs cardiac high-energy phosphate metabolism and cognitive function in healthy human subjects. *Am J Clin Nutr*. 2011;93:748-755
52. Holloway CJ, Montgomery HE, Murray AJ, Cochlin LE, Codreanu I, Hopwood N, Johnson AW, Rider OJ, Levett DZ, Tyler DJ, Francis JM, Neubauer S, Grocott MP, Clarke K. Cardiac response to hypobaric hypoxia: Persistent changes in cardiac mass, function, and energy metabolism after a trek to mt. Everest base camp. *FASEB J*. 2010;25:792-796
53. Hudsmith LE, Tyler DJ, Emmanuel Y, Petersen SE, Francis JM, Watkins H, Clarke K, Robson MD, Neubauer S. (31)p cardiac magnetic resonance spectroscopy during leg exercise at 3 tesla. *Int J Cardiovasc Imaging*. 2009;25:819-826
54. Pohmann R, von Kienlin M. Accurate phosphorus metabolite images of the human heart by 3d acquisition-weighted csi. *Magn Reson Med*. 2001;45:817-826
55. Robson MD, Tyler DJ, Neubauer S. Ultrashort te chemical shift imaging (ute-csi). *Magn Reson Med*. 2005;53:267-274
56. Naressi A, Couturier C, Castang I, de Beer R, Graveron-Demilly D. Java-based graphical user interface for mrui, a software package for quantitation of in vivo/medical magnetic resonance spectroscopy signals. *Comput Biol Med*. 2001;31:269-286
57. Naressi A, Couturier C, Devos JM, Janssen M, Mangeat C, de Beer R, Graveron-Demilly D. Java-based graphical user interface for the mrui quantitation package. *MAGMA*. 2001;12:141-152
58. Bottomley PA, Ouwerkerk R. Optimum flip-angles for exciting nmr with uncertain t1 values. *Magn Reson Med*. 1994;32:137-141
59. Blamire AM, Rajagopalan B, Radda GK. Measurement of myocardial ph by saturation transfer in man. *Magnetic Resonance in Medicine*. 1999;41:198-203
60. Lamb HJ, Doornbos J, denHollander JA, Luyten PR, Beyerbacht HP, vanderWall EE, deRoos A. Reproducibility of human cardiac p-31-nmr spectroscopy. *Nmr in Biomedicine*. 1996;9:217-227
61. Weiss RG, Bottomley PA, Hardy CJ, Gerstenblith G. Regional myocardial metabolism of high-energy phosphates during isometric exercise in patients with coronary artery disease. *N Engl J Med*. 1990;323:1593-1600
62. Buchthal SD, den Hollander JA, Merz CN, Rogers WJ, Pepine CJ, Reichek N, Sharaf BL, Reis S, Kelsey SF, Pohost GM. Abnormal myocardial phosphorus-31 nuclear magnetic resonance spectroscopy in women with chest pain but normal coronary angiograms. *N Engl J Med*. 2000;342:829-835
63. Yabe T, Mitsunami K, Okada M, Morikawa S, Inubushi T, Kinoshita M. Detection of myocardial ischemia by 31p magnetic resonance spectroscopy during handgrip exercise. *Circulation*. 1994;89:1709-1716
64. Schmidt O, Bunse M, Dietze GJ, Lutz O, Jung WI. Unveiling extracellular inorganic phosphate signals from blood in human cardiac 31p nmr spectra. *J Cardiovasc Magn Reson*. 2001;3:325-329
65. Labotka RJ, Glonek T, Hruby MA, Honig GR. Phosphorus-31 spectroscopic determinations of the phosphorus metabolite profiles of blood components: Erythrocytes, reticulocytes, and platelets. *Biochem Med*. 1976;15:311-329

66. Petersen A, Jacobsen JP, Horder M. 31p nmr measurements of intracellular ph and 2,3-diphosphoglycerate in erythrocytes. *Scand J Clin Lab Invest*. 1987;47:233-237
67. Lam Y, Lin A, Ho C. A phosphorus- 31 nuclear magnetic resonance investigation of intracellular environment in human normal and sickle cell blood. *Blood*. 1979;54:196-209
68. van den Boogaart A, Howe FA, Rodrigues LM, Stubbs M, Griffiths JR. In vivo 31p mrs: Absolute concentrations, signal-to-noise and prior knowledge. *NMR Biomed*. 1995;8:87-93
69. Gunal N, Saraclar M, Ozkutlu S, Senocak F, Topaloglu H, Karaaslan S. Heart disease in friedreich's ataxia: A clinical and echocardiographic study. *Acta Paediatr Jpn*. 1996;38:308-311
70. Unverferth DV, Schmidt WR, 2nd, Baker PB, Wooley CF. Morphologic and functional characteristics of the heart in friedreich's ataxia. *Am J Med*. 1987;82:5-10
71. Merante F, Tein I, Benson L, Robinson BH. Maternally inherited hypertrophic cardiomyopathy due to a novel t-to-c transition at nucleotide 9997 in the mitochondrial trna(glycine) gene. *Am J Hum Genet*. 1994;55:437-446
72. Tanaka T, Sohmiya K, Kawamura K. Is cd36 deficiency an etiology of hereditary hypertrophic cardiomyopathy? *J Mol Cell Cardiol*. 1997;29:121-127
73. Aoyama T, Souri M, Ushikubo S, Kamijo T, Yamaguchi S, Kelley RI, Rhead WJ, Uetake K, Tanaka K, Hashimoto T. Purification of human very-long-chain acyl-coenzyme a dehydrogenase and characterization of its deficiency in seven patients. *J Clin Invest*. 1995;95:2465-2473
74. Hardie DG, Carling D. The amp-activated protein kinase--fuel gauge of the mammalian cell? *Eur J Biochem*. 1997;246:259-273
75. Gollob MH, Green MS, Tang AS, Gollob T, Karibe A, Ali Hassan AS, Ahmad F, Lozado R, Shah G, Fananapazir L, Bachinski LL, Roberts R. Identification of a gene responsible for familial wolff-parkinson-white syndrome. *N Engl J Med*. 2001;344:1823-1831
76. Blair E, Redwood C, Ashrafian H, Oliveira M, Broxholme J, Kerr B, Salmon A, Ostman-Smith I, Watkins H. Mutations in the gamma(2) subunit of amp-activated protein kinase cause familial hypertrophic cardiomyopathy: Evidence for the central role of energy compromise in disease pathogenesis. *Hum Mol Genet*. 2001;10:1215-1220
77. Javadpour MM, Tardiff JC, Pinz I, Ingwall JS. Decreased energetics in murine hearts bearing the r92q mutation in cardiac troponin t. *J Clin Invest*. 2003;112:768-775
78. Spindler M, Saupe KW, Christe ME, Sweeney HL, Seidman CE, Seidman JG, Ingwall JS. Diastolic dysfunction and altered energetics in the alphamhc403/+ mouse model of familial hypertrophic cardiomyopathy. *J Clin Invest*. 1998;101:1775-1783
79. Jung WI, Sieverding L, Breuer J, Hoess T, Widmaier S, Schmidt O, Bunse M, van Erckelens F, Apitz J, Lutz O, Dietze GJ. 31p nmr spectroscopy detects metabolic abnormalities in asymptomatic patients with hypertrophic cardiomyopathy. *Circulation*. 1998;97:2536-2542
80. de Roos A, Doornbos J, Luyten PR, Oosterwaal LJ, van der Wall EE, den Hollander JA. Cardiac metabolism in patients with dilated and hypertrophic cardiomyopathy: Assessment with proton-decoupled p-31 mr spectroscopy. *J Magn Reson Imaging*. 1992;2:711-719
81. Sieverding L, Jung WI, Breuer J, Widmaier S, Staubert A, van Erckelens F, Schmidt O, Bunse M, Hoess T, Lutz O, Dietze GJ, Apitz J. Proton-decoupled myocardial 31p nmr spectroscopy reveals decreased pcr/pi in patients with severe hypertrophic cardiomyopathy. *Am J Cardiol*. 1997;80:34A-40A
82. Abozguia K, Elliott P, McKenna W, Phan TT, Nallur-Shivu G, Ahmed I, Maher AR, Kaur K, Taylor J, Henning A, Ashrafian H, Watkins H, Frenneaux M. Metabolic modulator perhexiline

corrects energy deficiency and improves exercise capacity in symptomatic hypertrophic cardiomyopathy. *Circulation*. 2010;122:1562-1569

83. Esposito A, De Cobelli F, Perseghin G, Pieroni M, Belloni E, Mellone R, Canu T, Gentinetta F, Scifo P, Chimenti C, Frustaci A, Luzi L, Maseri A, Maschio AD. Impaired left ventricular energy metabolism in patients with hypertrophic cardiomyopathy is related to the extension of fibrosis at delayed gadolinium-enhanced magnetic resonance imaging. *Heart*. 2009;95:228-233
84. Lamb HJ, Beyerbacht HP, Ouwerkerk R, Doornbos J, Pluim BM, van der Wall EE, van der Laarse A, de Roos A. Metabolic response of normal human myocardium to high-dose atropine-dobutamine stress studied by 31p-mrs. *Circulation*. 1997;96:2969-2977
85. Pluim BM, Lamb HJ, Kayser HW, Leujes F, Beyerbacht HP, Zwinderman AH, van der Laarse A, Vliegen HW, de Roos A, van der Wall EE. Functional and metabolic evaluation of the athlete's heart by magnetic resonance imaging and dobutamine stress magnetic resonance spectroscopy. *Circulation*. 1998;97:666-672
86. Lamb HJ, Beyerbacht HP, van der Laarse A, Stoel BC, Doornbos J, van der Wall EE, de Roos A. Diastolic dysfunction in hypertensive heart disease is associated with altered myocardial metabolism. *Circulation*. 1999;99:2261-2267
87. Morimoto S, Ohtsuki I. [calcium regulation of contraction and relaxation in skeletal muscle]. *Tanpakushitsu Kakusan Koso*. 1998;43:1744-1752
88. Unno K, Isobe S, Izawa H, Cheng XW, Kobayashi M, Hirashiki A, Yamada T, Harada K, Ohshima S, Noda A, Nagata K, Kato K, Yokota M, Murohara T. Relation of functional and morphological changes in mitochondria to myocardial contractile and relaxation reserves in asymptomatic to mildly symptomatic patients with hypertrophic cardiomyopathy. *Eur Heart J*. 2009;30:1853-1862
89. Lucas DT, Aryal P, Szweda LI, Koch WJ, Leinwand LA. Alterations in mitochondrial function in a mouse model of hypertrophic cardiomyopathy. *Am J Physiol Heart Circ Physiol*. 2003;284:H575-583
90. Kalsi KK, Smolenski RT, Pritchard RD, Khaghani A, Seymour AM, Yacoub MH. Energetics and function of the failing human heart with dilated or hypertrophic cardiomyopathy. *Eur J Clin Invest*. 1999;29:469-477
91. Shen W, Asai K, Uechi M, Mathier MA, Shannon RP, Vatner SF, Ingwall JS. Progressive loss of myocardial atp due to a loss of total purines during the development of heart failure in dogs: A compensatory role for the parallel loss of creatine. *Circulation*. 1999;100:2113-2118
92. Ingwall JS, Kramer MF, Fifer MA, Lorell BH, Shemin R, Grossman W, Allen PD. The creatine kinase system in normal and diseased human myocardium. *N Engl J Med*. 1985;313:1050-1054
93. Neubauer S, Horn M, Naumann A, Tian R, Hu K, Laser M, Friedrich J, Gaudron P, Schnackerz K, Ingwall JS, et al. Impairment of energy metabolism in intact residual myocardium of rat hearts with chronic myocardial infarction. *J Clin Invest*. 1995;95:1092-1100
94. Frenneaux MP, Porter A, Caforio AL, Odawara H, Counihan PJ, McKenna WJ. Determinants of exercise capacity in hypertrophic cardiomyopathy. *J Am Coll Cardiol*. 1989;13:1521-1526
95. Nihoyannopoulos P, Karatasakis G, Frenneaux M, McKenna WJ, Oakley CM. Diastolic function in hypertrophic cardiomyopathy: Relation to exercise capacity. *J Am Coll Cardiol*. 1992;19:536-540
96. Okeie K, Shimizu M, Yoshio H, Ino H, Yamaguchi M, Matsuyama T, Yasuda T, Taki J, Mabuchi H. Left ventricular systolic dysfunction during exercise and dobutamine stress in patients with hypertrophic cardiomyopathy. *J Am Coll Cardiol*. 2000;36:856-863

97. Werner GS, Jandt E, Krack A, Schwarz G, Mutschke O, Kuethe F, Ferrari M, Figulla HR. Growth factors in the collateral circulation of chronic total coronary occlusions: Relation to duration of occlusion and collateral function. *Circulation*. 2004;110:1940-1945
98. Werner GS, Ferrari M, Betge S, Gastmann O, Richartz BM, Figulla HR. Collateral function in chronic total coronary occlusions is related to regional myocardial function and duration of occlusion. *Circulation*. 2001;104:2784-2790
99. Panting JR, Gatehouse PD, Yang GZ, Grothues F, Firmin DN, Collins P, Pennell DJ. Abnormal subendocardial perfusion in cardiac syndrome x detected by cardiovascular magnetic resonance imaging. *N Engl J Med*. 2002;346:1948-1953
100. Cannon RO, 3rd, Schenke WH, Maron BJ, Tracy CM, Leon MB, Brush JE, Jr., Rosing DR, Epstein SE. Differences in coronary flow and myocardial metabolism at rest and during pacing between patients with obstructive and patients with nonobstructive hypertrophic cardiomyopathy. *J Am Coll Cardiol*. 1987;10:53-62
101. Li D, Dhawale P, Rubin PJ, Haacke EM, Gropler RJ. Myocardial signal response to dipyridamole and dobutamine: Demonstration of the bold effect using a double-echo gradient-echo sequence. *Magn Reson Med*. 1996;36:16-20
102. Fieno DS, Shea SM, Li Y, Harris KR, Finn JP, Li D. Myocardial perfusion imaging based on the blood oxygen level-dependent effect using t2-prepared steady-state free-precession magnetic resonance imaging. *Circulation*. 2004;110:1284-1290
103. Han JS, Mikulis DJ, Mardimae A, Kassner A, Poublanc J, Crawley AP, deVeber GA, Fisher JA, Logan WJ. Measurement of cerebrovascular reactivity in pediatric patients with cerebral vasculopathy using blood oxygen level-dependent mri. *Stroke*. 2011;42:1261-1269
104. Mandell DM, Han JS, Poublanc J, Crawley AP, Stainsby JA, Fisher JA, Mikulis DJ. Mapping cerebrovascular reactivity using blood oxygen level-dependent mri in patients with arterial steno-occlusive disease: Comparison with arterial spin labeling mri. *Stroke*. 2008;39:2021-2028
105. Rao SM, Salmeron BJ, Durgerian S, Janowiak JA, Fischer M, Risinger RC, Conant LL, Stein EA. Effects of methylphenidate on functional mri blood-oxygen-level-dependent contrast. *Am J Psychiatry*. 2000;157:1697-1699
106. Ziyeh S, Rick J, Reinhard M, Hetzel A, Mader I, Speck O. Blood oxygen level-dependent mri of cerebral co2 reactivity in severe carotid stenosis and occlusion. *Stroke*. 2005;36:751-756
107. Forster BB, MacKay AL, Whittall KP, Kiehl KA, Smith AM, Hare RD, Liddle PF. Functional magnetic resonance imaging: The basics of blood-oxygen-level dependent (bold) imaging. *Can Assoc Radiol J*. 1998;49:320-329
108. Towse TF, Slade JM, Meyer RA. Effect of physical activity on mri-measured blood oxygen level-dependent transients in skeletal muscle after brief contractions. *J Appl Physiol*. 2005;99:715-722
109. Utz W, Jordan J, Niendorf T, Stoffels M, Luft FC, Dietz R, Friedrich MG. Blood oxygen level-dependent mri of tissue oxygenation: Relation to endothelium-dependent and endothelium-independent blood flow changes. *Arterioscler Thromb Vasc Biol*. 2005;25:1408-1413
110. Vohringer M, Flewitt JA, Green JD, Dharmakumar R, Wang J, Jr., Tyberg JV, Friedrich MG. Oxygenation-sensitive cmr for assessing vasodilator-induced changes of myocardial oxygenation. *J Cardiovasc Magn Reson*. 2010;12:20
111. Egred M, Waiter GD, Al-Mohammad A, Semple SI, Redpath TW, Walton S. Blood oxygen level dependent (bold) mri: A novel technique for the detection of myocardial ischemia. *Eur J Intern Med*. 2006;17:551-555

112. Egred M, Waiter GD, Redpath TW, Semple SK, Al-Mohammad A, Walton S. Blood oxygen level-dependent (bold) mri: A novel technique for the assessment of myocardial ischemia as identified by nuclear imaging spect. *Eur J Intern Med*. 2007;18:581-586
113. Dharmakumar R, Arumana JM, Tang R, Harris K, Zhang Z, Li D. Assessment of regional myocardial oxygenation changes in the presence of coronary artery stenosis with balanced ssfp imaging at 3.0 t: Theory and experimental evaluation in canines. *J Magn Reson Imaging*. 2008;27:1037-1045
114. Murakami Y, Zhang Y, Cho YK, Mansoor AM, Chung JK, Chu C, Francis G, Ugurbil K, Bache RJ, From AH, Jerosch-Herold M, Wilke N, Zhang J. Myocardial oxygenation during high work states in hearts with postinfarction remodeling. *Circulation*. 1999;99:942-948
115. Beache GM, Herzka DA, Boxerman JL, Post WS, Gupta SN, Faranesh AZ, Solaiyappan M, Bottomley PA, Weiss JL, Shapiro EP, Hill MN. Attenuated myocardial vasodilator response in patients with hypertensive hypertrophy revealed by oxygenation-dependent magnetic resonance imaging. *Circulation*. 2001;104:1214-1217
116. Bauer WR, Nadler W, Bock M, Schad LR, Wacker C, Hartlep A, Ertl G. The relationship between the bold-induced t(2) and t(2)(*): A theoretical approach for the vasculature of myocardium. *Magn Reson Med*. 1999;42:1004-1010
117. Uren NG, Marraccini P, Gistri R, de Silva R, Camici PG. Altered coronary vasodilator reserve and metabolism in myocardium subtended by normal arteries in patients with coronary artery disease. *J Am Coll Cardiol*. 1993;22:650-658
118. Kjaer A, Meyer C, Wachtell K, Olsen MH, Ibsen H, Opie L, Holm S, Hesse B. Positron emission tomographic evaluation of regulation of myocardial perfusion in physiological (elite athletes) and pathological (systemic hypertension) left ventricular hypertrophy. *Am J Cardiol*. 2005;96:1692-1698
119. Kaul S, Jayaweera AR. Coronary and myocardial blood volumes: Noninvasive tools to assess the coronary microcirculation? *Circulation*. 1997;96:719-724
120. Johansson B, Morner S, Waldenstrom A, Stal P. Myocardial capillary supply is limited in hypertrophic cardiomyopathy: A morphological analysis. *Int J Cardiol*. 2008;126:252-257
121. Moon J, Cho IJ, Shim CY, Ha JW, Jang Y, Chung N, Rim SJ. Abnormal myocardial capillary density in apical hypertrophic cardiomyopathy can be assessed by myocardial contrast echocardiography. *Circ J*. 2010;74:2166-2172
122. Takahashi E, Asano K. Mitochondrial respiratory control can compensate for intracellular o(2) gradients in cardiomyocytes at low po(2). *Am J Physiol Heart Circ Physiol*. 2002;283:H871-878
123. van Dijk SJ, Dooijes D, dos Remedios C, Michels M, Lamers JM, Winegrad S, Schlossarek S, Carrier L, ten Cate FJ, Stienen GJ, van der Velden J. Cardiac myosin-binding protein c mutations and hypertrophic cardiomyopathy: Haploinsufficiency, deranged phosphorylation, and cardiomyocyte dysfunction. *Circulation*. 2009;119:1473-1483
124. La Gerche A, Taylor AJ, Prior DL. Athlete's heart: The potential for multimodality imaging to address the critical remaining questions. *JACC Cardiovasc Imaging*. 2009;2:350-363
125. Maron BJ, Pelliccia A, Spirito P. Cardiac disease in young trained athletes. Insights into methods for distinguishing athlete's heart from structural heart disease, with particular emphasis on hypertrophic cardiomyopathy. *Circulation*. 1995;91:1596-1601
126. Effects of enalapril on mortality in severe congestive heart failure. Results of the cooperative north scandinavian enalapril survival study (consensus). The consensus trial study group. *N Engl J Med*. 1987;316:1429-1435

127. Pfeffer MA, Braunwald E, Moye LA, Basta L, Brown EJ, Jr., Cuddy TE, Davis BR, Geltman EM, Goldman S, Flaker GC, et al. Effect of captopril on mortality and morbidity in patients with left ventricular dysfunction after myocardial infarction. Results of the survival and ventricular enlargement trial. The save investigators. *N Engl J Med*. 1992;327:669-677
128. A randomized trial of beta-blockade in heart failure. The cardiac insufficiency bisoprolol study (cibis). Cibis investigators and committees. *Circulation*. 1994;90:1765-1773
129. Feldman AM, Bristow MR. The beta-adrenergic pathway in the failing human heart: Implications for inotropic therapy. *Cardiology*. 1990;77 Suppl 1:1-32
130. Packer M, Carver JR, Rodeheffer RJ, Ivanhoe RJ, DiBianco R, Zeldis SM, Hendrix GH, Bommer WJ, Elkayam U, Kukin ML, et al. Effect of oral milrinone on mortality in severe chronic heart failure. The promise study research group. *N Engl J Med*. 1991;325:1468-1475
131. Fragasso G, Perseghin G, De Cobelli F, Esposito A, Palloshi A, Lattuada G, Scifo P, Calori G, Del Maschio A, Margonato A. Effects of metabolic modulation by trimetazidine on left ventricular function and phosphocreatine/adenosine triphosphate ratio in patients with heart failure. *Eur Heart J*. 2006;27:942-948
132. Beer M, Wagner D, Myers J, Sandstede J, Kostler H, Hahn D, Neubauer S, Dubach P. Effects of exercise training on myocardial energy metabolism and ventricular function assessed by quantitative phosphorus-31 magnetic resonance spectroscopy and magnetic resonance imaging in dilated cardiomyopathy. *Journal of the American College of Cardiology*. 2008;51:1883-1891
133. Stolen KQ, Kemppainen J, Kalliokoski KK, Luotolahti M, Viljanen T, Nuutila P, Knuuti J. Exercise training improves insulin-stimulated myocardial glucose uptake in patients with dilated cardiomyopathy. *J Nucl Cardiol*. 2003;10:447-455
134. Belardinelli R, Georgiou D, Cianci G, Purcaro A. Randomized, controlled trial of long-term moderate exercise training in chronic heart failure: Effects on functional capacity, quality of life, and clinical outcome. *Circulation*. 1999;99:1173-1182
135. Stolen KQ, Kemppainen J, Ukkonen H, Kalliokoski KK, Luotolahti M, Lehikoinen P, Hamalainen H, Salo T, Airaksinen KE, Nuutila P, Knuuti J. Exercise training improves biventricular oxidative metabolism and left ventricular efficiency in patients with dilated cardiomyopathy. *Journal of the American College of Cardiology*. 2003;41:460-467
136. Smart N, Marwick TH. Exercise training for patients with heart failure: A systematic review of factors that improve mortality and morbidity. *Am J Med*. 2004;116:693-706
137. Piepoli MF, Davos C, Francis DP, Coats AJ. Exercise training meta-analysis of trials in patients with chronic heart failure (extramatch). *BMJ*. 2004;328:189
138. Beer M, Wagner D, Myers J, Sandstede J, Köstler H, Hahn D, Neubauer S, Dubach P. Effects of exercise training on myocardial energy metabolism and ventricular function assessed by quantitative phosphorus-31 magnetic resonance spectroscopy and magnetic resonance imaging in dilated cardiomyopathy. *Journal of the American College of Cardiology*. 2008;51:1883-1891
139. Coats AJ, Adamopoulos S, Radaelli A, McCance A, Meyer TE, Bernardi L, Solda PL, Davey P, Ormerod O, Forfar C, et al. Controlled trial of physical training in chronic heart failure. Exercise performance, hemodynamics, ventilation, and autonomic function. *Circulation*. 1992;85:2119-2131
140. Myers J, Wagner D, Schertler T, Beer M, Luchinger R, Klein M, Rickli H, Muller P, Mayer K, Schwitter J, Dubach P. Effects of exercise training on left ventricular volumes and function in patients with nonischemic cardiomyopathy: Application of magnetic resonance myocardial tagging. *Am Heart J*. 2002;144:719-725

141. Page N. Weightlessness: A matter of gravity. *N Engl J Med*. 1977;297:32-37

# Table of Tables and Figures

## Chapter 1

**Figure 1.1**: Patterns of Cardiac Remodelling 13

**Figure 1.2**: Cardiac Energy Metabolism 16

**Figure 1.3**: Molecular structure of the sarcomere 18

## Chapter 2

**Figure 2.1**: Timeline for the scan protocol 29

**Figure 2.2**: Epicardial and endocardial contours 31

**Figure 2.3**: BOLD image a) rest and b) exercise 33

**Figure 2.4**: Sequential images during perfusion acquisition in a HCM patient 35

**Figure 2.5**: Myocardial intensity slope curves for normal and HCM subject 36

**Figure 2.6**: Epicardial and endocardial borders for LGE analysis. 37

## Chapter3

**Table 3.1**: Selection of published values of PCr/ATP measured 41

**Figure 3.1**: Top) Resting spectra. Bottom) placement of voxels 46

**Figure 3.2**: top) Bland Atlman plot of high resolution protocol ('long') versus the 8 minute protocol ('short'). Bottom) Bland- Altman plot of the intra subject repeatability 49

**Figure 3.3**: top) spectra acquired during rest, exercise and recovery. Bottom) anatomical images with spectroscopy grid overlay used to confirm voxel position before and after exercise 51

**Figure 3.4**: a) Nominal voxel and voxel. (b) The true volume of a voxel, as described by the point spread function (c) Potential for contamination by neighbouring tissues can be minimised. 54

**Figure 3.5**: (a) PSF of one voxel dimension acquired using standard spatial encoding. (b) PSF of the same voxel acquired using acquisition weighting:
55

**Figure 3.6:** Mismatch between nominal and true flip angle is due to coil loading differences. 57

## *Chapter 4*

**Table 4.1**: Values used in jMRUI simulation package to create simulated data with 40% synthetic random noise added to 16 simulations. 67

**Table 4.2**: A summary of the differences between the original and new prior knowledge for 2, 3 DPG. 70

**Table 4.3**: Sample size needed to detect a 10% change, α 0.05, power 80% ,using the mean and standard deviations of the PCr/ATP using the original and the new 2,3 DPG fit in the pilot patient data above. 79

**Figure 4.1**:Non-linear Least squares fitting to a noisy Gaussian function. 64

**Figure 4.2**: Molecular structure of 2, 3 DPG 64

**Figure 4.3**: Green arrow points to 2 DPG; blue arrow to 3 DPG. In the original fitting, note the great disparity in the sizes of these peaks even though the integration of these peaks should be roughly equal as they arise from the same molecule. Allowing AMARES to estimate these peaks particularly if there is noise in that area of the spectrum can lead to inaccuracies. With the new fit, 2 DPG=0.8x 3 DPG, AMARES can now fit these nuclei with more confidence. 68

**Figure 4.4**: Experimental data on human blood shows that 2 DPG and 3 DPG resonant at differing frequencies but still within a narrow range at phsiological pH. 69

**Figure 4.5**: Simulated data with 20% noise using the original and new 2, 3 DPG fits. 72

**Figure 4.6**: Simulated data with 40% noise using the original and new 2, 3 DPG fits. 73

**Figure 4.7**: Coefficient of variance of 2, 3 DPG measurements for normal volunteers, HCM and DCM cohorts using the original and new 2, 3 DPG fits. 74

**Figure 4.8*:*** Comparison of original 2, 3 DPG fit with new fit. 76

**Figure 4.9**: Examples of voxel content in HCM, DCM and normal controls. 78

## *Chapter 5*

**Table 5.1**: Summary of data published on PCr/ATP measurements in HCM. 83

**Table 5.2**: A comparisons of left ventricular mass in normal; primary pathological hypertrophy, HCM; physiological hypertrophy, Athletes. 86

**Figure 5.1**: The effect of exercise on PCr/ATP in normal controls, HCM, and Athletes, showing a reduction in the HCM group, but no change in athletes or normal 87

**Figure 5.2**: Correlation between change in energetics with exercise and resting PCr/ATP. 88

**Figure 5.3:** Examples of rest and exercise energetics in normal and HCM. 89

**Figure 5.4**: Illustrates the lack of relationship between resting energetics and change in energetic with exercise and hypertrophy, both physiological (athletes) and pathological (HCM). 90

**Figure 5.5**: Equation for free energy release of ATP hydrolysis 96

## *Chapter 6*

**Table 6.1:** Characteristics of study population. 104

**Table 6.2**: Clinical Risk Stratification and Medications in HCM *cohort*. 105

**Figure 6.1**: The mean and standard deviation of BOLD SIΔ% with adenosine stress in normal, athletes, and HCM patients with and without hypertrophy. 106

**Figure 6.2**: The mean and standard deviation of MPRI with adenosine stress in normal, athlete, HCM with and without hypertrophy. 107

**Figure 6.3**: ROC curves for BOLD and MPRI 110

***Figure 6.4***: Demonstrating the progressive importance of function, exercise studies and tissue characterization 117

***Figure 6.5*** Criteria for distinguishing an athlete's heart from HCM 118

## *Chapter7*

**Table 7.1**: Baseline characteristics of subjects 127

**Table 7.2**: Body weight and composition measurements in subjects before and after exercise training 128

**Table 7.3:** Cardiac parameters before and after training. 129

**Figure 7.1**: Time line describing study protocol. 126

**Figure 7.2**: Resting LVEF pre and post exercise training 130

**Figure 7.3**: Relationship between hours of weekly exercise before starting training and change in resting LVEF pre and post training. 131

**Figure 7.4**: Spectra measured at rest and during 8 min leg exercise pre and post 8 week exercise training 132

**Figure 7.5**: Examples of LGE patterns observed. 133

# Appendix 1 Minnesota Questionnaire

MINNESOTA LIVING WITH HEART FAILURE® QUESTIONNAIRE

The following questions ask how much your heart failure (heart condition) affected your life during the past month (4 weeks). After each question, circle the 0, 1, 2, 3, 4 or 5 to show how much your life was affected. If a question does not apply to you, circle the 0 after that question.

| **Did your heart failure prevent you from living as you wanted during the past month (4 weeks) by -** | **No** | | | **Very Little** | | **Very Much** |
|---|---|---|---|---|---|---|
| 1. causing swelling in your ankles or legs? | 0 | 1 | 2 | 3 | 4 | 5 |
| 2. making you sit or lie down to rest during the day? | 0 | 1 | 2 | 3 | 4 | 5 |
| 3. making your walking about or climbing stairs difficult? | 0 | 1 | 2 | 3 | 4 | 5 |
| 4. making your working around the house or yard difficult? | 0 | 1 | 2 | 3 | 4 | 5 |
| 5. making your going places away from home difficult? | 0 | 1 | 2 | 3 | 4 | 5 |
| 6. making your sleeping well at night difficult? | 0 | 1 | 2 | 3 | 4 | 5 |
| 7. making your relating to or doing things with your friends or family difficult? | 0 | 1 | 2 | 3 | 4 | 5 |
| 8. making your working to earn a living difficult? | 0 | 1 | 2 | 3 | 4 | 5 |
| 9. making your recreational pastimes, sports or hobbies difficult? | 0 | 1 | 2 | 3 | 4 | 5 |
| 10. making your sexual activities difficult? | 0 | 1 | 2 | 3 | 4 | 5 |
| 11. making you eat less of the foods you like? | 0 | 1 | 2 | 3 | 4 | 5 |
| 12. making you short of breath? | 0 | 1 | 2 | 3 | 4 | 5 |
| 13. making you tired, fatigued, or low on energy? | 0 | 1 | 2 | 3 | 4 | 5 |
| 14. making you stay in a hospital? | 0 | 1 | 2 | 3 | 4 | 5 |
| 15. costing you money for medical care? | 0 | 1 | 2 | 3 | 4 | 5 |
| 16. giving you side effects from treatments? | 0 | 1 | 2 | 3 | 4 | 5 |
| 17. making you feel you are a burden to your family or friends? | 0 | 1 | 2 | 3 | 4 | 5 |
| 18. making you feel a loss of self-control in your life? | 0 | 1 | 2 | 3 | 4 | 5 |
| 19. making you worry? | 0 | 1 | 2 | 3 | 4 | 5 |
| 20. making it difficult for you to concentrate or remember things? | 0 | 1 | 2 | 3 | 4 | 5 |
| 21. making you feel depressed? | 0 | 1 | 2 | 3 | 4 | 5 |

# *Appendix 2*
# *Borg score*

The Borg score is a simple method of rating perceived exertion:

- 0 - Nothing at all
- 1 - Very light
- 2 - Fairly light
- 3 - Moderate
- 4 - Somewhat hard
- 5 - Hard
- 6
- 7 - Very hard
- 8
- 9
- 10 - Very, very hard

# *Appendix 3*
# *Papers in Preparation*

EXERCISE ACUTELY EXACERBATES DERANGEMENT OF CARDIAC ENERGY METABOLISM IN HYPERTROPHIC CARDIOMYOPATHY, A $^{31}$ PHOSPHORUS MAGNETIC RESONANCE STUDY AT 3 TELSA

Accepted as oral presentation, American Heart Association scientific meeting 2011

DEVELOPMENT AND VALIDATION OF A SHORT 31P CARDIAC MAGNETIC RESONANCE SPECTROSCOPY PROTOCOL.

SOCIETY OF CARDIOVASCULAR MAGNETIC RESONANCE IMAGING 2010. ACCEPTED POSTER

EXERCISE TRAINING IMPROVES CARDIAC FUNCTION, QUALITY OF LIFE AND EXERCISE CAPACITY IN PATIENTS WITH DILATED CARDIOMYOPATHY.

SOCIETY OF CARDIOVASCULAR MAGNETIC RESONANCE IMAGING 2011. ACCEPTED POSTER.

EXERCISE OXYGENATION IS IMPAIRED IN HCM IN BOTH HYPERTROPHIED AND PRE HYPERTROPHIED STATES.